THEORY REVIEW & VALIDATION

BLEV (FIREBALL)

DATE: December 2023

This document describes the theory of the time-varying (Martinsen & Marx) and static (HSE and TNO) fireball models which are implemented in PHAST/SAFETI. The fireball is modelled as a sphere emitting radiation from its surface with uniform surface emissive power. The models predict the fireball maximum radius, duration, lift-off height, fraction of heat radiated from the flame's surface, and maximum surface emissive power of the flame. This document also includes results of a literature review on fireball modelling together with model validation results.

Reference to part of this report which may lead to misinterpretation is not permissible.

No.	Date	Reason for Issue	Prepared by	Verified by	Approved by
1	July 2004	PHAST 6.5 version	A. O. Oke	Henk Witlox	
2	September 2017	Safeti 8.0 version	A. O. Oke	Henk Witlox	
3	May 2021	Apply new template	D. Vatier		

Date: December 2023

Prepared by: Digital Solutions at DNV

© DNV AS. All rights reserved

This publication or parts thereof may not be reproduced or transmitted in any form or by any means, including copying or recording, without the prior written consent of DNV AS.

ABSTRACT

This document describes the theory of the time-varying (Martinsen & Marx) and static (HSE and TNO) fireball models (BLEV-HSE/BLEV-TNO) which are implemented in PHAST/SAFETI. The fireball is modelled as a sphere emitting radiation from its surface with uniform surface emissive power. The models employ empirical correlations that predict fireball maximum radius, duration, lift-off height, fraction of heat radiated from the flame's surface and maximum surface emissive power of the flame.

This document also includes the results of a literature review on fireball modelling. The review includes an overview of previous literature studies undertaken including the review by DNV Benelux for the Flemish Government.

Attention has been paid to models describing the dynamic behaviour of fireballs. Literature on dynamic fireball models have been discussed under two categories:

- Catastrophic vessel failure fireball models: these cover fireballs stemming from BLEVEs or pressure vessel bursts. Three models have been identified and reviewed in this document:
  - The BG/GL fireball model as reported by Pritchard (1985)
  - The Shell fireball model as detailed in Shield (1993 / 1995)
  - The Quest fireball model as described by Martinsen and Marx (1999)
- Pipeline release fireball models: these cover fireballs stemming from immediate/delayed ignited vertical (impulsive) jet releases from pipelines. Two models have been reviewed in this document:
  - The GL impulsive fireball model as reported by Cleaver and Halford (2014)
  - The Shell vertical jet fireball model as reported by Cracknell and Carlsey (1997)

A comparative analysis of the key characteristics of each model and associated performance of model predictions against experimental / field data has also been undertaken. Also included are results of the model validation of the Martinsen and Marx time-varying fireball model, as implemented in PHAST/SAFETI, against published experimental data for large scale (2tonne) propane and butane BLEVEs (Johnson et al., 1991) and medium to large scale propane BLEVEs reported by Roberts et al., 2000. The key conclusions from the model review, validation and comparative analysis are summarized below, where:

In terms of catastrophic vessel failure dynamic fireball models:

- All three models account for three distinct regimes in the fireball development, i.e., flame ignition to lift-off, lift-off to break-up and break-up to extinction and primarily differ in assumptions as to flame behaviour during these regimes.
- In terms of performance against experimental / field data:
  - The Quest model is observed to give the closest agreement with the range of data recorded during the Johnson et al. (1991) propane and butane BLEVE tests.
  - Only a limited amount of data (flame duration) was considered in the comparative analysis involving the Shell Shield model, as such only limited conclusions may be drawn from the analysis undertaken. In general, for the cases considered, the Shell Shield model is observed to give the closest agreement with measured data for flame durations. Furthermore, the BG Pritchard model is observed to give generally closer agreement with the range of data recorded during the JIVE (Roberts et al., 2000) propane BLEVE tests when compared against simulated data using the Quest model.
  - The Quest model shows overall very good agreement for radiation dose predictions except in the near-field for a limited number of cases.

In terms of the impulsive pipeline release fireball models:

- The Shell Cracknell and Carsley model is relatively simple and employs empirical correlations in describing flame characteristics. However, the BG/GL model is significantly more complicated and flame characterization requires the solution of mass, momentum and combustion differential equations.
- The BG/GL impulsive fireball model may only be applied to gas / vapour phase time-varying releases where the material is naturally buoyant. However, the Shell Cracknell and Carsley model may be applied to a wide variety of fluid states and materials but is only suited for steady state releases.

In general, it is not recommended to model the development of fireballs from impulsive pipeline releases using catastrophic vessel failure fireball models and vice-versa. For impulsive jet releases, the models described in this report may be used, albeit with care; readers are advised to take particularly note of the various model limitations documented in this report (see Sections 3.1 and 3.2).

Table of contents

ABSTRACT I

1 INTRODUCTION 1

2 STATIC FIREBALL MODELS IN SAFETI [TNO AND HSE MODELS] 4

2.1 Mathematical model 4
2.1.1 Determine the mass of fuel involved in the fireball 4
2.1.2 Calculate the maximum radius of the fireball 5
2.1.3 Determine the fireball duration 5
2.1.4 Calculate the lift-off height of the fireball 5
2.1.5 Calculate the surface emissive power (SEP) of the fireball 6
2.1.6 Calculate the flame co-ordinates 7

3 LITERATURE REVIEW OF DYNAMIC FIREBALL MODELS 8

3.1 Catastrophic vessel failure fireball models 8
3.1.1 BG/GL model (Pipesafe – Pritchard, 1985) 8
3.1.2 Shell model (Shepherd – Shield, 1993 & 1995) 12
3.1.2.1 Shield (1993) 12
3.1.2.2 Shield (1995) 15
3.1.2.3 Validation, Shield (1993 / 1995) 16
3.1.3 Quest model (CANARY - Martinsen and Marx) 18
3.1.4 Comparative analysis of key model characteristics 20
3.1.5 Comparative analysis of model predictions against selected field data 24
3.1.5.1 Johnson et al. (1991) large scale tests: Butane and Propane BLEVEs 24
3.1.5.2 Roberts et al. (2000) medium to large scale tests: Propane (LPG) BLEVEs 26
3.1.6 Literature review of fireballs by DNV Benelux for Flemish authorities 29

3.2 Impulsive pipeline release fireball models 32
3.2.1 GL model (Pipesafe – Cleaver and Halford, 2014) 32
3.2.2 Shell model (Shepherd – Cracknell, 1997) 33
3.2.3 Comparative analysis 35

4 DETAILED VALIDATION OF THE MARTINSEN AND MARX (1999) MODEL 37

4.1 Johnson et al. (1991) large scale tests: Butane and Propane BLEVEs 37
4.1.1 Radiation intensity versus time 38
4.1.2 Radiation Dose versus distance 39
4.1.3 Flame SEP versus time 40
4.1.4 Flame radius versus time 40
4.1.5 Flame height versus time 41

4.2 Roberts (2000) medium to large scale tests: Propane (LPG) BLEVEs 45
4.2.1 Radiation intensity versus time 45
4.2.2 Radiation dose versus distance 46
4.2.3 Flame SEP versus time 47

4.3 Overall results 48

5 CONCLUSIONS AND RECOMMENDATIONS 50

5.1 Conclusions 50

5.2 Recommendations 51
5.2.1 Catastrophic vessel failure fireball models 51
5.2.2 Impulsive pipeline release fireball models 51

NOMENCLATURE 52

APPENDICES 53
Appendix A. Verification of the static fireball (BLEV-HSE and BLEV-TNO) models 53
A1. Yellow Book example 6.6.5[4] 53
A2. Fireball radius 53
A3. Fireball duration 54
Appendix B. Sensitivity analysis on the static fireball (BLEV-HSE and BLEV-TNO) models 56

B1. Effect of increasing flammable mass 56
B2. Effect of increasing burst temperature/pressure 58
B3. Effect of increasing atmospheric pressure 59
B4. Effect of increasing burst vapour mass fraction 60

REFERENCES 64

Table of figures

Figure 1. Potential future dynamic fireball and jet fire model 1
Figure 2. Static fireball model in Phast and Safeti 2
Figure 3. Schematic representation of fireball co-ordinates based on the BLEV-HSE and BLEV-TNO models. 7
Figure 4. Validation of Pritchard (1985) model: incident radiation intensity versus time 11
Figure 5. Stages in the development of a fireball Shield (1993) 12
Figure 6. Validation of the Shield (1993) model: fireball characteristics and radiation flux 17
Figure 7. Validation of Martinsen and Marx model (Test 1, Johnson et al.) – radiation intensity versus time 20
Figure 8. Validation of Martinsen and Marx model (Tests 2-5, Johnson et al.) – radiation dose 20
Figure 9. Comparison of predicted maximum durations: BG, Quest, TNO and HSE models 22
Figure 10. Comparison of fireball dimensions and duration for TNO, HSE, Quest and SFPE models 30
Figure 11. Comparison of SEP for TNO, HSE, Quest and SFPE models 31
Figure 12. Validation of the GL impulsive jet "stalk" model (Cleaver and Halford, 2014) 33
Figure 13. Validation of the GL impulsive fireball model (Cleaver and Halford, 2014): peak incident radiation intensities. 33
Figure 14. Validation of the Shell impulsive fireball model (Cracknell and Carlsey, 1997): radiation intensity versus time. 35
Figure 15. Validation of Martinsen and Marx model (Tests 1R – 5, Johnson et al., 1991) – radiation intensity versus time 39
Figure 16. Validation of Martinsen and Marx model (Tests 1R – 5, Johnson et al., 1991) – radiation dose versus distance 41
Figure 17. Validation of Martinsen and Marx model (Tests 1R – 5, Johnson et al., 1991) – flame SEP versus time 42
Figure 18. Validation of Martinsen and Marx model (Tests 1R – 5, Johnson et al., 1991) – flame radius versus time 43
Figure 19. Validation of Martinsen and Marx model (Tests 1R – 5, Johnson et al., 1991) – flame centroid height versus time 44
Figure 20. Instrument layout for (1708kg) propane BLEVEs (Roberts et al., 2000) 45
Figure 21. Validation of Martinsen and Marx model (Roberts et al., 2000) – radiation intensity versus time 46
Figure 22. Validation of Martinsen and Marx model (Roberts et al., 2000) – radiation dose versus distance 47
Figure 23. Validation of Martinsen and Marx model (Roberts et al., 2000) – flame SEP versus time 48
Figure 24. Validation of Martinsen and Marx model (Johnson et al., 1991; Roberts et al., 2000) –radiation dose 49
Figure 25. Validation of Martinsen and Marx model (Johnson et al., 1991; Roberts et al., 2000) – peak radiation intensity 49
Figure 26 Variation of predicted fireball radius with flammable mass using Microsoft Excel, the BLEV-HSE and BLEV-TNO models. 54
Figure 27 Variation of predicted fireball duration with flammable mass using Microsoft Excel, the BLEV-HSE and BLEV-TNO models. 55
Figure 28 Sensitivity analyses on the BLEV-HSE and BLEV-TNO models showing the variation of simulated fireball radius with flammable mass. 57
Figure 29 Sensitivity analyses on the BLEV-HSE and BLEV-TNO models showing the variation of simulated fireball duration with flammable mass. 57
Figure 30 Sensitivity analyses on the BLEV-HSE and BLEV-TNO models showing the variation of simulated fireball lift-off height with flammable mass. 58
Figure 31 Sensitivity analyses on the BLEV-HSE and BLEV-TNO models showing the variation of simulated fireball surface emissive power with flammable mass. 58
Figure 32 Sensitivity analyses on the BLEV-HSE and BLEV-TNO models showing the variation of simulated fireball surface emissive power with fluid saturated vapour temperature at the moment of vessel rupture. 59
Figure 33 Sensitivity analyses on the BLEV-HSE and BLEV-TNO models showing the variation of simulated fireball surface emissive power with the prevailing ambient pressure. 60
Figure 34 Sensitivity analyses on the BLEV-HSE and BLEV-TNO models showing the variation of simulated fireball radius with vapour mass fraction from the released inventory. 61
Figure 35 Sensitivity analyses on the BLEV-HSE and BLEV-TNO models showing the variation of simulated fireball duration with vapour mass fraction from the released inventory. 61

Figure 36 Sensitivity analyses on the BLEV-HSE and BLEV-TNO models showing the variation of simulated fireball lift-off height with vapour mass fraction from the released inventory.....62
Figure 37 Sensitivity analyses on the BLEV-HSE and BLEV-TNO models showing the variation of simulated fireball surface emissive power with vapour mass fraction from the released inventory.....62

List of tables

Table 1 Fireball parameters as a fraction of total flame duration (Pritchard, 1985)..... 9
Table 2 Validation of Pritchard (1985) model: predicted versus measured data.....10
Table 3 Comparison of key characteristics of the BG, Shell and Quest dynamic fireball model 23
Table 4 Comparison of dynamic fireball model predictions against experimental data (Johnson et al., 1991).....25
Table 5 Comparison of dynamic fireball model predictions against experimental data (Roberts et al., 2000).....28
Table 6 Comparison of key characteristics of the BG and Shell impulsive jet fireball models.....36
Table 7 Summary of test and ambient conditions: butane and propane BLEVEs (Johnson et al., 1991).....37
Table 8 Summary of test and ambient conditions: propane BLEVEs (Roberts et al., 2000).....45
Table 9 Pertinent information relating to the simulation of fireball characteristics following the failure of a propane road tanker 53
Table 10 Comparison of simulated fireball characteristics using the BLEV-TNO model against published results in the “TNO- Yellow Book” example 6.6.5[4] 53
Table 11 Parameter variations employed in the sensitivity analyses of the BLEV-HSE and BLEV-TNO models.....56

1 INTRODUCTION

Fireballs are short-lived flames which generally result from the ignition and combustion of turbulent vapour/two-phase (i.e., aerosol) fuels in air[1]. Releases that fuel fireballs are usually near instantaneous and commonly involve the catastrophic failure of pressurised vessels/pipelines. Fireballs could dissipate large amounts of thermal radiation, which, away from their visible boundaries, may transmit heat energy that could be hazardous to life and property. As such, in the evaluation of the hazard posed by fireballs, the accurate determination of the likelihood of object engulfment and/or the amount of radiant energy received by objects at a distance from the flame is of primary importance.

Fireball models developed for estimating flame shape and incident radiation at a given distance can be broadly divided into two categories, i.e. Dynamic and Static models[1]:

- Dynamic models account for the variation of flame shape and surface emissivity with time. Dynamic models may be further sub-divided into two categories:
  - Catastrophic vessel failure models
  - Pipeline release fireball models

- Static models, on the other hand, assume the fireball to exist at its maximum size over its lifespan and ignore transient flame characteristics. These models are only applicable to immediately ignited flames following catastrophic pressure vessel bursts or BLEVEs.

Both Static and Dynamic models generally rely on empirical correlations in simulating fireballs. The former, when compared with the latter, are mathematically simpler, easier to understand and formulate, quicker to implement in computer programs, and provide conservative flame shape and incident radiation estimates for hazard assessment studies[1].

However in reality the fireball will not be static. In case of a ground-level release resulting from a catastrophic vessel failure, the fireball will initially start from the ground and subsequently rise to the atmosphere. In case of a long pipeline, there will be an initial mushroom like 'composite' flame comprising of a fireball at its apex (i.e., with the fireball starting from the ignition / release source[i] and rising to the atmosphere) and a truncated cone-shaped 'jet fire' at its base. The mushroom like flame (i.e. on disintegration of the fireball) is followed by a jet fire (with reducing radiation because of reducing pipeline release rate); see Figure 1. Thus, because of the moving fireball and the reducing jet fire, the radiation will vary as a function of time at a given downwind location. In addition, the radiation may vary as a function of the time, because the observer is not located at a fixed position but may move away from the fire.

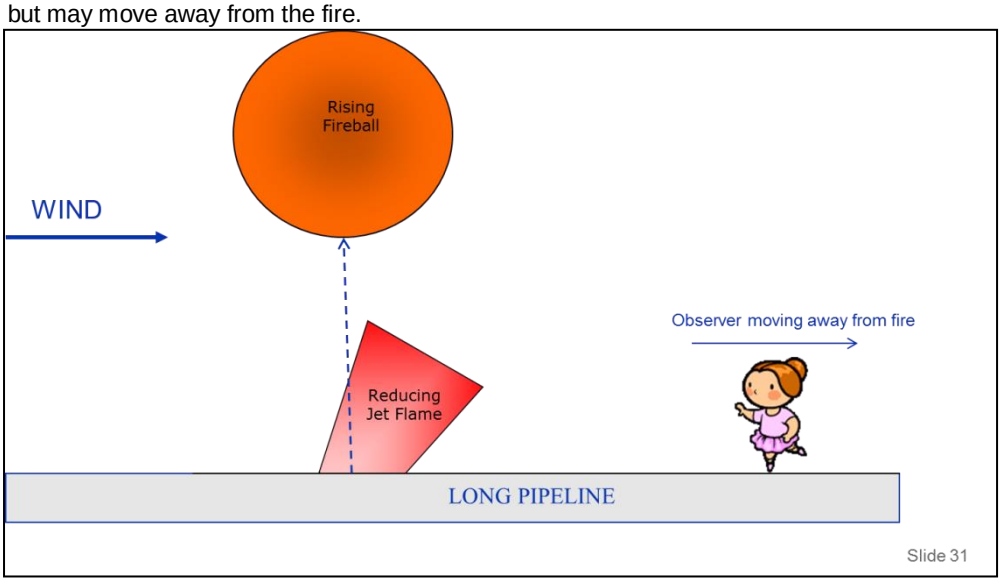

Figure 1. Potential future dynamic fireball and jet fire model

[i] With long pipeline releases, it is generally believed (i.e., from observations gathered during field tests) that fireballs may only ensue where the ignition source is close to the release and ignition is undertaken relatively within a short period (ca. ≤ 30s) following the release.

Static fireball models in Phast, Safeti and Safeti-NL

Chapter 2 provides a detailed description of the underlying theory for the static fireball models available in Phast, Safeti and Safeti-NL. Further information on model verification, sensitivity analysis and validation against available fireball field data[2, 3] are included in Appendix A and Appendix B.

The static fireball model calculates the fireball dimensions (radius, lift-off height), the surface emissive power and the fireball duration. These output data are derived using simple correlations derived from either the TNO[4] or HSE (Roberts)[5] models. These models assume that the fireball radiation and fireball location is fixed and does not vary over time during the fireball duration. In case of the HSE model, the fireball is assumed to be located on the ground, while the TNO model assumes the lift-off height of the plume (distance between ground and the centre of the fireball) equals the fireball diameter; see Figure 2. Furthermore, the model assumes that for radiation calculations the observer is located at a fixed position and does not move.

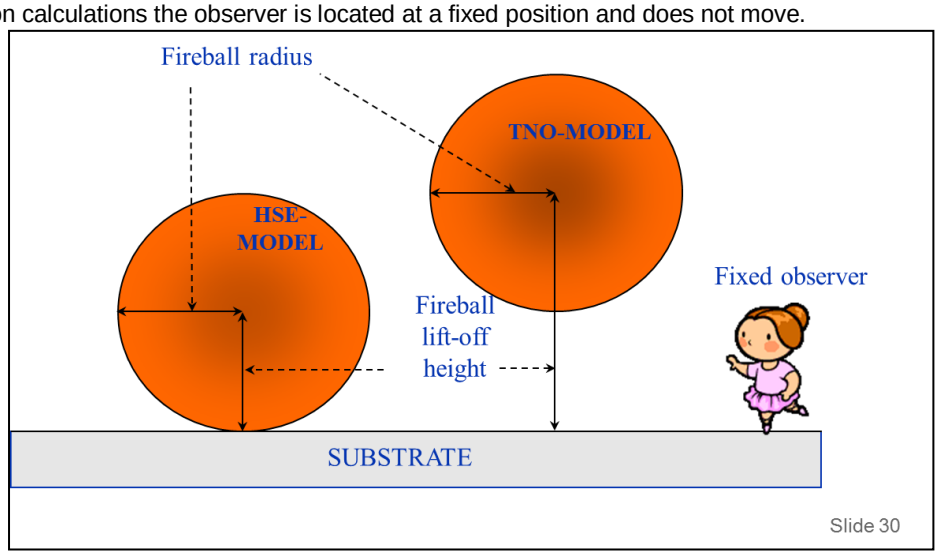

Figure 2. Static fireball model in Phast and Safeti

Literature review

Chapter 3 includes the results from a brief literature review carried out to establish state-of-the-art logic for time-varying fireballs. This included investigation of the following references:

- Previous literature reviews
  - Overview of fireball models from Loss Prevention book (Mannan[6]).
  - Review of fireball models from Dutch Yellow Book[4]
  - Description and overview of fireball modelling in the CCPS book[7]. This refers to the paper by Roberts et al. (2000)[8] and the dynamic fireball model by Martinsen and Marx (1999)[1].
  - Report[9] produced by DNV Benelux (partly carried out with feedback from DNV Digital Solutions) for the Flemish Authorities in an investigation of the use of consequence models for QRA's.

- Models from GL (previously Advantica and British Gas). Acton et al.[10,11] describe the PIPESAFE program for modelling the release of natural gas (methane) from a buried long pipeline. PIPESAFE includes the model IMPJET to predict the radiation from a time-varying fireball in case of immediate ignition, and the model CRYSTAL for modelling the delayed ignition (quasi steady-state jet fire (CRYSTAL includes a crater source model, a flame structure model and a radiation model. The GL programs FROST and ORDER programs use the Pritchard fireball model FYRBL.

- The methodology included in Shepherd[12] is based on the time-varying fireball model developed by Simon Shield (1993, 1994, 1995)[13,14,15].

- The paper by Martinsen and Marx (1999)[1]. This paper appears to be based on extensive literature, detailed tests and allows for lift-off.

Details of the theoretical basis including the results of a comparative analysis undertaken on the pertinent models is presented.

The Martinsen and Marx model has been implemented in the new time-varying model TVFM within Phast, Safeti and Safeti-NL. TVFM allows for modelling time-varying radiation (because of changing geometry of fireball and/or jet fire) and employs the existing radiation model RADS to calculate the radiation at a specific time. TVFM obtains radiation dose via integration of the RADS results, and subsequently radiation probit and probability of death are calculated as previously (using the probit function from the TNO Green Book). This new numerical model could be further extended in the future to account for time-varying radiation effects because of people moving away from the fire (with a given constant velocity).

Model validation

Chapter 4 describes results using the static (as far as feasible) and dynamic Phast models against relevant experiments found as identified as part of the literature survey.

Recommendations

In chapter 5, the document closes with suggestions on possible improvements to the static and dynamic BLEV-fireball models.

2 STATIC FIREBALL MODELS IN SAFETI [TNO AND HSE MODELS]

Section 2.1 documents the mathematical model underlying the HSE and TNO static fireball models (BLEV-HSE/BLEV-TNO) which are implemented in PHAST/SAFETI. The fireball is modelled as a sphere emitting radiation from its surface with uniform surface emissive power. The models employ empirical correlations that predict fireball maximum radius, duration, lift-off height, fraction of heat radiated from the flame's surface and maximum surface emissive power of the flame. The flame shape and duration are correlated as functions of the fireball fuel mass while the fraction of heat radiated is correlated as a function of the fuel's pre-explosion vapour pressure. Both the TNO and HSE models ignore time varying effects. In the HSE model, the sphere is assumed to be grounded while the TNO model predicts a degree of flame lift-off above ground.

The detailed verification of the TNO and HSE models are detailed in Appendix A. Each model has been verified by comparison against simulated data generated in Microsoft Excel and published worked example data for an LPG (propane) tank BLEVE as detailed in the "TNO-Yellow Book" (example 6.6.5[4]). In all studied cases, very close agreement in simulated results is observed.

The outcome of a detailed sensitivity analyses on the BLEV-HSE and BLEV-TNO models is also documented in Appendix B. The results from sensitivity analyses show the predicted fireball maximum radius, lift-off height and duration to increase exponentially with the ignited fuel mass/ vapour mass fraction while flame surface emissive power is observed to increase with fuel pre-explosion temperature or vapour pressure. In general, for a given release scenario, the BLEV-TNO model generally predicts wider fireball radius, longer flame duration, higher lift-off heights and smaller flame surface emissive power when compared with simulated results from the BLEV-HSE model.

A third modelling option in PHAST/SAFETI (a.k.a. "Roberts/TNO hybrid") combines the surface emissive power model of the BLEV-HSE with the BLEV-TNO's maximum fireball radius, lift-off height and duration models.

2.1 Mathematical model

Figure 2 is a schematic representation of the fireball shapes as modelled using the HSE and TNO models respectively. For these models, the algorithm involved in the estimation of the fireball shape and surface emissivity can be summarised as follows:

1. Determine the mass of fuel involved in the fireball
2. Calculate the maximum radius of the fireball
3. Determine the fireball duration
4. Calculate the lift-off height of the fireball
5. Calculate the surface emissive power of the fireball
6. Calculate the flame co-ordinates

In the following, the equations employed in the BLEV-HSE and BLEV-TNO models are presented.

2.1.1 Determine the mass of fuel involved in the fireball

The first step in estimating flame dimension and surface emissivity involves the calculation of the mass of fuel involved in the fireball. Where two-phase inventory is concerned, all or some of the mass contained within a vessel prior to its rupture can contribute to the fireball. The total mass contributing to the fireball is strongly influenced by the fuel's degree of superheat with reference to its boiling point at ambient pressure. Increase in the fuel's degree of superheat prior to loss of containment results in increased flash vaporisation of the liquid inventory and larger amounts of released inventory contributing to the fireball.

From experimental studies on fireballs, Hasegawa and Sato (1977)[16] and Roberts (1982)[17] recommend that: if adiabatic flash vaporisation of the fuel upon loss of containment exceeds 35% by mass, the mass of fuel involved in the fireball equals the total mass of fuel released.

The CCPS (2010)[18] suggest a modified form of the Roberts' rule, which is summarised as follows: if adiabatic flash vaporisation of the fuel exceeds 1/3 of the released inventory, the mass of fuel involved in the fireball equals the total mass of fuel released. Otherwise, the mass involved equals three times the adiabatic flash vapour mass fraction. The latter proposition accounts for the mass contributed to the released vapour cloud as a result of entrained

liquid droplets following a BLEVE. The CCPS recommendation is employed in the BLEV-HSE and BLEV-TNO[ii] models and is expressed mathematically as:

$$M_{\text{Flammable}} = \begin{cases} M_{\text{Input}} & f_{\text{Vapour}} \geq \dfrac{1}{f_{\text{correction}}} \\ f_{\text{correction}} f_{\text{Vapour}} M_{\text{Input}} & f_{\text{Vapour}} < \dfrac{1}{f_{\text{correction}}} \end{cases} \quad \textbf{(1)}$$

Where:

$M_{Flammable}$	=	Mass of fuel involved in the fireball [kg]
M_{Input}	=	Total inventory released following vessel rupture [kg]
f_{Vapour}	=	Mass fraction of vapour released following vessel rupture [-]
$f_{correction}$	=	Mass correction factor (CCPS recommended value = 3) [-]

2.1.2 Calculate the maximum radius of the fireball

The flame radius, r_{Flame}, is generally correlated as a function of $M_{Flammable}$. Based on the HSE and TNO fireball models, r_{Flame} can be calculated respectively as:

The HSE model[5]:

$$r_{\text{Flame}} = 2.9 M_{\text{Flammable}}^{0.333} \quad \textbf{(2)}$$

The TNO "Yellow Book" model[4]:

$$r_{\text{Flame}} = 3.24 M_{\text{Flammable}}^{0.325} \quad \textbf{(3)}$$

2.1.3 Determine the fireball duration

The flame duration, t_{Flame}, is generally correlated as a function of $M_{Flammable}$. Based on the HSE and TNO fireball models, t_{Flame} can be calculated respectively as:

The HSE model[5]:

$$t_{\text{Flame}} = \begin{cases} 0.45 M_{\text{Flammable}}^{0.333} & M_{\text{Flammable}} < 37000 \\ 2.59 M_{\text{Flammable}}^{0.167} & M_{\text{Flammable}} \geq 37000 \end{cases} \quad \textbf{(4)}$$

The TNO "Yellow Book" model[4]:

$$t_{\text{Flame}} = 0.852 M_{\text{Flammable}}^{0.26} \quad \textbf{(5)}$$

2.1.4 Calculate the lift-off height of the fireball

The flame lift-off height, H_{Flame}, is defined as the height from the centre of the fireball to the ground under the fireball (ref: TNO). Based on the HSE and TNO fireball models H_{Flame} can be calculated respectively as:

The HSE model I[5]:

[ii] In the TNO fireball model, the mass involved in the fireball is assumed to be equal to the released inventory. Thus, $M_{Flammable} = M_{Input}$. This corresponds to specifying a very large value for the mass correction factor ($f_{correction}$) such that $f_{correction} f_{vapour} \geq 1$. The use of $M_{Flammable} = M_{Input}$ could be inaccurate especially where the released inventory is non-volatile (e.g. heavy-crude). In such cases, the CCPS approach would rightly predict the non-occurrence of a fireball while the TNO model would simulate the converse. As such, the CCPS method has been adopted for the BLEV-HSE and BLEV-TNO fireball models.

$$H_{\text{Flame}} = r_{\text{Flame}} \quad \textbf{(6)}$$

The TNO "Yellow Book" model[4]:

$$H_{\text{Flame}} = 2r_{\text{Flame}} \quad \textbf{(7)}$$

From equations (6) and (7) it can be seen that the HSE model assumes the fireball to be grounded while the TNO model predicts an amount of flame lift-off above ground level.

2.1.5 Calculate the surface emissive power (SEP) of the fireball

The Roberts' correlation[17] for the flame SEP is employed in the HSE and TNO models. It is given by:

$$E_f = \frac{f_s M_{\text{Flammable}} \Delta H_C}{4\pi r_{\text{Flame}}^2 t_{\text{Flame}}} \quad \textbf{(8)}$$

Where

E_f	=	Surface emissive power of the flame [W/m^2]
f_s	=	Fraction of total available heat energy radiated by the flame [-]
ΔH_C	=	Net available heat for radiation [J/kg]

Roberts (1982) [17] correlated f_s in terms of the fuel's saturated-vapour/vessel-burst pressure (P_{Sat} [N/m^2]) at the point of vessel failure as[iii, iv]:

$$f_s = 0.27\left(\frac{P_{\text{Sat}}}{10^6}\right)^{0.32} \quad \textbf{(9)}$$

For the HSE and TNO models, ΔH_C is defined respectively as:

The HSE model[5]:

$$\Delta H_C = \Delta H_{Comb} \quad \textbf{(10)}$$

The TNO "Yellow Book" model[4,v]

$$\Delta H_C = \Delta H_{Comb} - \left[\min\left(1, f_{vapour} f_{correction}\right) - f_{vapour}\right]\left[\Delta H_{Vap} + C_{p,Liq}\left(T_{Flame} - T_{Amb}\right)\right] \quad \textbf{(11)}$$

Where:

ΔH_{Comb}	=	Heat of combustion of the fuel [J/kg]
ΔH_{Vap}	=	Latent heat of vaporisation of the fuel at its boiling point [J/kg]
$C_{p,Liq}$	=	Specific heat capacity of the fluid at constant pressure [J/kg/K]
T_{Flame}	=	Flame temperature (≈2000K) [K]
T_{Amb}	=	Ambient temperature [K]

[iii] In the implementation of BLEV-HSE model, the right hand side of equation (9) is slightly modified and re-expressed in a dimensionless form as: $f_s = 0.27(P_{Sat}/(10P_{Atm}))^{0.32}$. Where: P_{Atm} is the ambient pressure [N/m^2]. The modified expression suggests a plausible dependence of f_s on P_{Atm}. Any error introduced by this assumption will be generally negligible as in most practical cases: $P_{Atm} \approx 10^5$ N/m^2.

[iv] P_{Sat} is currently set in the BLEV models to be subject to the following constraint: $P_{Sat} = \max(P_{Atm}, P_{Sat})$. Where P_{Sat} is unknown/undefined, its value is taken as the fluid's saturated vapour pressure at the lower of the ambient or critical temperature: i.e., $P_{Sat}(\min(T_{crit}, T_{Amb}))$. T_{crit} is the fluid's critical temperature.

[v] Equation (11) is rather ambiguous. The term $C_{p,Liq}(T_{Flame} - T_{Amb})$ appears to suggest that the liquid boils at T_{Flame} and is discharged at T_{Amb}. A more accurate rendition of this term would be: $\int_{T_{sar}}^{T_{ref}} C_{p,Liq}\,dT - \int_{T_{ref}}^{T_{Flame}} C_{p,gas-products}\,dT$, where T_{sat} and T_{ref} are the fluid's release temperature and boiling point respectively while $C_{p,gas-products}$ represents the specific heat capacity of the combustion products. In all, Roberts (1982) calculates the total available energy in the fireball as "MH": where M is the mass of fuel that burns in the fireball and H is the heat of combustion of the fuel. Thus, the HSE model appears to be a more accurately implementation of the Roberts (1982) model. Note: The use of equation (10) in place of equation (11) would significantly simplify model calculations and predict conservative estimates of the flame's SEP.

2.1.6 Calculate the flame co-ordinates

The co-ordinates of the fireball simulated by the BLEV models are always defined by a set of ten circles equally spaced along the flame length (in this case along the flame diameter). Each circle *i* is described by four co-ordinates, x_i and, z_i which correspond to the centre of the circle, r_i the radius of the circle, and $\varphi_i = 0$ the inclination of the circle from horizontal (see Figure 3).

The co-ordinates for each circle are calculated as:

$$x_i = 0; \quad z_i = H_{\text{Flame}} - r_{\text{Flame}} \cos \vartheta_i; \quad r_i = r_{\text{Flame}} \sin \vartheta_i; \quad \varphi_i = 0; \quad \vartheta_i = \frac{\pi(i-1)}{N-1} \qquad \textbf{(12)}$$

Where:

x_i	=	Horizontal position of the centre of circle *i* [m]
z_i	=	Vertical height of the centre of circle *i* above ground level[m]
N	=	Total number of circles (N is currently equal to 10)
ϑ_i	=	Angle between the vertical and the cord joining the fireball centre to the circumference of circle *i* [º]

From equation (12), ϑ_i will range from 0º to 180º and thus cover the entire diameter of the fireball.

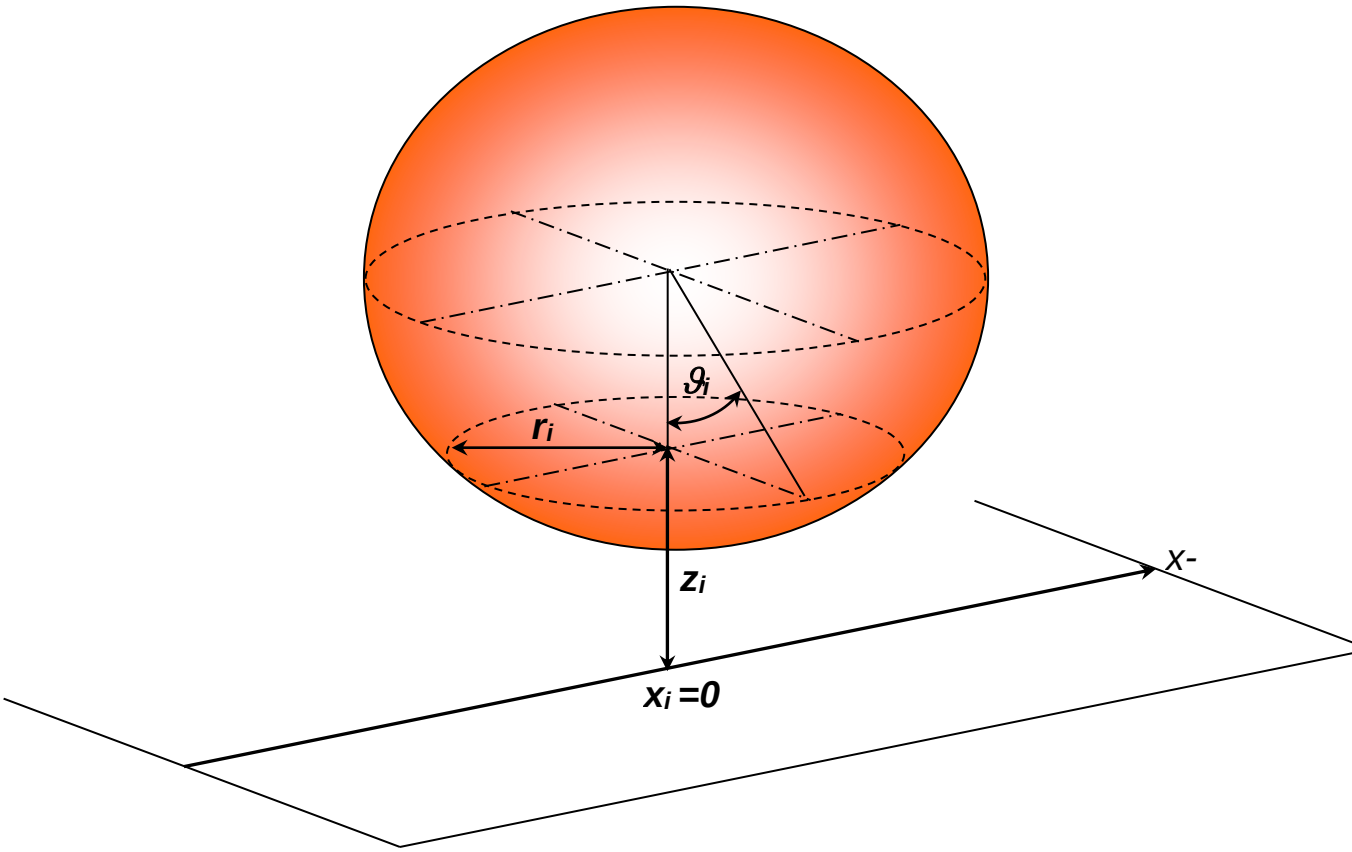

Figure 3. Schematic representation of fireball co-ordinates based on the BLEV-HSE and BLEV-TNO models.

3 LITERATURE REVIEW OF DYNAMIC FIREBALL MODELS

As indicated in Chapter 1, a significant amount of published literature and model reviews on static fireball models have been undertaken. Recent comprehensive reviews, with guidelines, have been published by the Center for Chemical Process Safety (CCPS)[7], the TNO (Yellow Book)[4] and more recently, within the DNV report "Research on models for use in Quantitative Risk Assessment" (2012)[9] for the Flemish Authorities.

These reviews have primarily focussed on static fireball models associated with catastrophic vessel failures. The CCPS and DNV reviews also touch on the dynamic fireball model published by Martinsen and Marx (1999)[1] but do not describe any others.

Whilst a number of dynamic fireball models exist and have been described in literature, a detailed review and comparative assessment of the characteristics of well-established dynamic fireball models has not been undertaken. The following presents the results of a literature review carried out to assess the various characteristics of time-varying fireball models available within open literature. The review also assesses model performance against field / experimental data with the aim of identifying the model which best represents state-of-art logic.

This literature review is concerned with models describing the dynamic behaviour of fireballs stemming from:

- the immediate ignition of flammable material following a catastrophic vessel failure (BLEVEs or pressure vessel bursts);
- the delayed ignition of vertical steady-state jets of flammable fluids (e.g. propane) from a pipeline or pressurized vessel (leak scenario only) following a leak or full-bore rupture, provided the ignition occurs close to the release source and has allowed a flammable cloud to form (to steady state).
- the immediate (or early < 30s) ignition of vertical jets of flammable fluids from a pipeline following a major (>1") leak or full-bore rupture event

This chapter discusses dynamic fireball models for the above fireball scenarios under the following two categories:

- Catastrophic vessel failure fireball models: these cover fireballs stemming from BLEVEs or pressure vessel bursts
- Pipeline release fireball models: these cover fireballs stemming from immediate/delayed ignited vertical (impulsive) jet releases from pipelines.

3.1 Catastrophic vessel failure fireball models

3.1.1 BG/GL model (Pipesafe – Pritchard, 1985)

Following a review of experimental data on fireballs, Pritchard (1985)[19,20] proposed an empirical model for predicting flame characteristics and attendant radiant heat effects from fireballs. The proposed model is comprised of equations that describe the variation of fireball size, motion and flame emissive power with time. The model does not account for rainout as it assumes the entire inventory, following catastrophic vessel failure, contributes to the ensuing fireball. Fireball characteristics were described in terms of:

- Fireball shape
- Fireball lifetime
- Fireball radius and height:
- Flame surface emissive power:

The Pritchard (1985) model was later extended (Halford, 2014)[21] to account for wind-drift.

Fireball Shape

Pritchard (1985) assumes the fireball to be spherical in shape throughout its lifetime. On ignition, the fireball flame envelope is assumed to expand at ground level and thereafter start to rise off the ground. Soon after flame lift-off, the fireball reaches its maximum diameter and continues to rise at a constant volume. A maximum visible height is then attained at which time the fireball starts to fragment, while its centre remains at the same height. During this period, the fireball is represented as a gradually shrinking sphere until flame extinction occurs.

Flame lifetime and development

The lifespan of the fireball (i.e. following ignition) is characterised in terms of 3 main time periods:

- Flame growth: this covers the period from ignition to the time the fireball attains its maximum radius (t_{MXR})
- Flame rise: this spans the period the flame commences lifting off (at time t_{lo}) till the time the flame attains its maximum visible height (t_{MXH})
- Flame decay: this spans the time the flame begins to break-up ($t_{break\text{-}up}$) till it burns out (t_{Flame}). Both t_{MXH} and $t_{break\text{-}up}$ are assumed to coincide.

The total flame duration (t_{Flame}) is determined as an empirical function of the mass of fuel released (M_{input}, kg),

$$t_{\text{Flame}} = \begin{cases} 7.4(M_{input}/1000)^{0.333} & M_{input} < 2000\,kg \\ 8.2(M_{input}/1000)^{0.167} & M_{input} \geq 2000\ kg \end{cases} \quad \textbf{(13)}$$

The times to the different fireball stages (t_{MXR}, t_{MXH}, t_{lo} and $t_{breakup}$) are given in Table 1 as a fraction of total flame duration t_{Flame}.

Parameter	Time (as a fraction of t_{Flame})
Time to flame lift-off [t_{lo} / t_{Flame}]	0.3
Time to flame maximum radius [t_{MXR} / t_{Flame}]	0.4
Time to flame maximum visible height [t_{MXH} / t_{Flame}]	0.75
Time to start of fireball breakup [$t_{breakup}$ / t_{Flame}]	0.75
Total flame duration [t_{Flame} / t_{Flame}]	1

Table 1 Fireball parameters as a fraction of total flame duration (Pritchard, 1985)

Flame radius and height

Pritchard (1985) modelled the variation of fireball radius ($r_f(t)$) and the distance between ground and fireball base ($H_B(t)$) as polynomial functions of time (t) for each time period. The polynomial expressions were empirically derived and the variations of $r_f(t)$ and $H_B(t)$ with time were presented in dimensionless form.

For the fireball growth period, $H_B(t) = 0$ for $t \leqslant t_{lo}$, while $r_f(t)$ is given by ($0 \leq t \leqslant t_{MXR}$)

$$\frac{r_f(t)}{r_{Flame}} = 0.02122 + 2.946\frac{t}{t_{MXR}} - 3.339\left(\frac{t}{t_{MXR}}\right)^2 + 1.381\left(\frac{t}{t_{MXR}}\right)^3 \quad \textbf{(14)}$$

where r_{Flame} is the maximum fireball radius predicted from the HSE correlation [see equation (2)].
During the fireball rise period, $r_f(t) = r_{Flame}$ for $t_{MXR} \leqslant t \leqslant t_{MXH}$, while $H_B(t)$ is given by[vi]:

$$\frac{H_B(t)}{H_{MAXB}} = 0.01195 + 0.1802\left(\frac{t - t_{lo}}{t_{MXH} - t_{lo}}\right) + 0.7962\left(\frac{t - t_{lo}}{t_{MXH} - t_{lo}}\right)^2 \quad \textbf{(15)}$$

Where:

H_{MAXB} Maximum visible height of fireball base above ground [m]; H_{MAXB} is derived from the maximum visible height of the fireball centre, H_{Flame} (lift-off height). H_{Flame} is given by equation (16) from which H_{MAXB} is derived, assuming a spherical flame, from equation (17).

$$H_{Flame} = 3r_{Flame} \quad \textbf{(16)}$$

$$H_{MAXB} = 2r_{Flame} \quad \textbf{(17)}$$

For the fireball decay period, the fireball centre remains at H_{Flame}, while the fireball starts to fragment and breakup with its radius $r_f(t)$ given by[vii]:

$$\frac{r_f(t)}{r_{Flame}} = 0.9975 + 0.6313\left(\frac{t - t_{breakup}}{t_{Flame} - t_{breakup}}\right) - 1.035\left(\frac{t - t_{breakup}}{t_{Flame} - t_{breakup}}\right)^2 \quad \textbf{(18)}$$

Flame surface emissive power

Pritchard (1985) assumes the fireball SEP increases from ignition to its maximum value ($E_{f,\max}$) at the commencement of lift-off (t_{lo}). Thereafter, the flame SEP is assumed to remain constant at its maximum value

[vi] At time $t=t_{lo}$, one would expect $H_B(t)=0$ to avoid a discontinuity
[vii] Equation (18) suggests that the fireball seizes to be an effective radiation emitter (i.e. flame burn out will occur) at an effective radius ≈ 0.594 r_{Flame}

until it burns out. The maximum flame SEP is calculated in terms of the initial vapour pressure, $P_{vap,init}$, and is given by:

$$E_{f,\max} = 235 P_{vap,init}^{0.39} \quad \textbf{(19)}$$

Where:

$E_{f,\max}$	Maximum fireball SEP [kW/m^2]
$P_{vap,init}$	Initial vapor pressure at the point of vessel failure [MPa];

Equation (19) is valid for $0.5 \leqslant P_{vap,init} \leqslant 2$MPa. Where the initial / failure vapour pressure is not known, Pritchard (1985) suggests that the flame SEP should be between 180 and 308kW/m^2 and would depend on the amount of fuel consumed. For releases involving 1 tonne or more of fuel, Pritchard (1985b)[20] recommends capping the flame SEP at 308kW/m^2, while for small fuel releases (ca. 10kg) a cap of 180kW/m^2 is recommended.

Similar to the flame radius and base height, Pritchard (1985) modelled the variation of the flame's surface emissive power ($E_f(t)$) as a function of time (t) using empirically derived polynomial equations. The variation of $E_f(t)$ [kW/m^2] with time for the period spanning ignition to flame lift-off was presented in dimensionless form and is given by:

$$\frac{E_f(t)}{E_{f,\max}} = 0.136 + 3.638\left(\frac{t}{t_{lo}}\right) - 5.425\left(\frac{t}{t_{lo}}\right)^2 + 2.691\left(\frac{t}{t_{lo}}\right)^3 \quad \textbf{(20)}$$

Validation

Pritchard (1985) presented the results of the validation of the BG fireball model against field data recorded during vessel / pipeline fracture tests conducted at BG's Midland Research Station (MRS) facility. The fracture tests involved the release of 27 tonnes of natural gas. Details of the prevailing atmospheric or vessel failure conditions at the time of the test were not provided.

The results from the comparison of predicted results using the BG fireball model against field data for the fracture test are summarized in Table 2. Pritchard (1985) also presented the predicted radiation intensity versus time profile as compared to measured data for an observer (radiometer) located 362m away from the ruptured containment and tilted 22° from the vertical (see Figure 4).

The results of the validation exercise show the Prichard (1985) model to over-predict the measured fireball duration data by ca 30% and under-predict the maximum flame radius by ca 24%. Good agreement between predicted and measured incident radiation fluxes (dose and peak intensities) at various observer positions is observed, with the BG fireball model under-predicting measured data by 14% on average.

Fireball parameter	Measured Data	Predicted Data (Pritchard, 1985)
Fireball mass (tonnes)	27	N/A
Fireball duration (s)	11	14.2
Maximum flame radius (m)	115	87
Maximum SEP (kW/m^2)	308	308[viii]

Radiation Effects					
Observer standoff distance (m)	**Observer tilt from vertical (°)**	**Total Heat Received (kJ/m^2)**		**Maximum incident flux (kW/m^2)**	
		Measured	**Predicted**	**Measured**	**Predicted**
262	32	139	124	22	19.2
312	26	123	94	20	14.0
362	22	80	73	12	10.8
372	19	64	69	11	10.1

Table 2 Validation of Pritchard (1985) model: predicted versus measured data

[viii] Maximum SEP taken from measured data

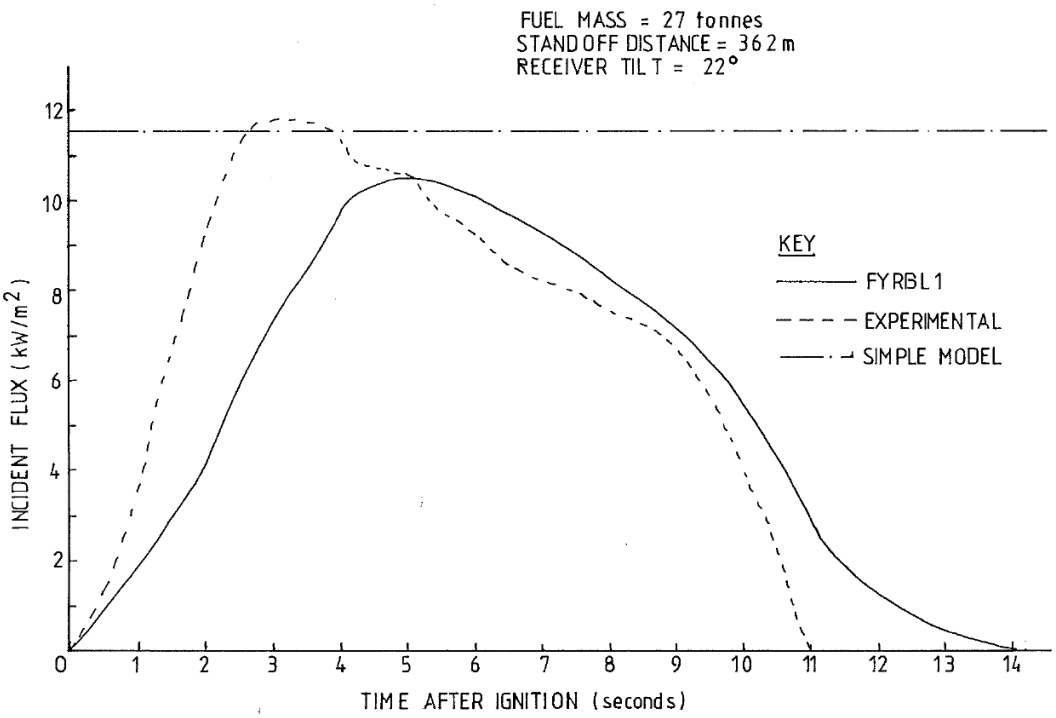

Figure 4. **Validation of Pritchard (1985) model: incident radiation intensity versus time**
The plot depicts the variation of measured and predicted (see legend: FRYBL1) radiation intensity with time at an observer location 362m away from a 27 tonne natural gas fireball.

3.1.2 Shell model (Shepherd – Shield, 1993 & 1995)

Shield (1993, 1995)[13, 15] described a semi-empirical dynamic model for simulating the growth, decay and radiation characteristics of a fireball[ix]. Fireball characteristics were described in terms of fireball:

- Shape;
- Diameter;
- Lifetime;
- Rise velocity;
- Thermal radiation characteristics;

3.1.2.1 **Shield (1993)**

The Shield (1993) fireball model was derived from an analysis of field data reported by Johnson et al. (1991)[24] relating to 6 large-scale (up to 2 tonne) LPG BLEVE experiments. The BLEVE process is modelled as developing in 5 stages, summarised below:

1. Stage 1: vessel fails, ejecting any missiles as the walls collapse and generating an initial pressure pulse whose source is the energy in the vapour in the vessel just before failure.
2. Stage 2: the bursting vessel ejects a cloud of liquid droplets which flash adiabatically as the pressure in the cloud drops. There is little mixing with the surrounding air and if the expansion velocity exceeds the speed of sound in the rarefaction wave following the initial pressure pulse, a flashing liquid blast wave is generated.
3. Stage 3: the cloud continues to grow, and air is entrained due to the turbulence.
4. Stage 4: ignition takes place and the ignited cloud grows to a fireball as the flashed vapour is consumed.
5. Stage 5: combustion continues, fuelled by evaporation of the remaining droplets, and the fireball rises into the air before extinction.

The Shield (1993) fireball model also makes the following key assumptions:

- No energy dissipation (isenthalpic expansion) as the turbulence is produced.
- There is no mechanism that causes liquid to rain out of the cloud rather than flash off.
- Except in the conditions mentioned above (i.e. flash off[x]), all the liquid is completely burnt in the fireball.
- The fireball radiates as a perfect black body.

Fireball Shape

Shield (1993) describes the fireball at its inception in terms of an expanding hemispherical shape attached to grade. The hemispherical shaped flame grows to its maximum size at constant velocity as the last visible part of the vapour cloud is consumed by the flame (fireball stages 1 – 4). Subsequently, the fireball rises (stage 5) at approximately constant velocity and volume to become a sphere sitting on the ground and thereafter assumes a typical mushroom shape on lift-off. Afterwards, the visible flame area decreases, becomes patched with sooty combustion products and upon complete combustion, the smoky toroid of combustion products rises, expands and dissipates away. The development of the fireball, as described above, is illustrated in Figure 5.

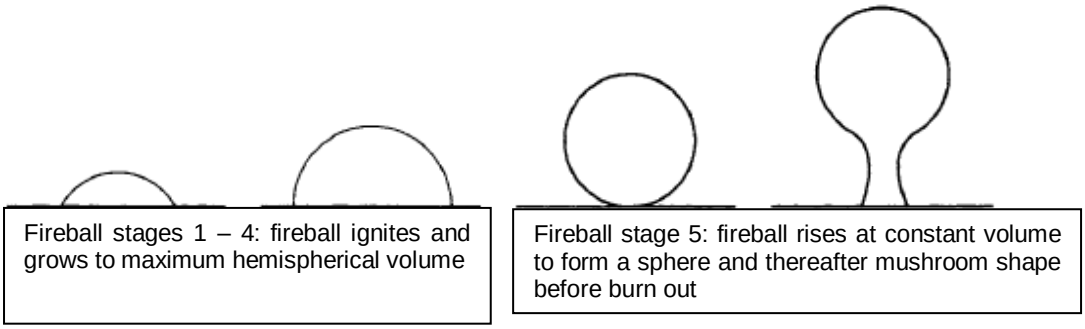

Figure 5. Stages in the development of a fireball Shield (1993)

Fireball diameter

[ix] The Shield (1993, 1995) model appears to be suitable for modelling BLEVES only (i.e. two-phase containment) as its governing equations breakdown for potential fireballs generated from pure vapour releases.

[x] Shield (1993) suggests that if the initial saturation pressure is lower than 6 – 7 bara, then insufficient air is mixed into the expanding cloud for complete combustion of the fuel. In which case, the fireballs will have a relatively low SEP, but the lifetime will be curtailed (in essence, a proportion of liquid droplets will only flash-off and not be burnt, with the flashing effect producing a cooling effect)

The fireball growth is described in terms of a 'peak' hemispherical diameter given by equation (21). From ignition to peak diameter, the flame radius and surface emissive power are assumed to increase linearly (i.e. at a constant velocity) with time (Shield, 1995). Thereafter, the fireball volume at the 'peak' hemispherical diameter is assumed to remain constant throughout the remainder of its lifetime. The flame is assumed to gradually rise at constant volume and velocity to form a grounded sphere which later develops into a mushroom-shaped flame (represented by a sphere with a cylindrical base connected to the ground).

$$V_f = \frac{\pi}{12} D_f^3 = G_1 N^3 L^3 f_1 (T_c / T_0) \quad \textbf{(21)}$$

Where:

V_f	Is the fireball volume after expansion [m^3];
D_f	The 'peak' hemispherical flame diameter [m];
G_1	Is given by 4π/3
N	The total number of eddies in the expanded cloud radius; N is given by equation (22)
L	The turbulent length-scale of eddies generated by the expanding cloud [m]; L is given by equation (23)
f_1	A fuel dependent factor, close to unity, which reflects the volumetric change which occurs in combustion due to the increased volume of the combustion products at constant temperature[xi];
T_c	The average temperature of the fireball when expanded to its maximum size [K]; T_c is given by equation (24) and is derived from an energy balance for the complete combustion of the flashed-off vapor fraction[xii]. Shield (1993) assumes that as the fireball expands, only the flashed-off vapor fraction is consumed by the flame front.
T_0	The saturation temperature [K] of the fluid at ambient pressure P_0

$$N = \left[\left(P_0 / \left(G_1 \rho_a u_L^2 \right) \right) - \left(\rho_{v0} / \left(G_1 \alpha \beta \rho_a \right) \right) + \left(1 / G_1 \right) + \left(1 - \beta \right) \left(\rho_{v0} / \left(G_1 \beta \rho_{l0} \right) \right) \right]^{1/3} \quad \textbf{(22)}$$

$$L = \left[\alpha \beta M / \rho_{v0} \right]^{1/3} \quad \textbf{(23)}$$

$$T_c = T + h_c / \left(c_{pv} + c_{pa} \left(P_0 / \left(\rho_{v0} u_L^2 \right) - 1 / \alpha \beta \right) \right) \quad \textbf{(24)}$$

Where:

M	Fluid mass / total fuel inventory prior to catastrophic vessel failure [kg];
P_0	Ambient pressure [N/m^2];
ρ_a	Density of air at ambient conditions [kg/m^3];
u_L	The turbulent velocity associated with eddies with characteristic size L: u_L has been derived empirically and is given by equation (25)
ρ_{v0}	The saturated fuel vapor density at ambient pressure [kg/m^3];
α	The initial liquid mass fraction (before vessel rupture)
β	The mass fraction of vapor flashed from the liquid assuming an isenthalpic thermodynamic trajectory
ρ_{l0}	The saturated fuel liquid density at ambient pressure [kg/m^3];
T	The air + fuel post mixing temperature: T is given by equation (26) and is derived from an energy balance assuming complete mixing of entrained air and flashed-off vapor from the expanding liquid inventory.
h_c	The gross calorific value / heat of combustion of the fuel vapor [J/kg]
c_{pv}	Specific heat at constant pressure of fuel vapor [J/kg/K][xiii]
c_{pa}	Specific heat at constant pressure of air [J/kg/K]

$$u_L = 39.85 \left(\rho_a^2 / \left(\rho_{vT} \rho_{v0} \right) \right)^{1/9} (\alpha\beta)^{1/9} \quad \textbf{(25)}$$

[xi] CLARIFY: Shield (1993/1995) does not provide any value for f_1. It is assumed that this parameter can be determined from the equation of complete combustion of the fuel: the ratio of the total number of moles of combustion products (including Nitrogen) and total number of moles of reactants (fuel + air).

[xii] JUSTIFY: the energy balance does not include any heat loss terms to the (evaporating) liquid droplets within the burning cloud

[xiii] CLARIFY: It appears the specific heats at constant pressure employed in the Shield (1993/1995) model does not account for temperature dependence or perhaps the author assumes average values over the temperature range of interest (although the latter is not explicitly stated)

$$T = \frac{\left(M_a c_{pa} T_a + \alpha\beta M c_{pv} T_0\right)}{\left(M_a c_{pa} + \alpha\beta M c_{pv}\right)} \quad (26)$$

Where:

ρ_{vT}	The fuel vapor density at ambient temperature and pressure [kg/m^3];
M_a	Is the mass of air entrained into the cloud [kg]; M_a is given by equation (27) and is derived from an energy balance where the energy available to do work against the atmosphere (i.e. due to the flashing liquid) is equated to the turbulent kinetic energy of the vapor + air cloud mixture[xiv].
T_a	Ambient temperature [K];

$$M_a = L^3\left\{\left(P_0/u_L^2\right) - \left(\rho_{v0}/(\alpha\beta)\right)\right\} \quad (27)$$

Fireball lifetime

Shield (1993) broadly divides the duration of the fireball into two phases: the expansion phase duration (t_{exp}), where the fireball grows to its maximum hemispherical size, and the period following the expansion phase (t_s) where the fireball is assumed to remain at a constant volume for the remainder of its lifetime. Hence, the total duration of the fireball (t_{Flame}) is given by:

$$t_{\text{Flame}} = t_{\text{exp}} + t_s \quad (28)$$

Where:

t_{exp}	The duration of the fireball flame expansion phase [s]; t_{exp} is given by equation (29) by assuming the fireball grows at a constant (root mean square: r.m.s) expansion velocity.
t_s	The duration of the post-expansion (constant volume) phase of the fireball [s]; t_s is given by equation (30) and is approximated from a heat balance, assuming the complete combustion of the non-flashed-off fuel liquid droplets. The liquid droplets are assumed to be heated to T_c and evaporated, whilst most of the heat produced remains in the combustion products and excess air at T_c.[xv]

$$t_{\text{exp}} = r_f / u' \quad (29)$$

$$t_s = \frac{\alpha(1-\beta)M\left(h_c - \lambda - \left(c_{pl}\left(T_c - T_0\right)\right)\right)}{\pi D_f^2 \sigma T_c^4} \quad (30)$$

Where:

r_f	The 'peak' hemispherical flame radius [m]; $r_f = D_f / 2$ (see equation (21))
u'	The r.m.s turbulent velocity [m/s]; u' is given by equation (31) assuming isotropic turbulence.
λ	Fuel heat of vaporization [J/kg]
σ	Stefan-Boltzmann's constant

$$u' = u_L\sqrt{2/3} \quad (31)$$

Fireball rise velocity

The Shield (1993) model assumes the fireball lifts-off after the expansion phase at a constant rise velocity (u_{rise}) given by:

$$u_{rise} = u'/2 \quad (32)$$

The fireball continues to rise until its radiation pulse effectively dies out. Shield (1993) suggests that the time to cessation of any significant radiation pulse from the fireball (t_{rad}) can be estimated from equation (33), noting that t_{rad} is always less than t_{Flame}.

$$t_{rad} = 3t_{\text{exp}} \quad (33)$$

Thermal radiation characteristics

Shield (1993) observed that the radiation "pulse" at the receiver can be considered in three parts. First, as the hemispherical fireball grows, the observer view factor increases since the fireball radius and SEP are increasing

[xiv] i.e., vapour + air cloud mixture formed after fluid post-expansion but before significant dissipation to ambient has occurred

[xv] Again, equation (30) assumes the fluid properties (i.e. c_{pl}) to be temperature independent. Furthermore, Shield (1993) noted that the application of equation (30) must take cognizance of the amount of air entrained (M_a) and consumed during the combustion of the fuel (vapour and liquid) (see equation (27)). From equations (23) and (27), low values of β (i.e. lower superheat) will result in lower masses of air entrained in the fuel, which may result in incomplete combustion of the liquid droplets.

linearly to a maximum. This increase in received heat flux terminates at the end of the flame expansion phase, t_{exp}, given by equation (29).

The second part, which also is taken to last for approximately t_{exp}, the fireball becomes spherical while still attached to the ground. The flame SEP remains at around 90% of the peak value and may be estimated from equation (34) assuming that the fireball is a perfect black body.

In the third part, the flame SEP drops rapidly to zero due to the cooling effects as a result of evaporating of liquid fuel and soot obscuration. Shield (1993) suggests that the heat pulse contribution from the third part ("tail") of the fireball radiation process is little when compared against earlier stages and does not warrant specific consideration.

$$E_{f,90\%} = \sigma T_c^4 \qquad \textbf{(34)}$$

3.1.2.2 Shield (1995)

Shield (1995) further extended his original model by determining the fireball lifetime in terms of the lifespan (evaporation through to combustion) of a representative droplet generated following the loss of containment event. The revised model also allows for droplet rainout to occur should evaporating droplets hit the ground before evaporation is complete. Rained out droplets are assumed to ignite to form a pool extending over the maximum (spherical) fireball diameter. The model characterises the lifespan of the fireball (i.e. following ignition) in terms of 3 distinct time phases:

- Flame expansion phase: corresponds to the duration covering ignition and growth of the flame to maximum fireball size (t_{exp}, see equation (29))
- Flame rise to onset of break-up ($t_{breakup}$): this spans the period the flame starts rising from the 'peak' hemispherical shape till flame break-up, i.e., t_{exp} to $t_{breakup}$
- Flame decay: this spans the flame break-up time to its burn out time (t_{Flame}), i.e., $t_{breakup}$ to t_{Flame}. The flame ceases to be an effective emitter beyond t_{Flame}.

The key elements of the extended fireball model are summarised below where:

- For the flame expansion phase (i.e. ignition to peak diameter), the fireball parameters are as determined by the Shield (1993) model with the flame radius and surface emissive power increasing linearly with time.
- During the rise period, the flame is assumed to rise at a constant velocity (and volume) as given by equation (32). The flame shape starts off as a hemisphere and later rises to form a sphere, but unlike the 'mushroom' flame shape assumption in Shield (1993), the flame is assumed to remain spherical until extinction.
- The average temperature of the fireball at break-up, T_{end}, is found by an energy balance which assumes complete combustion of as much fuel as can be burned by the air contained within the fireball. Based on experimental data, Shield (1995) suggests that the break-up temperature should never fall below 0.88 of the fireball peak temperature, T_{peak}. Details of the energy balance to be employed in deriving T_{end} and T_{peak} were not provided.[xvi]
- The time to fireball break-up ($t_{breakup}$) is calculated from the lifetime of a characteristic droplet of diameter D_{drop}, using standard equations for droplet evaporation assuming constant temperature of the droplet surroundings (T_{end}). D_{drop} is derived empirically and given by equation (35), while specific details on the standard equations for droplet evaporation employed are not stated[xvii].

$$D_{drop} = 2.805\alpha^{2/15}\beta^{1/6}\left(\frac{\vartheta}{\rho_{v0}}\right)^{0.6}\left(\beta N^3 \varepsilon\right)^{-0.4} \qquad \textbf{(35)}$$

Where:

ϑ Fluid surface tension [kg/s^2];

[xvi] CLARIFY: It is assumed that T_{peak} may be derived from T_c and the maximum SEP, see equations (24) and (34) assuming that T_{peak} corresponds to the flame temperature at the peak SEP (i.e. $E_{f,peak} = E_{f,90\%} / 0.9$); while T_{end} may be derived from a similar energy balance as in equation (24) but assuming the complete consumption of the fuel (αM) or oxygen in the entrained air ($0.21 \times M_a$, see equation (27)), whichever is lesser in quantity.

[xvii] CLARIFY: It is not clear what is meant by "standard equations for droplet evaporation", in particular, the modelled heat source terms and sinks in the droplet evaporation equation (energy balance).

ε Energy dissipation rate per unit mass [m^2/s^3]; Shield (1995) does not provide an expression for estimating ε.[xviii]

- For the purposes of flame SEP calculation, the fireball temperature (from which the flame SEP is calculated, see equation (34)) is modelled as decreasing linearly with time from T_{peak} to T_{end} (i.e. over time period t_{exp} to $t_{breakup}$), and thereafter is assumed to be fixed at T_{end}.
- The total duration of the fireball (t_{Flame}) is effectively calculated from equation (36). Shield (1995) assumes that droplets which ignited immediately burn out at onset of flame break-up ($t_{breakup}$), while break-up is complete (i.e. flame extinction) when droplets which were not ignited until the end of stage 4, i.e., the termination of the fireball expansion phase (t_{exp}), had themselves burnt out. Given that the temperature of the surroundings under which fuel droplets are assumed to evaporate is fixed (i.e., T_{end}), hence, the droplet evaporation duration[xix] may be assumed to be constant and to correspond to $t_{breakup}$. As such, the fireball duration may be estimated as the sum of t_{exp} and $t_{breakup}$ (i.e. equation (36)).

$$t_{\text{Flame}} = t_{\text{exp}} + t_{breakup} \quad \textbf{(36)}$$

- During the break-up phase the radius of the fireball is assumed to decrease linearly with time but with the flame temperature (hence SEP) remaining constant at T_{end}.

3.1.2.3 Validation, Shield (1993 / 1995)

The Shield (1993 / 1995) models have been validated against the following sets of experimental / field data:

- Hasegawa and Sato (1977)[16]
  The Hasegawa and Sato [HS] tests comprise of small scale tests involving fireballs created following the rupture of glass vessels and metal containers partly filled with superheated propane, n-pentane and n-octane. The experimental data assessed in the validation exercise include, maximum fireball diameter, SEP and flame duration.

- Maurer, Hess, Giesbrecht and Leuckel [MGL] (1977)[22]
  The MGL experiments relate to fireballs created following the rupture of model rail car tanks filled with liquid propylene and heated to internal pressures between 22 and 39bar. Maximum fireball diameter data were recorded during the MGL tests.

- Schultz-Forberg, Droste and Charlett [SDC] (1984)[23]
  The SDC tests involved BLEVEs of commercial propane tanks due to fire engulfment. Maximum fireball diameter and flame duration data were recorded during the SDC tests.

- Johnson et al. [JP] (1991)[24]
  The JP tests involved seven large scale (up to 2 tonne) BLEVEs of LPG vessels. Six of the experiments involved the release of commercial grade butane at different initial pressures and tank fill. Four of butane releases were ignited to form fireballs. A single ignited (2 tonne) propane experiment was also conducted to complete the set. Maximum fireball diameter, SEP, flame duration, peak incident heat flux and radiation dose at various observer locations were recorded during the JP tests.

Figure 6 shows the reported results of the validation of the Shield (1993) fireball model against experimental data for maximum flame diameter, flame SEP, flame duration and radiation flux (peak incident heat flux / intensity and radiation dose) respectively. From Figure 6, it can be observed that the Shield (1993) model shows good agreement with measured fireball and radiation data. The JP flame durations are generally under-predicted, hence the need for further improvement of the Shield (1993) model as discussed by Shield (1995).

Shield (1995) presented the results of the validation of the updated fireball model [improved Shield (1993) model] against experimental data for time to fireball break-up. The predicted data from the Shield (1995) model was observed to show better agreement with observed fireball duration data when compared against results from its earlier version (Shield, 1993).

Shield (1995) also presented the predicted radiation intensity versus time profile as compared to measured data for an observer (radiometer) located 175m west of the JP 2tonne butane BLEVE from an initial pressure

[xviii] CLARIFY: Shield (1995) suggests that the energy dissipation rate per unit mass ε is "a product of the existing turbulence model". It is assumed that "the existing turbulence model" makes reference to the model discussed in Shield (1993). There is no mention of

[xix] i.e., based on the characteristic droplet size (assuming evaporation at constant temperature, T_{end})

of 7.7barg. The simulated data from the Shield (1995) model was observed to show very good agreement with logged data at the specified observer location.

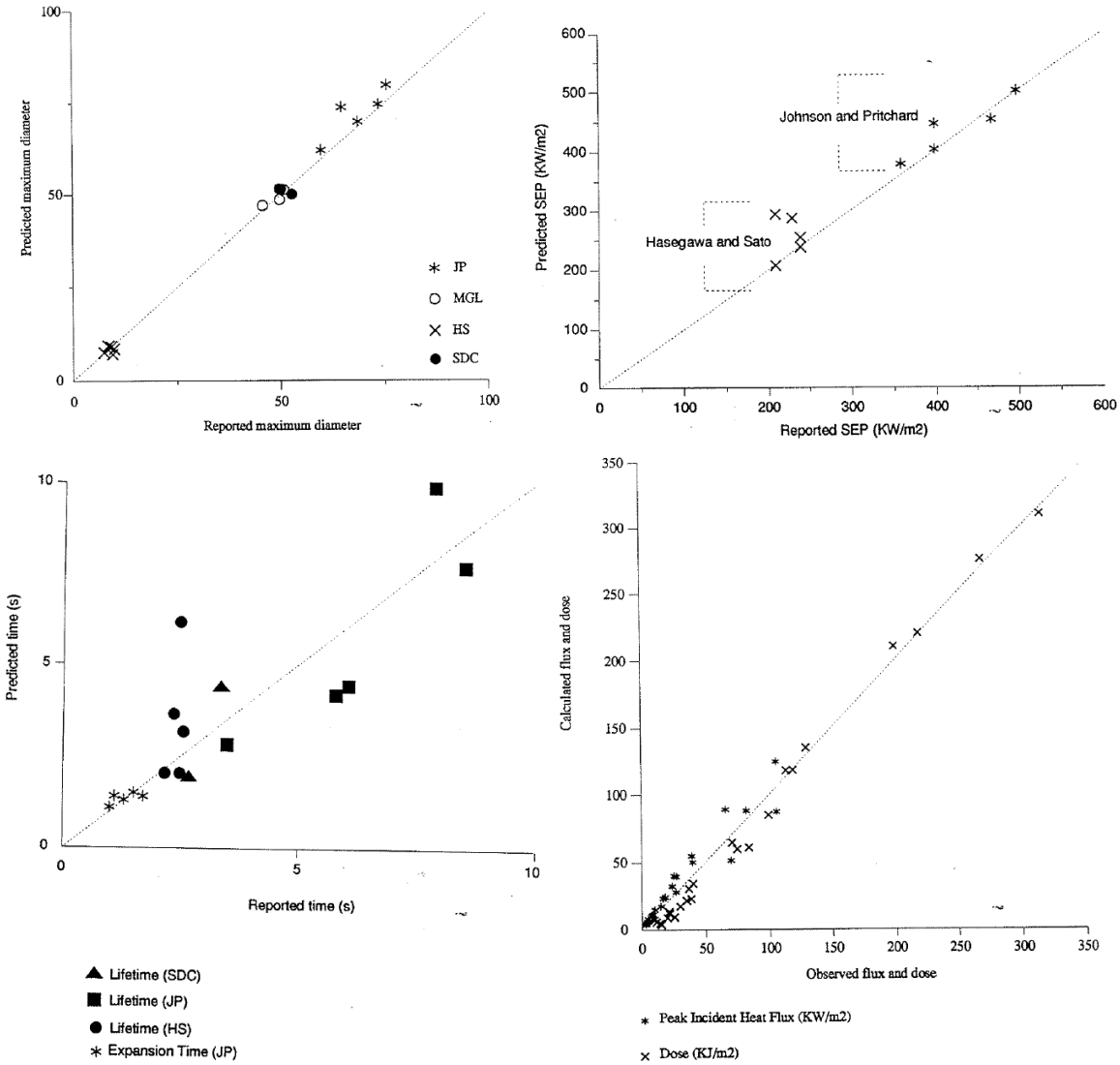

Figure 6. **Validation of the Shield (1993) model: fireball characteristics and radiation flux**
The plot depicts predicted versus measured data for various fireball characteristics: maximum diameter, flame SEP, flame duration and radiation flux (peak incident heat flux and radiation dose), respectively.

3.1.3 Quest model (CANARY - Martinsen and Marx)

Martinsen & Marx (1999)[1] described an integrated model for predicting the flame characteristics and attendant radiant heat effects from fireballs created by near-instantaneous releases of superheated flammable liquids. The authors proposed a suite of equations that were judged to provide a more realistic representation of the true behaviour of fireballs. The proposed equations account for fireball growth, lift-off and changing radiative characteristics. Fireball characteristics were described in terms of:

- Fireball shape
- Mass of fuel involved
- Fireball duration
- Fireball diameter and location:
- Flame surface emissive power:

Fireball Shape

Martinsen and Marx (1999) assume the fireball to be spherical in shape throughout its lifetime.

Mass of fuel involved

The mass of fuel involved in the fireball is based on the CCPS (1994)[7] correlation as expressed mathematically by equation (1).

Fireball duration

Martinsen and Marx (1999) estimates the fireball duration using a slight variation of the TNO equation (see equation (5)). The authors propose the following relationship for the flame duration:

$$t_{\text{Flame}} = 0.9 M_{\text{Flammable}}^{0.25} \qquad (37)$$

The authors observe that the predicted durations from equation (37) is nearly identical to that of the TNO correlation until the flammable mass exceeds 10,000 kg and slightly shorter than the durations predicted by the TNO correlation when the flammable mass exceeds 10,000 kg. When compared against the predicted durations from the HSE flame duration correlations (see equation (4)), the authors observe that equation (37) predicts slightly longer durations for masses less than 5,000 kg or more than 300,000 kg, and predicts lower durations otherwise.

Fireball diameter and location

At inception, the fireball is assumed to increase in diameter with time, remaining tangent to grade as it grows. Martinsen and Marx (1999) propose the following expression for the fireball radius as a function of elapsed time (t), $r_{flame}(t)$, during its growth phase:

$$r_{flame}(t) = 4.332\, M_{Flammable}^{1/4} t^{1/3}; \qquad t \le t_{lo} \qquad (38)$$

Where:

t	Is the elapsed time from ignition [s];
t_{lo}	Flame lift-off time given by equation (40);

On reaching its maximum diameter, the fireball is assumed to rise into the air at a constant velocity and diameter until the flame burns out. The maximum flame radius is predicted based on the HSE correlation (see equation (2)), while the flame is assumed to burn out when its centre is at a height corresponding to three times its maximum radius, i.e.:

$$H_{\text{Flame}} = 3 r_{\text{Flame}} \qquad \textbf{(39)}$$

Similar to the assumptions adopted in Shield (1993), the fireball is assumed to reach its maximum diameter and commence lifting off at the end of the first third of its duration. Hence the flame lift-off time (t_{lo}), which also corresponds to the time to reach flame maximum diameter (i.e. termination of the growth phase) is given by:

$$t_{\text{lo}} = t_{\text{Flame}} / 3 \qquad \textbf{(40)}$$

Subsequently, the fireball is assumed to move upward at a constant rate from its pre-lift-off position (i.e. $H_{lo} = r_{Flame}$) to H_{Flame} over a duration corresponding to two-thirds of the fireball's existence.

Flame emissive power

Martinsen and Marx (1999) assume the flame SEP starts off and remains at a constant, time-averaged, value until the fireball reaches its maximum diameter. Thereafter, the flame SEP is assumed to linearly decrease from its maximum value to zero over the last two-thirds of the fireball duration. The adopted time-averaged flame SEP is derived based on a slight variation of the Roberts' correlation [see equations (8) and (9))]. Equation (9) from Roberts correlation for the radiative heat fraction f_s has been applied without changes. Equation (8) has been replaced by the following equation for the time-averaged SEP [imposing an upper limit of 400kW/m^2]:

$$E_f = Min\left(\frac{f_s M_{\text{Flammable}} \Delta H_C}{0.8888 \times 4\pi r_{\text{Flame}}^2 t_{\text{Flame}}},\ 400000 \right) \quad \textbf{(41)}$$

Where

$0.8888 \times 4\pi r_{\text{Flame}}^2$ = Time-averaged surface area of the fireball [m^2][xx]

Substituting r_{Flame} and t_{Flame} in Equation (41) with Equation **(38)** [at lift-off time given by Equation (40)] and equation (37) respectively, equation (41) can be re-written as[xxi]

$$E_f = Min\left(0.0118 f_s M_{Flammable}^{1/12} \Delta H_C,\ 400000\right) \quad \textbf{(42)}$$

Validation

Martinsen and Marx (1999) present the validation of the Quest fireball model against field data recorded by Johnson et al. (1991)[24] for BLEVEs of LPG vessels (see Section 3.1.2.3 for further details).

Figure 7 shows an outcome of the validation exercise comparing the measured and predicted ("Dynamic Model") variation in radiation intensity at an observer location 50m away from the release point for a 2tonne butane BLEVE from an initial pressure of 15.1barg (Test 1). The observer is tilted so as to receive approximately the maximum radiation from the fireball. From Figure 7 it can be seen that the predicted results using the Quest dynamic fireball model follows the general shape of logged data, but slightly over-predicts the maximum incident heat flux whilst showing a slight offset in time.

Martinsen and Marx (1999) also presented results comparing predicted radiation dose at various observer locations against logged data from the Johnson et al. (1991) BLEVE tests (Tests 2 – 5) (see Figure 8). From Figure 8, good agreement is observed between predicted and measured doses at pertinent observer locations. The authors point out that the data presented in Figure 8 only covers measured doses below 350kJ/m^2 (thirty-one data points).

[xx] The authors provide no expression for deriving the time averaged area. However, from an analysis of the underlying equations, it appears the time averaged area corresponds to $(\int A_{Flame} t\ d(A_{Flame} t)) / (4\pi(\int r_{flame}(t)\ dt)^2$; where $A_{Flame} = 4\pi$. However, a more logical definition of time-averaged area is $\int A_{flame} dt / t_{Lo} = 0.6\ A_{fl}^{max}$ with time-averaging over time t_{Lo} prior to lift-off.

[xxi] This Equation differs from equation quoted in Martinsen & Marx (1999), who mention a constant of 0.0133 instead of 0.0118. They derived their equation by substituting rFlame and tFlame in equation (41) with equation (2) and equation (37) respectively.

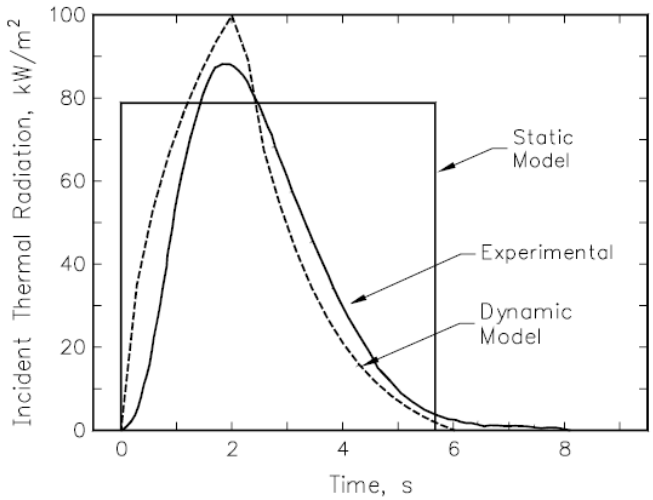

Figure 7. **Validation of Martinsen and Marx model (Test 1, Johnson et al.) – radiation intensity versus time**
The plot depicts the variation of radiation intensity with time at an observer location 50m west of a 2 tonne butane BLEVE from an initial pressure of 15.1barg.

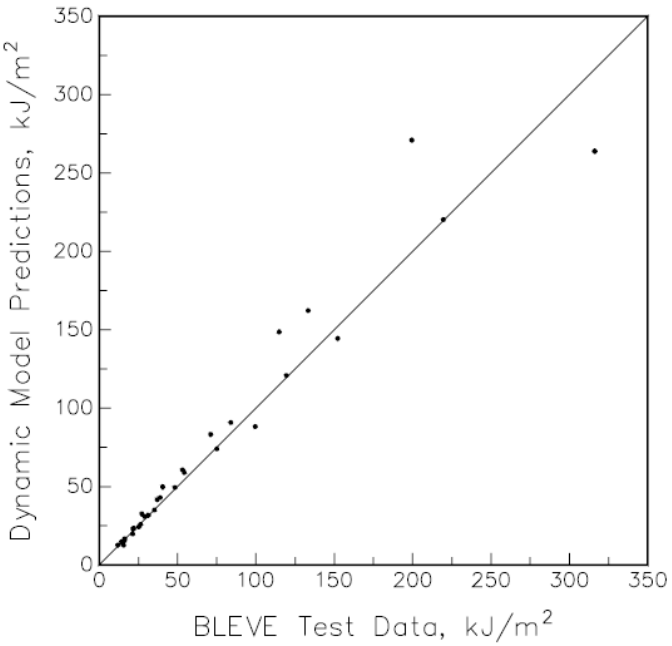

Figure 8. **Validation of Martinsen and Marx model (Tests 2-5, Johnson et al.) – radiation dose**
The plot depicts predicted versus measured radiation dose for large scale propane and butane BLEVEs.

3.1.4 Comparative analysis of key model characteristics

Table 3 presents a comparison of the key characteristics of the BG (Pritchard, 1985), Shell (Shield, 1993 and 1995) and the Quest (Martinsen and Marx, 1999) time-varying fireball models.

From Table 3, it can be observed that:

- Fireball shape
  The BG and Quest models assume a spherical flame over the duration of the fireball, while the Shell model assumes the flame to start-off as a grounded hemisphere. The Shield (1993, 1995) appears to be particularly suited for fireballs stemming from grounded (or close-to-ground) catastrophic vessel failures; the fireball shape for above ground / elevated vessel failures is unlikely to start off as a grounded hemisphere.

- Mass of fuel involved
  The BG model conservatively assumes the entire contents of the ruptured containment to contribute to the developing fireball, while both the Shell and Quest models allow for potential droplet rainout. It should be noted that the Shell model appears to be only suitable for modelling fireballs stemming from BLEVEs and may not support the modelling of fireballs arising from the rupture of pressurized gas/vapour vessels.

- Fireball duration
  Figure 9 shows a comparison of the predicted maximum fireball durations using the BG, Quest, TNO and HSE models as a function of total fireball mass. It is not possible to provide a direct comparison of the aforementioned models with the Shell model as the durations predicted by the Shell model varies with other case specific data (e.g. amount of superheat, droplet size, air entrained, evaporation / combustion rate). A close look at Figure 9 shows that:
    - Durations predicted by the Quest model as compared to TNO model are nearly identical. Below 10kg, the Quest model predicts marginally longer fireball durations than the TNO and BG models.
    - The BG correlation predicts the longest flame durations for fireball fuel masses between ca. 10kg and 300,000kg noting that above, 37,000kg, the HSE and BG flame duration models are the same. The TNO model predicts the longest flame durations above 300,000kg closely followed by the Quest model.
    - Below 5,000kg, the HSE and above 300,000kg, the BG/HSE models predict the shortest flame durations.

- Fireball diameter
  Both the BG and Quest models employ similar correlations for the maximum fireball radius r_{flame}. All three models assume the fireball radius to increase with time until flame lift-off. The BG and Quest models assume the fireball radius to remain constant after lift-off until the onset of flame break-up. During flame break-up, the Quest model assumes the flame radius to remain constant (with SEP assumed to decrease linearly with time, i.e. post flame lift-off), while the BG model assumes the flame radius to decrease with time (with SEP constant) until flame extinction. The Shell model assumes the fireball to maintain a constant volume between flame lift-off and breakup, followed by a linear decrease in fireball radius until flame extinction.

- Fireball height
  Both the BG and Quest models employ similar correlations for the maximum fireball height and assume the fireball height to increase with time until flame breakup or extinction, respectively. The BG model assumes the fireball height remains constant during flame break-up until extinction. The Shell model assumes the flame height to increase linearly with time (i.e. at a fixed rise velocity) with the maximum flame diameter occurring while the flame is grounded and hemispherical in shape.

- Flame surface emissive power
  The Quest model assumes the flame SEP to start at a peak value until flame lift-off commences and to subsequently decrease linearly to zero at the point of flame extinction. Both the Shell and BG models assume the flame SEP to initially increase with time and to reach a maximum value at the commencement of flame lift-off. Thereafter, the BG model assumes the flame SEP to remain constant until flame extinction, while the Shell model assumes the flame SEP to decrease linearly between flame lift-off and break-up and to remain constant until flame extinction.

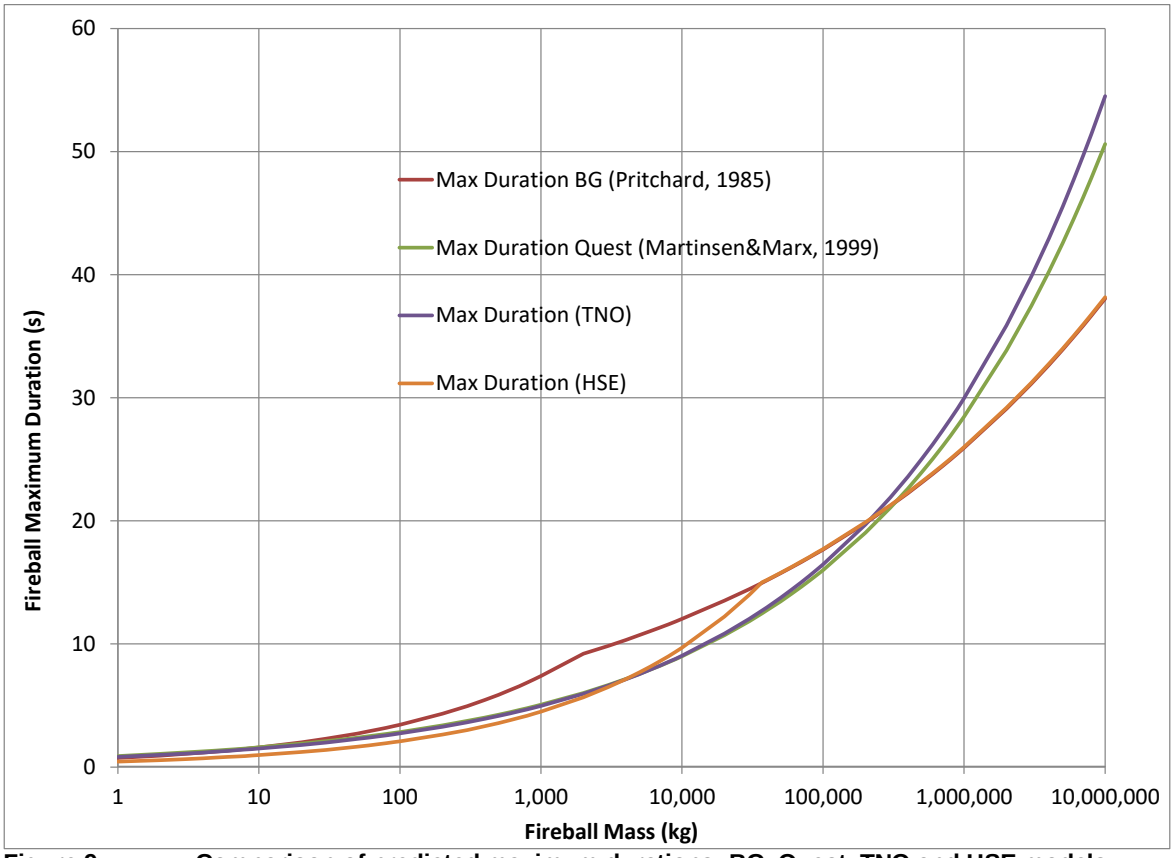

Figure 9. Comparison of predicted maximum durations: BG, Quest, TNO and HSE models

Model parameter	Pritchard (1985)	Martinsen & Marx (1999)	Shield (1993/1995)
Flame shape	Spherical	Spherical	Hemispherical ➔ spherical ➔ mushroom shaped (Shield, 1993)
Mass of fuel contributing to fireball	M_{Input} = total released mass	$M_{\text{Flammable}} = \begin{cases} M_{\text{Input}} & f_{\text{Vapour}} \geq \frac{1}{f_{\text{correction}}} \\ f_{\text{correction}} f_{\text{Vapour}} M_{\text{Input}} & f_{\text{Vapour}} < \frac{1}{f_{\text{correction}}} \end{cases}$	Derived from energy balance (fuel combustion)
Flame duration (s)	$t_{\text{Flame}} = \begin{cases} 7.4\left(M_{Input}/1000\right)^{0.333} & M_{Input} < 2000 \\ 8.2\left(M_{Input}/1000\right)^{0.167} & M_{Input} \geq 2000 \end{cases}$	$t_{\text{Flame}} = 0.9 M_{\text{Flammable}}^{0.25}$	Derived from energy balance for complete evaporation of characteristic droplets from onset of release
Flame lift-off time (s)	$t_{lo} = 0.3 t_{\text{Flame}}$	$t_{lo} = t_{\text{Flame}}/3$	$t_{exp} = t_{lo} = t_{\text{Flame}}/3$ (Shield, 1993)
Flame radius (m)	$\frac{r_f(t)}{r_{Flame}} = 0.02122 + 2.946\frac{t}{t_{MXR}} - 3.339\left(\frac{t}{t_{MXR}}\right)^2 + 1.381\left(\frac{t}{t_{MXR}}\right)^3$; $t \leq t_{lo}$ $t_{MXR} = 0.4 t_{\text{Flame}}$	$2r_f(t) = 8.664 M_{Flammable}^{1/4} t^{1/3}$; $t \leq t_{lo}$	Linear increase in hemispherical flame radius to peak radius (r_{flame}); $t \leq t_{exp} = t_{lo}$
	$r_f(t) = r_{\text{Flame}} = 2.9 M_{\text{Flammable}}^{0.333}$; for $t_{MXR} \leq t \leq t_{MXH} = t_{breakup}$; $t_{MXH} = 0.75 t_{Flame}$	$r_{\text{Flame}} = 2.9 M_{\text{Flammable}}^{0.333}$; $t \geq t_{lo}$	Hemisphere gradually turns to sphere at constant volume; $t_{exp} < t \leq t_{breakup}$
	$\frac{r_f(t)}{r_{Flame}} = 0.9975 + 0.6313\left(\frac{t - t_{breakup}}{t_{Flame} - t_{breakup}}\right) - 1.035\left(\frac{t - t_{breakup}}{t_{Flame} - t_{breakup}}\right)^2$; for $t > t_{breakup}$; $t_{MXH} = t_{breakup} = 0.75 t_{Flame}$		Linear decrease in fireball radius until flame extinction; $t_{breakup} < t \leq t_{Flame}$ $t_{Flame} = t_{exp} + t_{breakup}$
Flame height (m)	$H_f(t) = r_f(t)$; $t \leq t_{lo}$	$H_f(t) = r_f(t)$; $t \leq t_{lo}$	$H_f(t) = 0$; $t \leq t_{exp}$ (hemisphere)
	$\frac{H_B(t)}{H_{MAXB}} = 0.01195 + 0.1802\left(\frac{t - t_{lo}}{t_{MXH} - t_{lo}}\right) + 0.7962\left(\frac{t - t_{lo}}{t_{MXH} - t_{lo}}\right)^2$ $t_{lo} \leq t \leq t_{MXH}$; $H_f(t) = H_B(t) + r_f(t)$; $H_{MAXB} = 2 r_{Flame}$	$H_f(t) = r_{Flame}\left(1 + \frac{3}{t_{Flame}}\left(t - t_{lo}\right)\right)$; $t > t_{lo}$	$H_f(t) = u_{rise} t + H_{f,c}$; $t_{exp} < t \leq t_{Flame}$ $H_{f,c}$ = centroid of fireball at t_{exp}; Fireball is assumed to rise at a constant velocity (u_{rise})
	$H_f(t) = H_{Flame} = 3 r_{Flame}$; $t > t_{MXH}$;		
Flame SEP (kW/m²)	$\frac{E_f(t)}{E_{f,\max}} = 0.136 + 3.638\left(\frac{t}{t_{lo}}\right) - 5.425\left(\frac{t}{t_{lo}}\right)^2 + 2.691\left(\frac{t}{t_{lo}}\right)^3$; $t \leq t_{lo}$	$E_{f,\max} = Min\left(0.0133 f_s M_{Flammable}^{1/12} \Delta H_C,\ 400000\right)$; $t \leq t_{lo}$	Derived from energy balance (flame temperature). Linear increase in SEP to peak SEP at t_{exp}, followed by linear decrease to flame SEP at $t_{breakup}$.
	$E_{f,\max} = 235 P_{vap,init}^{0.39}$; $t > t_{lo}$	$E_f(t) = E_{f,\max}\left[1 - \left(t - t_{lo}\right)/\left(2t_{lo}\right)\right]$; $t > t_{lo}$	Constant SEP: $t_{breakup} \leq t \leq t_{Flame}$

Table 3 Comparison of key characteristics of the BG, Shell and Quest dynamic fireball model

3.1.5 Comparative analysis of model predictions against selected field data

The following presents a comparison of the BG (Pritchard, 1985), Shell (Shield, 1993 and 1995) and Quest (Martinsen and Marx, 1999) time-varying fireball model predictions (where available) against the following experimental data sets:

- Johnson et al. (1991)[24] for BLEVEs of LPG vessels (see section 3.1.2.3 for further details).
- Roberts et al. (2000)[8] medium to large scale tests: Propane (LPG) BLEVEs.

3.1.5.1 Johnson et al. (1991) large scale tests: Butane and Propane BLEVEs

Table 4 presents the results of the comparison of the BG, Shell and Quest dynamic fireball model predictions against measured data recorded during the Johnson et al. (1991) LPG BLEVE tests.

From Table 4, it can be observed that:

- Fireball duration.
  Predicted duration data from the Quest model generally shows better agreement with measured data as compared to the BG model. The BG model tends to over-predict measured duration data by up to 70% (Test 2). The Shell model only slightly under-predicts measured data for Test 4 with the Quest model showing best agreement with measured data of the three models.

- Fireball lift-off time.
  Both the BG and Quest models tend to under-predict flame lift-off times with the former model predictions showing better agreement with measured data as compared to the latter.

+

- Time to maximum flame diameter.
  The BG and Quest models tend to over-predict times to maximum flame diameter with the latter model predictions showing better agreement with measured data as compared to the former.

- Maximum flame diameter and height.
  Both the BG and Quest models show equally good agreement with measured flame diameter data, but generally over-predict maximum flame heights. The Shell model shows good agreement with measured flame diameter data for Test 4 and best agreement with flame height data of the 3 models.

- Flame SEP.
  The BG and Quest models tend to under-predict flame SEP, while closer agreement with measured data is observed with the Quest model predictions as compared to the BG model. The Shell model significantly over-predicts measured data for Test 4 with the Quest model showing best agreement with measured data of the three models.

In general, for the cases compared and experimental data reviewed, the Quest model is observed to give the closest agreement with the range of data recorded during the Johnson et al. (1991) LPG BLEVE tests. The above observation may not totally apply to the Shell model as only a limited amount of data (Test 4) was considered in the comparative analysis. It should be noted that both the Quest and Shell models were largely fitted against the Johnson et al. (1991) test data and as such may not constitute an independent basis for model performance assessment.

Table 4 Comparison of dynamic fireball model predictions against experimental data (Johnson et al., 1991)

Parameter Description	Test Information / Measured Data	Model Predictions		
		Quest (Martinsen and Marx, 1999)	BG (Pritchard, 1985)	Shell (Shield, 1993 / 1995)[22]
Test number	1R			
Released Material	Butane			
Released mass [kg]	2000			
Vessel volume [m^3]	5.659			
Liquid fill ratio [%]	77			
Burst pressure [Mpa]	1.51			
Time to ignition [s]	0.5			
Fireball duration [s]	5.8	6.0	9.3	–
Fireball lift-off time [s]	3.2	2.0	2.8	–
Time to max. diameter [s]	2.0	2.0	3.7	–
Maximum diameter [m]	68 – 84	73.1	73.1	–
Maximum height [m]	90	109.6	109.6	–
Average SEP [kW/m^2]	347 – 388	313.8	276.0	–
Peak SEP [kW/m^2]	400			–
Test number	2			
Released Material	Butane			
Released mass [kg]	1000			
Vessel volume [m^3]	5.659			
Liquid fill ratio [%]	39			
Burst pressure [Mpa]	1.52			
Time to ignition [s]	0.2			
Fireball duration [s]	4.3	5.1	7.4	–
Fireball lift-off time [s]	2.7	1.7	2.2	–
Time to max. diameter [s]	1.2	1.7	3.0	–
Maximum diameter [m]	56 – 64	58.0	58.0	–
Maximum height [m]	45	87.0	87.0	–
Average SEP [kW/m^2]	347	296.9	276.0	–
Peak SEP [kW/m^2]	560			–
Test number	3			
Released Material	Butane			
Released mass [kg]	2000			
Vessel volume [m^3]	5.659			
Liquid fill ratio [%]	68			
Burst pressure [Mpa]	0.77			
Time to ignition [s]	0.5			
Fireball duration [s]	7.9	6.0	9.3	–
Fireball lift-off time [s]	3.9	2.0	2.8	–
Time to max. diameter [s]	2.2	2.0	3.7	–
Maximum diameter [m]	64 – 74	73.1	73.1	–
Maximum height [m]	70	109.6	109.6	–
Average SEP [kW/m^2]	282 – 329	253.0	210.1	–
Peak SEP [kW/m^2]	440			–

[22] Shell Fireball data as reported by Skrinsky et al. (2013). "Validation possibilities of the BLEVE thermal effects", Journal of Safety Research and Applications (JOSRA), vol. 2, 2013.

Parameter Description	Test Information / Measured Data	Model Predictions		
		Quest (Martinsen and Marx, 1999)	BG (Pritchard, 1985)	Shell (Shield, 1993 / 1995)[22]
Test number	4			
Released Material	Butane			
Released mass [kg]	2000			
Vessel volume [m^3]	10.796			
Liquid fill ratio [%]	40			
Burst pressure [Mpa]	1.51			
Time to ignition [s]	0.4			
Fireball duration [s]	6.1	6.0	9.3	5.9
Fireball lift-off time [s]	3.6	2.0	2.8	–
Time to max. diameter [s]	1.5	2.0	3.7	–
Maximum diameter [m]	60 – 88	73.1	73.1	83
Maximum height [m]	85	109.6	109.6	77
Average SEP [kW/m^2]	336 – 353	313.8	276.0	440
Peak SEP [kW/m^2]	353			
Test number	5			
Released Material	Propane			
Released mass [kg]	2000			
Vessel volume [m^3]	5.659			
Liquid fill ratio [%]	80			
Burst pressure [Mpa]	1.52			
Time to ignition [s]	0.6			
Fireball duration [s]	8.6	6.0	9.3	–
Fireball lift-off time [s]	4.0	2.0	2.8	–
Time to max. diameter [s]	1.9	2.0	3.7	–
Maximum diameter [m]	64 – 66	73.1	73.1	–
Maximum height [m]	90	109.6	109.6	–
Average SEP [kW/m^2]	336 – 355	318.7	276.0	–
Peak SEP [kW/m^2]	530			–

3.1.5.2 Roberts et al. (2000) medium to large scale tests: Propane (LPG) BLEVEs

Roberts et al. (2000)[8] reported the results of experiments involving BLEVEs of four pressure tanks filled with different amounts of propane, ranging from 279 to 1708 kg. The experiments were conducted as part of the Commission of the European Community (CEC) funded project investigating the hazardous consequences of Jet-Fire Interaction with VEssels containing pressurized liquids (JIVE).

Each pressure tank was fitted with pressure relief valves and exposed to an impinging jet flame up to the point of BLEVE failure. Maximum fireball diameter, SEP, flame duration, peak incident heat flux and radiation dose at various observer locations were recorded during the JIVE tests. In each case, the entire vessel inventory was largely observed to contribute to the ensuing fireball (negligible droplet rainout). Flame characteristics (duration, maximum diameter, height and SEP) were recorded in terms of upwind (U/W) and crosswind (C/W) behaviour. The granularity of the measured data (U/W and C/W) provide further detail on the variation in flame characteristics relative to downwind / crosswind observers and enable better understanding of the variation in radiation measurements at pertinent observer locations.

Table 5 presents the results of the comparison of the BG, Shell and Quest dynamic fireball model predictions against measured data recorded during the JIVE (Roberts et al., 2000) propane (LPG) BLEVE tests.

From Table 5, it can be observed that:

- Fireball duration
  Predicted duration data from the Shell and Quest models generally show better agreement with measured data as compared to the BG model, with the Shell model results arguably showing the closest agreement with measured data of the 3 models. Again, the BG model tends to over-predict measured duration data.
- Fireball lift-off time
  Both the BG and Quest models tend to under-predict flame lift-off times with the BG model predictions showing better agreement with measured data as compared to the latter.

- Time to maximum flame diameter
  The BG and Quest models tend to under-predict times to maximum flame diameter with the BG model predictions showing significantly better agreement with measured data as compared to the latter.
- Maximum flame diameter and corresponding flame height
  Both the BG and Quest models show equally good agreement with measured maximum flame diameter data, but generally under-predict the corresponding flame heights. The BG flame height at maximum diameter predictions generally show closer agreement with measured data as compared to predicted results using the Quest model.
- Flame SEP
  The predicted flame SEPs using the BG and Quest models tend to show good agreement with the range of measured average to peak flame SEPs. Both models tend to over-predict average flame SEPs and under-predict peak flame SEPS, while closer agreement with measured data is observed with the BG model predictions as compared to predicted results using the Quest model.

Only a limited amount of data (flame duration) was considered in the comparative analysis involving the Shell model, as such only limited conclusions may be drawn from the analysis undertaken. In general, for the cases considered, comparisons undertaken and dynamic fireball models studied, the Shell model is observed to give the closest agreement with measured data for flame durations. Furthermore, the BG model is observed to give generally closer agreement with the range of data recorded during the JIVE (Roberts et al., 2000) propane BLEVE tests when compared against simulated data using the Quest model.

Parameter Description	Test Information / Measured Data	Model Predictions		
		Quest (Martinsen and Marx, 1999)	BG (Pritchard, 1985)	Shell (Shield, 1993 / 1995)[22]
Test number	1			
Released Material	Propane			
Released mass [kg]	279			
Liquid fill ratio [%]	20			
Burst pressure [Mpa]	1.65			
Fireball duration [s]	3 – 3.8	3.7	4.8	3.3
Fireball lift-off time [s]	2.2	1.2	1.5	–
Time to max. diameter [s]	2.08 – 2.21	1.2	1.9	–
Maximum diameter [m]	41 – 45	37.9	37.9	–
Height at max. diameter [m]	22	18.9	22.4	–
Average SEP [kW/m^2]	188 – 295			–
Peak SEP [kW/m^2]	554 – 650	277.7	285.7	–
Test number	2			
Released Material	Propane			
Released mass [kg]	710			
Liquid fill ratio [%]	41			
Burst pressure [Mpa]	2.13			
Fireball duration [s]	4.6 – 5	4.6	6.6	4.6
Fireball lift-off time [s]	3	1.5	2.0	–
Time to max. diameter [s]	2 – 2.84	1.5	2.6	–
Maximum diameter [m]	43 – 45	51.7	51.7	–
Height at max. diameter [m]	33	25.9	30.6	–
Average SEP [kW/m^2]	196			–
Peak SEP [kW/m^2]	484	325.7	315.6	–
Test number	3			
Released Material	Propane			
Released mass [kg]	1272			
Liquid fill ratio [%]	60			
Burst pressure [Mpa]	1.86			
Fireball duration [s]	5.9 – 6.5	5.4	8.0	5.7
Fireball lift-off time [s]	3.4	1.8	2.4	–
Time to max. diameter [s]	3.12 – 4.18	1.8	3.2	–
Maximum diameter [m]	74 – 75	62.8	62.8	–
Height at max. diameter [m]	31.5	31.4	37.2	–
Average SEP [kW/m^2]	117 – 287			–
Peak SEP [kW/m^2]	482 – 486	327.4	299.3	–
Test number	4			
Released Material	Propane			
Released mass [kg]	1708			
Liquid fill ratio [%]	85			
Burst pressure [Mpa]	2.44			
Fireball duration [s]	6.6 – 7	5.8	8.8	6
Fireball lift-off time [s]	3.7	1.9	2.7	–
Time to max. diameter [s]	3.64 – 3.69	1.9	3.5	–
Maximum diameter [m]	71 – 85	69.3	69.3	–
Height at max. diameter [m]	49	34.7	41.0	–
Average SEP [kW/m^2]	212 – 312			–
Peak SEP [kW/m^2]	523 – 556	366.0	332.8	

Table 5 Comparison of dynamic fireball model predictions against experimental data (Roberts et al., 2000)

3.1.6 Literature review of fireballs by DNV Benelux for Flemish authorities

A literature review was recently carried out by DNV Benelux (partly carried out with feedback from DNV Digital Solutions) for the Flemish Authorities in an investigation of the use of consequence models for QRA's, and the results of this were reported in the report "Research on models for use in Quantitative Risk Assessment" (2012)[9].

Section V.1 of the above report includes the results of the above review for fireball models.

Description of fireball sub-models

It first provides an overview of the fireball sub-models for:

- Fireball mass $M_{flammable}$
  This may account for possible rainout. The report includes a discussion on the selection of the appropriate choice for the mass correction factor $f_{correction}$ in Equation (1). Based on the experiments form Hasegawo and Sato (1977)[16], Roberts (1982)[17] recommends a value of 3 in line with recommendations by CCPS(2010)[7] and the assumption for the existing Phast static fireball models. It also refers to the separate Flemish guideline (ANIMAL, 1987; 'Richtlijn voor berekenen van flash and spray'). It is also noted the flash fraction ($1-f_{vapour}$) in Equation (1) depends on the method of evaluation of, e.g. usage of isentropic or adiabatic assumption.

- Fireball duration
  Here distinction is made between a momentum-dominated fireball (dominated by initial momentum resulting of expansion to atmospheric pressure) and a gravity-dominated fireball (fireball rise due to hot combustion products). An overview of empirical power-law correlations of the form $t_{flame} = a\ M_{flammable}^{b}$ from the literature are given.

- Fireball diameter. An overview of empirical power-law correlations of the form $D_f = a\ M_{flammable}^{b}$ from the literature are given.

- Surface emissive power

- Fireball height

Description and comparison of fireball models

Subsequently the report includes a description and comparison of a range of fireball models. This includes the static models (TNO, HSE) and dynamic model (Martinsen and Marx) as described in the current report. In addition it includes the SFPE model (Beyler, 2002)[xxv].

In analogy with our Table 3, a table is given to compare the empirical correlations between these four different models. Also graphs are produced to compare the empirical correlations for maximum diameter $2r_{flame}$, fireball duration t_{flame}, fireball height H_{flame} as function of $M_{flammable}$; see Figure 10. And a graph is produced for the empirical correlation of maximum SEP versus tank failure pressure; see Figure 11.

In analogy with our Table 4 and Table 5, the above models are compared against the British Gas (Johnson et al., 1991) and Roberts's et al. (2000) experiments. It is concluded that the dynamic model may lead to under-prediction of the thermal dose primarily since it does not account for the effect of the wind. For the statics models this does not lead to under-prediction since they involve a larger degree of conservatism.

In addition, the models are compared for four examples involving a propane fireball, where the fireball mass $M_{flammable}$ and the tank failure pressure P are varied. Cases considered are a momentum-dominated fireball (25000 kg, 1.8MPa), a gravity-dominated propane fireball (50000 kg, 1.8MPa), small fireball mass (5000 kg, 1.8MPa) and a larger failure pressure (25000kg, 6MPa). Results of fireball height versus time and thermal dose and thermal lethality versus distance are compared. It is concluded that the TNO produces considerable lower lethalities due to the larger fireball height.

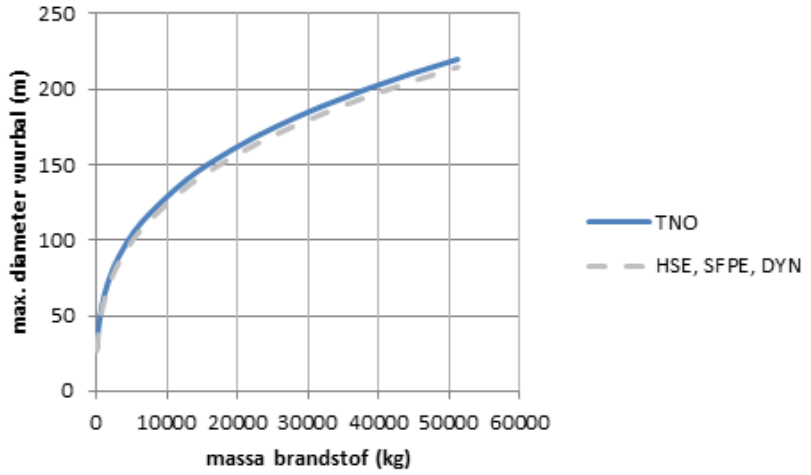

(a) Maximum flame diameter $2r_{flame}$ (m) versus mass $M_{flammable}$ (kg)

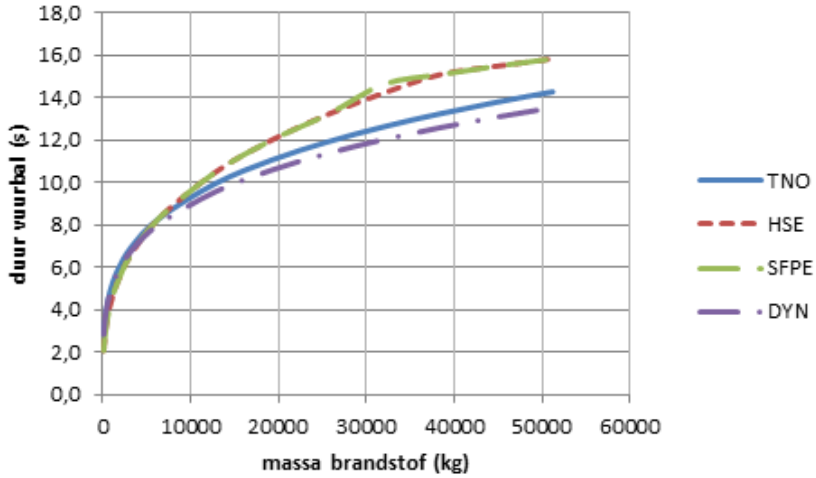

(b) Fireball duration t_{flame} (s) versus mass $M_{flammable}$ (kg)

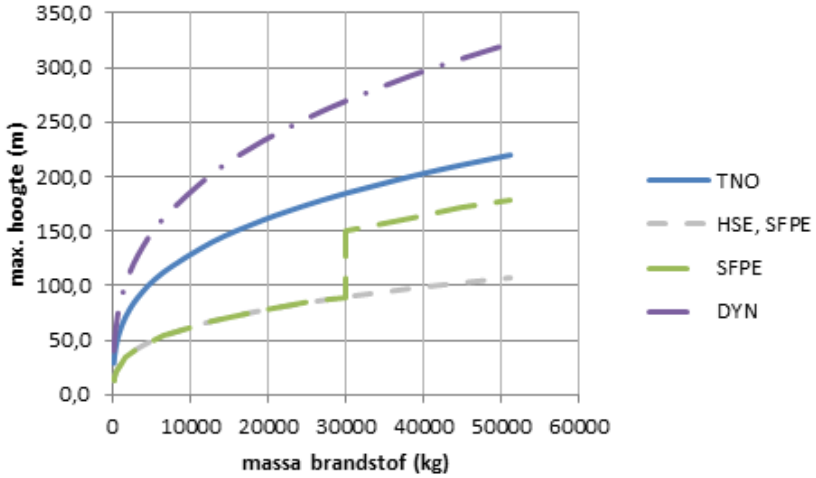

(c) Maximum flame height H_{flame} (m) versus mass $M_{flammable}$ (kg)

Figure 10. **Comparison of fireball dimensions and duration for TNO, HSE, Quest and SFPE models**
Figures taken from DNV Benelux report[9]

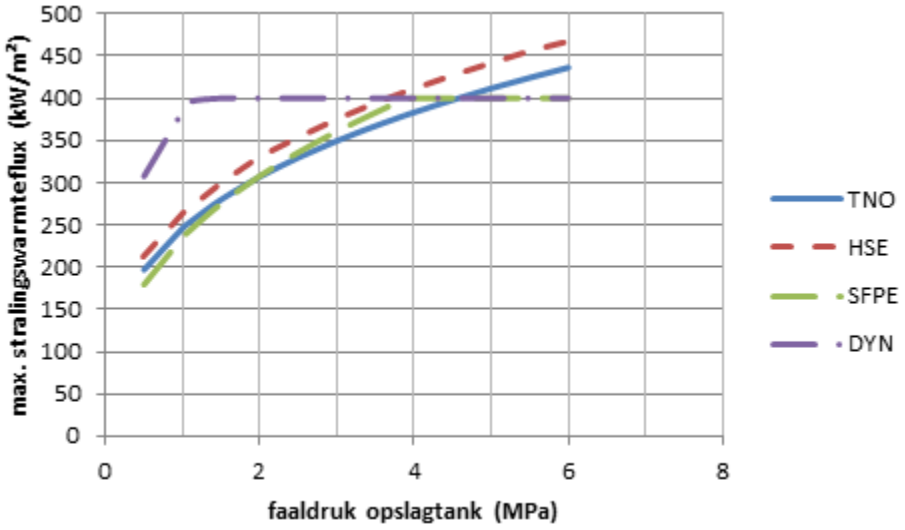

Figure 11. **Comparison of SEP for TNO, HSE, Quest and SFPE models**
Figure taken from DNV Benelux report[9] ; the figure plots the maximum surface emissive power (kW/m^2) verus the tank failure pressure P (MPa)

3.2 Impulsive pipeline release fireball models

3.2.1 GL model (Pipesafe – Cleaver and Halford, 2014)

Cleaver and Halford (2014)[xxvi] describe an integral or similarity type model developed for use within the PIPESAFE risk assessment software for predicting the transient flame characteristics and radiation emitted following the immediate ignition a full-bore rupture gas pipeline release. The model assumes that the impulsively started flow, on immediate ignition, produces a growing fireball ('cap') that sits on top of an underlying burning jet (plume or 'stalk'). The fireball is assumed to rapidly burn out as the 'stalk' is established. The established 'stalk' is modelled as a series of quasi steady-state jet fires at later times. For releases from buried pipelines, the model takes into account the impact of crater and soil effects on the release momentum, dilution and attendant flame and radiation characteristics.

The Cleaver and Halford (2014) model derives from a model published by Turner (1962)[xxvii], for an unignited, impulsively started plume produced by a constant rate release with no cross wind. Cleaver and Halford (2014) extended the Turner (1962) model to include combustion within the stalk and cap plus the effects of a cross-wind. Mass, momentum and combustion differential equations were developed and solved for the stalk and cap, with the flow from the stalk into the cap linking the two sets of equations.

The spherical cap formed at the onset of the release is modelled as entraining air from its surroundings as it rises. The amount of air entrained into the stalk and the cap are determined from semi-empirical correlations accounting for wind, plume / cap momentum and crater effects. The cap is modelled as rising more slowly than the local velocity in the stalk at the base of the cap; hence, fluid is fed into the cap from the stalk below. The stalk is modelled as a truncated conical frustum attached to the base of the cap with its dimensions described in terms of a bulk stalk radius at the point of overlap with the cap.

Other key assumptions adopted within the Cleaver and Halford (2014) model include:

- Ideal gas behaviour: fuel + air + combustion product mixture.
- Fraction of heat radiated from the stalk and cap are assumed to be constant, with the stalk radiative fraction determined empirically in terms of the fuel mass flow rate and wind speed. The radiative fraction from the cap is 60% greater than the radiative fraction from the stalk.
- The specific heat capacities of the fuel, air and combustion products do not vary with temperature, while changes in ambient air temperature with height are negligible compared to the temperature differences between the jet fire and the ambient air.
- The predicted timescale of the fireball is defined as the earliest time in the calculations that no fuel remains in the cap, and no fuel flows into the cap from the stalk.
- For time-varying releases, a representative average release rate is used to model the transient flame development and radiation process. An iterative scheme is used to find the time, t, such that, using the average flow rate over a time 1.2 t, a fireball timescale of t is predicted.

The authors present a comparison of the impulsive fireball model against field and scaled experimental data (up to 100bar and pipelines up to 36 inch) and conclude that the predicted values of thermal radiation are generally observed to lie within a factor of 2 of observed values. Other intermediate parameters, such as flame height and trajectory are also compared with available data and shown to generally agree to within about 25% of observed values.

Validation

Cleaver and Halford (2014) presented the results of the validation of the BG/GL impulsive fire (fireball and jet-fire) and radiation model against field data logged following the rupture of natural gas pipelines. The experimental data considered cover a wide range of scales (pipeline sizes up to 36" and containment pressures of 100barg) and include:

- Full scale experimental study of fires following the rupture of natural gas transmission pipelines as recorded by Acton et al. (2000)[xxviii].
- Reduced scale (one-sixth linear scaled) experiments conducted at BG/GL's test site at Spadeadam as reported by Norris (1994)[xxix].

Figure 12 shows the results of the validation of the BG/GL impulsive fire and radiation model comparing the measured and predicted radiation intensities at various observer locations after 32 seconds for the full scale experiments reported by Acton et al. (2000).

Figure 13 shows the comparison of the BG/GL impulsive fire and radiation model predictions against measured peak radiation data at various observer locations for the one-sixth linear scaled experiments with and without soil backfill, respectively, as reported by Norris (1994).

From Figure 12 and Figure 13, it can be observed that the BG/GL impulsive fire and radiation model predictions generally lie within a factor of 2 of measurements.

Cleaver and Halford (2014) also present data comparing other intermediate impulsive fire parameters, such as flame height and trajectory against measured data and affirm that predicted results generally agree to within ca 25% of observed values.

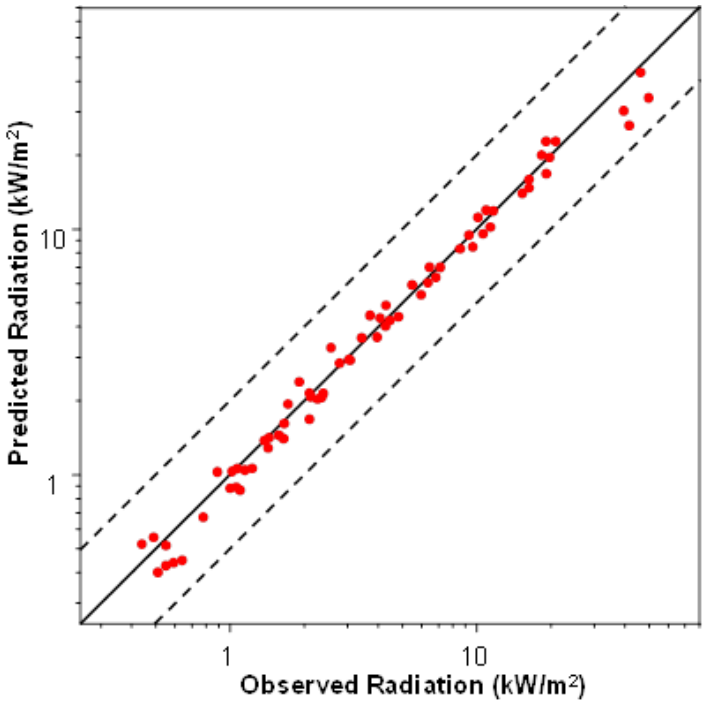

Figure 12. **Validation of the GL impulsive jet "stalk" model (Cleaver and Halford, 2014)**
The plot depicts the comparison of predictions from the "stalk" model against measured radiation intensities after 32 seconds for the full scale experiments reported by Acton et al. (2000). Dotted lines show differences of a factor of 2 between observed and predicted values.

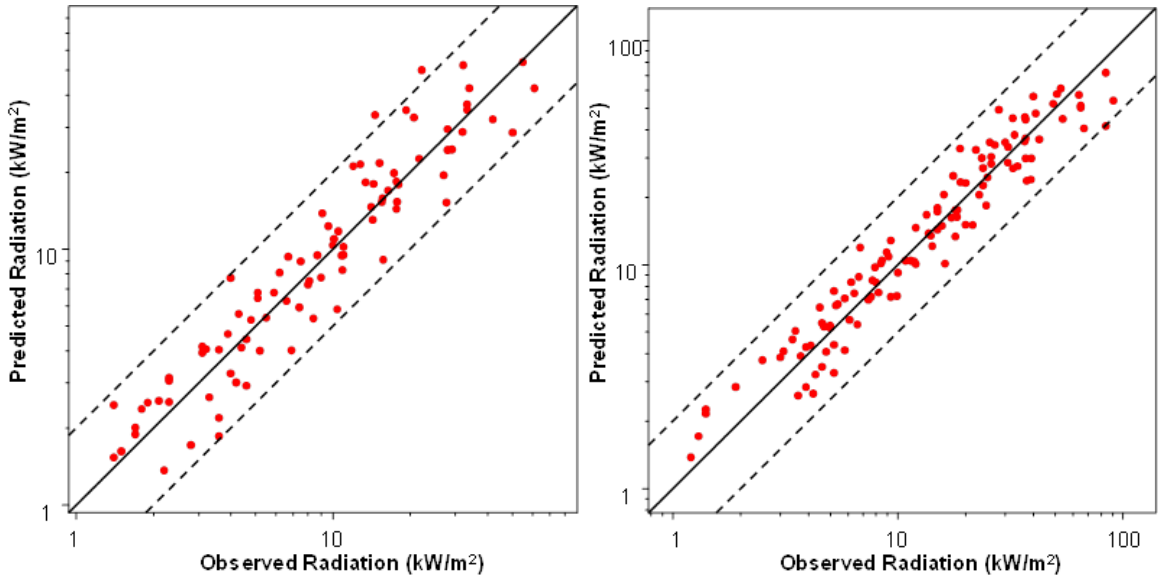

Figure 13. **Validation of the GL impulsive fireball model (Cleaver and Halford, 2014): peak incident radiation intensities.**
The plot depicts the comparison of predicted and measured peak incident radiations for the one-sixth linear scaled experiments with and without soil backfill, respectively, as reported by Norris (1994). Dotted lines show differences of a factor of 2 between observed and predicted values.

3.2.2 Shell model (Shepherd – Cracknell, 1997)

Model Overview

Hirst (1986)[xxx], while conducting field tests, observed that fireballs will form upon the delayed ignition of flammable vertical jets, provided the ignition occurs close to the release source and release conditions have allowed a flammable cloud to form (to steady state). As such, Cracknell and Carlsey (1997)[xxxi] proposed an empirical model for predicting flame

characteristics and attendant radiant heat effects from fireballs stemming from vertical steady state jet releases[23]. The ensuing fireball is assumed to be followed by a steady-state jet fire. The authors do not describe / provide a transitioning relationship between the fireball and the steady-state jet fire.

Cracknell and Carlsey's (1997) model correlations were fitted against field data reported by Hirst (1986) for a series of vertical propane (flashing) jet releases. The authors claim that the proposed fireball model may be applied to other hydrocarbons and suggest that predicted results are expected to be valid (but slightly conservative) for releases of gases lighter than propane. For liquids with lesser propensity to flash, the authors suggest that predicted results from the fireball model will be somewhat conservative, particularly where rain-out is seen or predicted to likely occur.

Model Description

The Cracknell and Carlsey (1997) model is comprised of equations that describe the variation of fireball size, motion and flame emissive power with time. The model does not account for rainout as it conservatively assumes the escaping fuel, in its entirety, contributes to the ensuing fireball. Fireball characteristics were described in terms of:

- Fireball shape
- Fireball radius (growth) and duration
- Fireball height (rise)
- Flame surface emissive power

Fireball Shape

Cracknell and Carlsey (1997) assume the fireball to be spherical in shape throughout its lifetime.

Fireball growth (diameter) and duration

Upon ignition, the ensuing flame is assumed to start off as a buoyant fireball that grows until it attains a maximum diameter ($D_{if,max}$).

Cracknell and Carlsey (1997) propose the following empirical expression for the maximum fireball diameter ($D_{if,max}$[m]) as a function of fuel mass flow rate (Q [kg/s]) and wind speed (u_w [m/s]):

$$\frac{D_{\mathrm{if,max}}}{Q^{2/5}} = 4 + 6\exp\left(-0.25u_w\right) \qquad \textbf{(43)}$$

Equation (43) suggests that the maximum fireball diameter increases with fuel release rate but decreases with wind speed[24].

At inception, the fireball is assumed to grow linearly with time until it reaches its maximum diameter. Thereafter, the fireball remains at its maximum width until extinguished / succeeded by the steady-state jet fire. As such, the fireball diameter (D_{if} (t)) as a function of time is given by:

$$D_{\mathrm{if}}(t) = D_{if,\max}\frac{t}{t_{if,\max}} \qquad t \le t_{if,\max}$$
$$D_{\mathrm{if}}(t) = D_{if,\max} \qquad t > t_{if,\max} \qquad \textbf{(44)}$$

Where:

$t_{if,max}$ Elapsed time from ignition to maximum fireball diameter [s];

The authors propose the following relationship for $t_{if,max}$:

$$t_{\mathrm{if,max}} = 0.11D_{if,\max} \qquad \textbf{(45)}$$

Fireball rise (height)

The fireball height (measured from the point of release to the fireball centre), H_{if}(t), is assumed to equal the fireball diameter while the flame is growing to its maximum size. Upon reaching its maximum size, Cracknell and Carlsey (1997) assume the fireball height to increase linearly with time. The fireball height, H_{if}(t), is given by:

$$H_{\mathrm{if}}(t) = D_{if}(t) \qquad t \le t_{if,\max}$$
$$H_{\mathrm{if}}(t) = D_{if,\max}\frac{t}{t_{if,\max}} \qquad t > t_{if,\max} \qquad (46)$$

Fireball duration

Cracknell and Carlsey (1997) do not provide a relationship for the overall fireball duration.

[23] The authors do not indicate the release containment type (storage vessel or pipeline). It is expected that the release rate following a rupture (pipelines) or large leaks (leak size > 2") will be time-varying.

[24] This appears to be the only mention as to the impact of wind on flame characteristics. Cracknell and Carlsey (1997) make no other mention of the impact of crosswinds (e.g. wind drift) on fireball behaviour.

Flame surface emissive power

Cracknell and Carlsey (1997) assume the fireball SEP to remain constant for its entire duration, irrespective of release conditions, flame size or fuel properties. However, the authors confirm that field evidence suggests otherwise, i.e., impulsive jet fireballs remain luminous up to the point where they reach maximum diameter and thereafter become abruptly less luminous (decrease in SEP). Nevertheless, the authors suggest assuming a 'best' fixed value of 250kW/m^2 for the flame SEP.

Validation

Cracknell and Carlsey (1997) presented the results of the validation of the Shell impulsive fire (fireball and jet-fire) and radiation model against field data recorded by Hirst (1986) for a 41kg/s vertical propane release (test 23).

Figure 14 shows the outcome of the validation exercise comparing the measured and predicted variation in radiation intensity at an observer location 108m away from the release point. The observer is tilted so as to receive approximately the maximum radiation from the fireball. Cracknell and Carlsey (1997) conclude that the proposed impulsive fireball and radiation model shows reasonable agreement with experiment both in terms of fireball duration[25] and radiation with the radiation from the impulsive fire decaying following the fireball event to a value appropriate to a steady state jet fire.

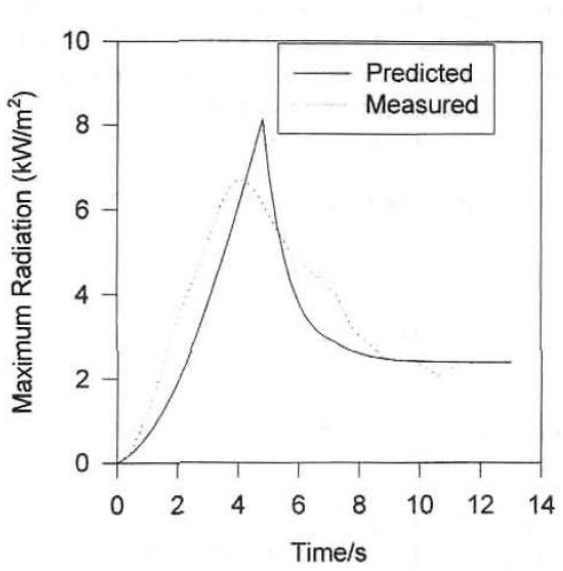

Figure 14. Validation of the Shell impulsive fireball model (Cracknell and Carlsey, 1997): radiation intensity versus time.
The plot depicts the variation of measured and predicted radiation intensity with time at an observer location 108m away from a 41kg/s vertical propane jet.

3.2.3 Comparative analysis

Table 6 presents a comparison of the key features / characteristics of the BG/GL (Cleaver and Halford, 2014)[xxvi] and the Shell (Cracknell and Carlsey, 1997)[xxxi] impulsive jet time-varying fireball models discussed in sections 3.2.1 and 3.2.2.

From Table 6 it can be observed that:

- Model complexity and flame characteristics: the Shell model is relatively simple and employs empirical correlations in describing flame characteristics. However, the BG/GL model is significantly more complicated and flame characterization requires the solution of mass, momentum and combustion differential equations.
- Fluid phase / material and release characteristics: The BG/GL impulsive fireball model may only be applied to gas / vapour phase time-varying releases where the material is naturally buoyant. However, the Shell model may be applied to a wide variety of fluid states and materials but is only suited for steady state releases.

[25] Note that Cracknell and Carlsey (1997) do not provide an expression for the overall fireball duration.

Model parameter	BG/GL (Cleaver and Halford, 2014)	Shell (Cracknell and Carlsey, 1997)
Flame shape	Composite flame: Spherical cap attached to a truncated cone (stalk)	Spherical
Variation of release rate with time	Modelled	Constant flow rate
Fluid phase	Gas / Vapour phase only	Applicable to gas/vapour, two-phase/ flashing liquids
Material characteristics	Limited to materials naturally buoyant in air (natural gas)	Applicable to any hydrocarbon: buoyant or heavier than air releases
Impact of wind speed on flame size	Modelled (via air entrainment terms)	Modelled
Wind drift	Modelled	Not mentioned as modelled
Mass of fuel contributing to fireball	Derived from the solution of mass, momentum and combustion differential equations	Total mass flow
Flame duration (s)		Details not provided
Time to maximum flame diameter (s)		$t_{\mathrm{if,max}} = 0.11 D_{if,\mathrm{max}}$
Flame diameter (m)		$\frac{D_{\mathrm{if,max}}}{Q^{2/5}} = 4 + 6\exp\left(-0.25 u_w\right)$ $D_{\mathrm{if}}(t) = D_{if,\mathrm{max}} \frac{t}{t_{if,\mathrm{max}}} \quad t \le t_{if,\mathrm{max}}$ $D_{\mathrm{if}}(t) = D_{if,\mathrm{max}} \quad t > t_{if,\mathrm{max}}$
Flame height (m)		$H_{\mathrm{if}}(t) = D_{if}(t) \quad t \le t_{if,\mathrm{max}}$ $H_{\mathrm{if}}(t) = D_{if,\mathrm{max}} \frac{t}{t_{if,\mathrm{max}}} \quad t > t_{if,\mathrm{max}}$
Flame SEP (kW/m^2)	Varies with flame characteristics (size, physical properties). Fraction of heat radiated assumed constant but varies between cap and stalk	Constant value

Table 6 Comparison of key characteristics of the BG and Shell impulsive jet fireball models

4 DETAILED VALIDATION OF THE MARTINSEN AND MARX (1999) MODEL

The following presents the results of the detailed validation of the implementation[26] of the Martinsen and Marx [M&M] (1999)[1] time-varying fireball model within the Phast Time Varying Fire and Radiation Model (TVFM). The predicted radiation dose and peak intensity at various observer locations based on the PHAST/SAFETI "Roberts/TNO hybrid" static fireball model ("TVFM_DNVR") are also presented for comparison. The TVFM Martinsen and Marx model (TVFM_M&M) has been validated against the following published experimental data sets:

- Johnson et al. (1991)[24] large scale tests: LPG BLEVEs
  - Radiation intensity versus time
  - Radiation Dose versus distance
  - Flame SEP versus time
  - Flame radius versus time
  - Flame height versus time
- Roberts et al. (2000)[8] medium to large scale tests: Propane (LPG) BLEVEs
  - Radiation intensity versus time
  - Radiation dose versus distance
  - Flame SEP versus time

4.1 Johnson et al. (1991) large scale tests: Butane and Propane BLEVEs

Table 7 presents a summary of the prevailing test and ambient conditions during the butane and propane BLEVEs reported by Johnson et al. (1991) (see section 3.1.2.3 for further details).

Description	Test Number / Identifier				
	1R	2	3	4	5
Released Material	Butane	Butane	Butane	Butane	Propane
Released mass [kg]	2000	1000	2000	2000	2000
Vessel volume [m^3]	5.659	5.659	5.659	10.796	5.659
Liquid fill ratio [%]	77	39	68	40	80
Burst pressure [Mpa]	1.51	1.52	0.77	1.51	1.52
Time to ignition [s]	0.5	0.2	0.5	0.4	0.6
Average wind speed [m/s]	8.2	14.8	5.1	4.9	5.2
Wind direction from magnetic North [°]	120	305	240	230	315
Ambient temperature [°C]	16.5	10	13	23	16
Relative humidity [%]	92.9	70	82	57	75
Ambient pressure [bara]	0.976	0.98	0.982	0.994	0.987

Table 7 Summary of test and ambient conditions: butane and propane BLEVEs (Johnson et al., 1991)

Incident thermal radiation measurements were taken at 50m and 75m north and at 50m, 75m, 100m, 125m, 150m, 175m, 200m and 250m west of the BLEVEs. Both slow response (Land / Medtherm: "Land" / "MT") and fast response (International Research and Development: "IRD1", "IRD2", "IRD3" and "IRD4") wide-angle radiometers were employed. The response times[27] for the Land, Medtherm and IRD radiometers were estimated as 0.3s, 1.5s and 0.02s, respectively. The accuracies of the slow response (Land / Medtherm) and IRD radiometers were reported as ±3% and ±10%, respectively.

Flame surface emissive power (SEP) measurements were taken using the wide-angled IRD radiometers and more precisely by a narrow angle radiometer ("Narrow") aimed at a point 30m above the ruptured vessels. Fireball radii, heights and areas were determined from cine film records from cameras located at various positions relative to the ruptured vessels.

[26] Implementation of the Martinsen and Marx (1999) model in Phast/Safeti/SafetiNL 8.0

[27] Response time is defined as the time for a radiometer to respond to 90% of the final output level

4.1.1 Radiation intensity versus time

Figure 15 shows the measured and predicted ("TVFM_M&M") variation in radiation intensity at observer locations 50m and 75m north and west of the BLEVEs reported by Johnson et al. (1991), i.e. Tests 1R – 5 (see Table 7). In each case, the observer is tilted so as to receive approximately the maximum radiation from the fireball.

From Figure 15, the following can be observed:

- The Martinsen and Marx model generally tends to under-predict peak incident radiation intensities particularly for near field radiometer positions (i.e., radiometer location 50m north/west). Johnson et al. (1991) observe that the generally significant differences in measured radiation intensities at the north as compared to the west equidistant radiometer locations can be attributed to:
    - Directional effects, i.e., non axi-symmetrical shape of the ensuing fireballs. In essence, the fireball characteristics (shape and duration) as viewed from the various equidistant locations were different. Johnson et al. (1991) observed that the flame size in the east-west plane was generally larger than in the north-south plane, particularly for test 4 (hence the higher north radiometer readings).
    - Wind-drift effects as a result of the prevailing wind. From Table 7 it can be observed the wind would mainly blow to the east for tests 2-5 and west for test 1R. This may also explain data for test 1R where the radiation measurement North are larger, while for tests 2-5 the radiation measurements West are larger.
- The predicted radiation intensity versus time profiles are rather similar to measured data, each showing a rapid increase to a peak value followed by a gradual decay in intensity as the flame goes to extinction. It should be noted that the predicted results are based on perfect (zero) radiometer response times, hence the apparent offset in the incident radiation versus time profiles of the measured (slow-response) as against the predicted results.
- The Martinsen and Marx model tends to under-predict, but in general, show relatively good agreement with predicted incident radiation intensity durations at the various observer locations.

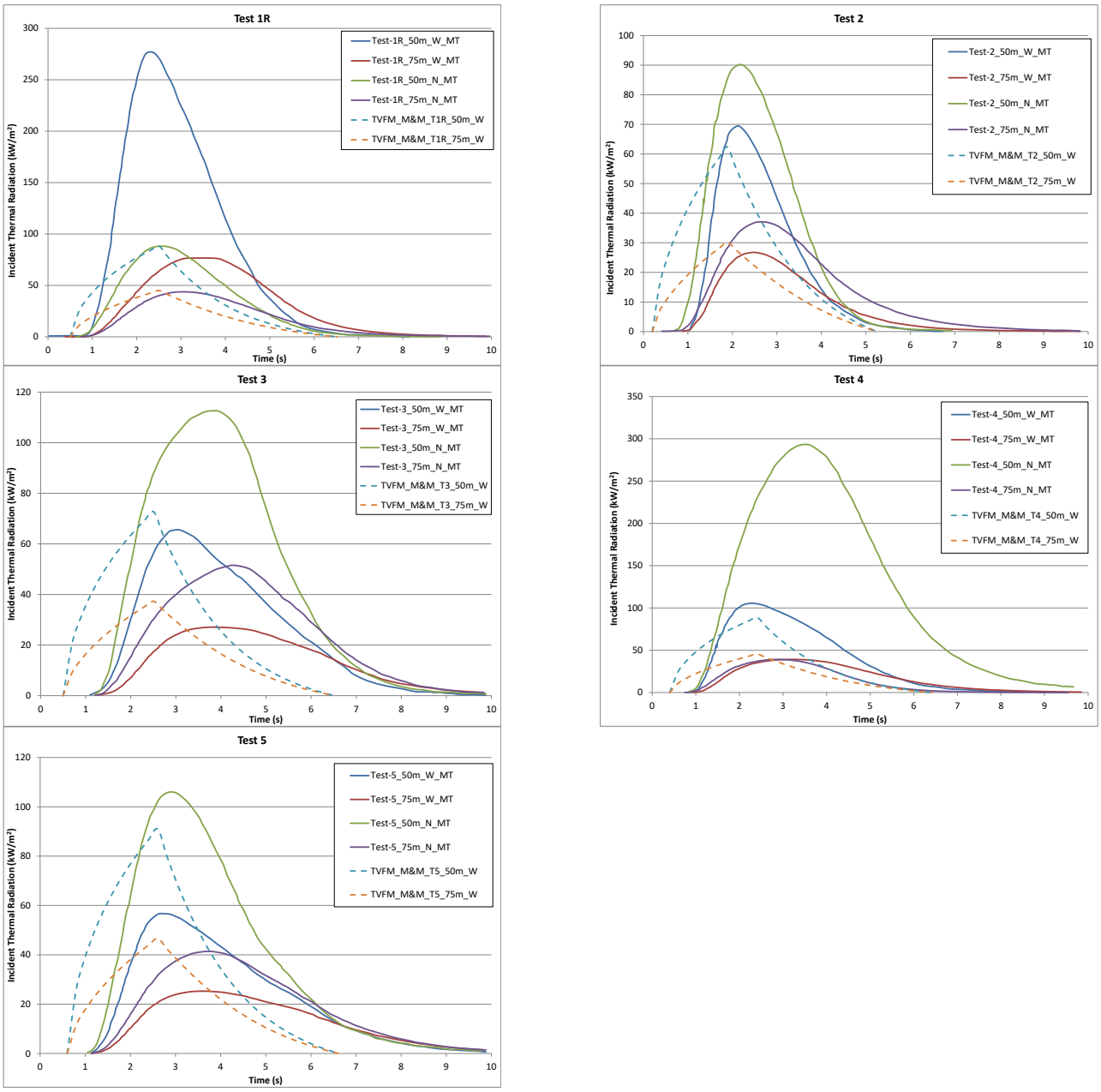

Figure 15. **Validation of Martinsen and Marx model (Tests 1R – 5, Johnson et al., 1991) – radiation intensity versus time**
The plots depict the variation of measured and predicted radiation intensity with time at observer locations 50m and 75m, north and west of butane (tests 1R-4) and propane (test 5) BLEVEs.

4.1.2 Radiation Dose versus distance

Figure 16 shows the measured and predicted ("TVFM_M&M") variation in radiation dosage at various observer locations north and west of the BLEVEs reported by Johnson et al. (1991), i.e. Tests 1R – 5 (see Table 7). For comparison, Figure 16 also shows the predicted variation in radiation dosage at pertinent observer locations as derived from the PHAST/SAFETI "Roberts/TNO hybrid" static fireball and radiation model ("TVFM_DNVR").

From Figure 16, the following can be observed:

- With the exception of data reported for Test 1R and near-field data (50m) reported for tests 3 and 4, the Martinsen and Marx model generally shows very good agreement with measured radiation dosage data. On average, the Martinsen and Marx model shows better agreement with measured data as compared to the static "Roberts/TNO hybrid" fireball model, with the "Roberts/TNO hybrid" fireball model tending to under-predict measured data in the near field and over-predict in the far-field.
- The poor agreement of predicted results against measured data in the near-field (and for Test 1R in general) may be due to the reasons proffered in section 4.1.1 (i.e. direction and wind-drift effects). Furthermore, the static "Roberts/TNO hybrid" model is more likely to under-predict radiation dose in the near field, particularly for

ground/close-to-ground level observers as it assumes the ensuing fireball to be instantaneously elevated and to remain elevated over its duration. For far-field ground/close-to-ground level observers, the “Roberts/TNO hybrid” model will tend to over-predict measured radiation dosage as it conservatively assumes the ensuing fireball, albeit elevated, to remain at a constant flame SEP and size over its duration.

- In either case, the predicted trend in the decay of radiation dosage with distance generally shows good agreement with measured data, with radiation dose showing a rapid decay in the near field and a less dramatic decrease in slope with increasing separation distance.

4.1.3 Flame SEP versus time

Figure 17 shows the measured and predicted (“TVFM_M&M”) variation in flame SEP with time for the BLEVEs reported by Johnson et al. (1991), i.e. Tests 1R – 5 (see Table 7).

From Figure 17, the following can be observed:

- The Martinsen and Marx model generally under-predicts the peak measured flame SEP. The predicted flame SEP should, by definition, ideally be compared against the time-averaged (or weighted) flame SEP prior to flame lift-off. From the discussion in section 3.1.5, the predicted time-averaged flame SEP is observed to show relatively good agreement with measured data (though still tending to under-predict).
- The predicted trend in flame SEP with distance generally shows good/moderate agreement with measured data. The Martinsen and Marx model assumes instantaneous rise to peak flame SEP, i.e. upon ignition. This modelling assumption is to a large extent confirmed by measured data. However, following the attainment of the peak flame SEP, measured data appears to suggest the flame SEP to initially gradually decay with time before rapidly decaying to zero. The Martinsen and Marx model assumes (i.e. post maximum flame SEP) flame SEP to remain constant prior to flame lift-off (for a third of the fireball duration) and to linearly decrease to zero upon flame extinction.

4.1.4 Flame radius versus time

Figure 18 shows the measured and predicted (“TVFM_M&M”) variation in flame radius with time for the BLEVEs reported by Johnson et al. (1991), i.e. Tests 1R – 5 (see Table 7).

From Figure 18, the following can be observed:

- The Martinsen and Marx model generally shows very good agreement with measured data during the fireball growth regime.
- Furthermore, measured data seems to confirm a period of relatively constant fireball radius followed by a relatively rapid decrease in fireball radii to a finite size at the point of flame extinction. The Martinsen and Marx model largely shows good agreement with measured data for a large proportion of the constant flame radii period but fails to account for the decrease in effective fireball radii as indicated in the reported data.

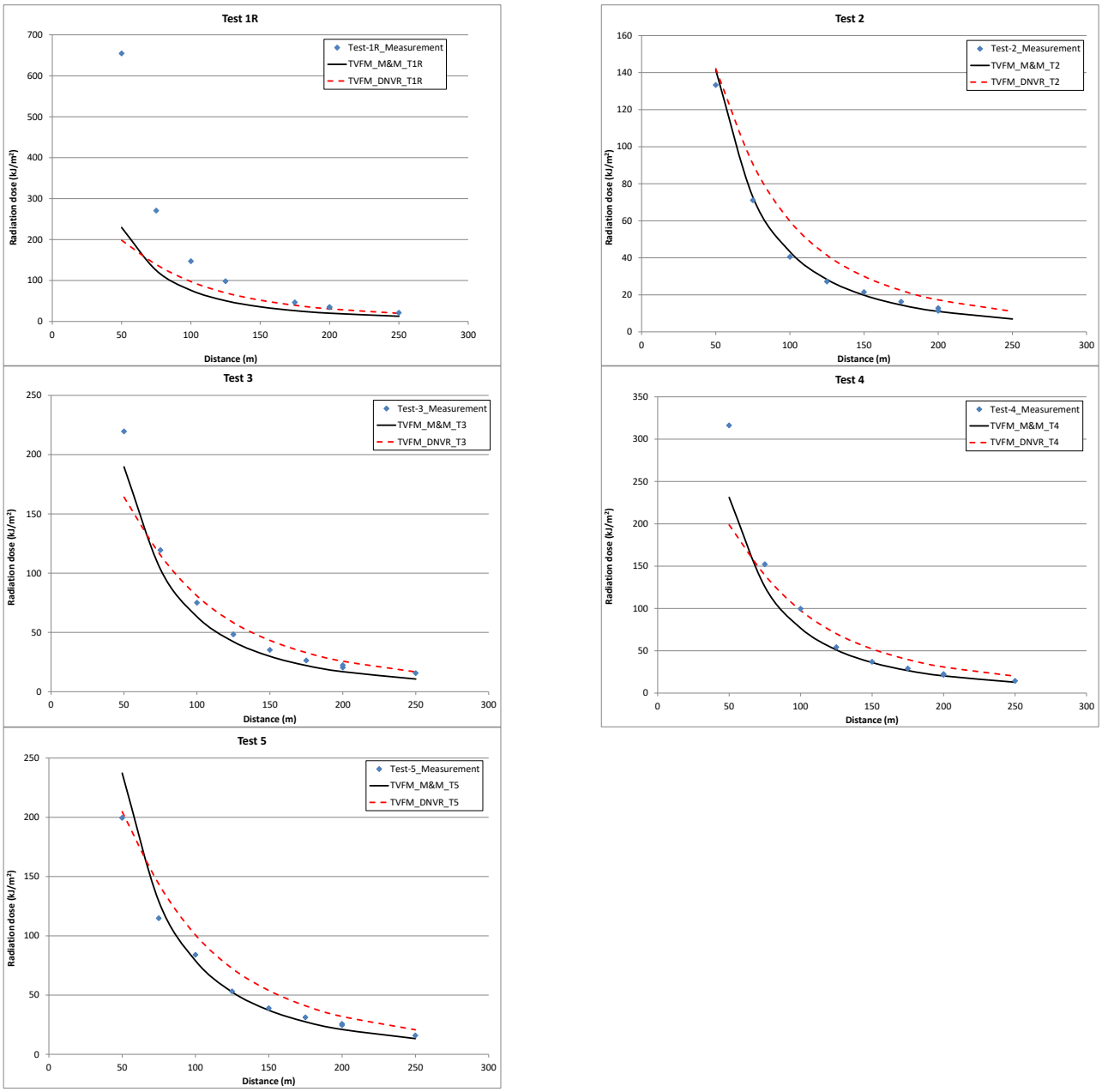

Figure 16. Validation of Martinsen and Marx model (Tests 1R – 5, Johnson et al., 1991) – radiation dose versus distance

The plots depict the variation of measured and predicted radiation dose with distance at various observer locations, north and west of butane (tests 1R-4) and propane (test 5) BLEVEs.

4.1.5 Flame height versus time

Figure 19 shows the measured and predicted ("TVFM_M&M") variation in flame height with time for the BLEVEs reported by Johnson et al. (1991), i.e. Tests 1R – 5 (see Table 7).

From Figure 19, the following can be observed:

- The Martinsen and Marx model generally tends to (marginally) over-predict flame heights with time, particularly as the flame goes to extinction.
- The predicted trend / shape in the flame height versus time shows very good agreement with measured data with flame height seemingly increasing with time gradually, for an intervening period of time and thereafter rapidly as the flame goes to extinction.

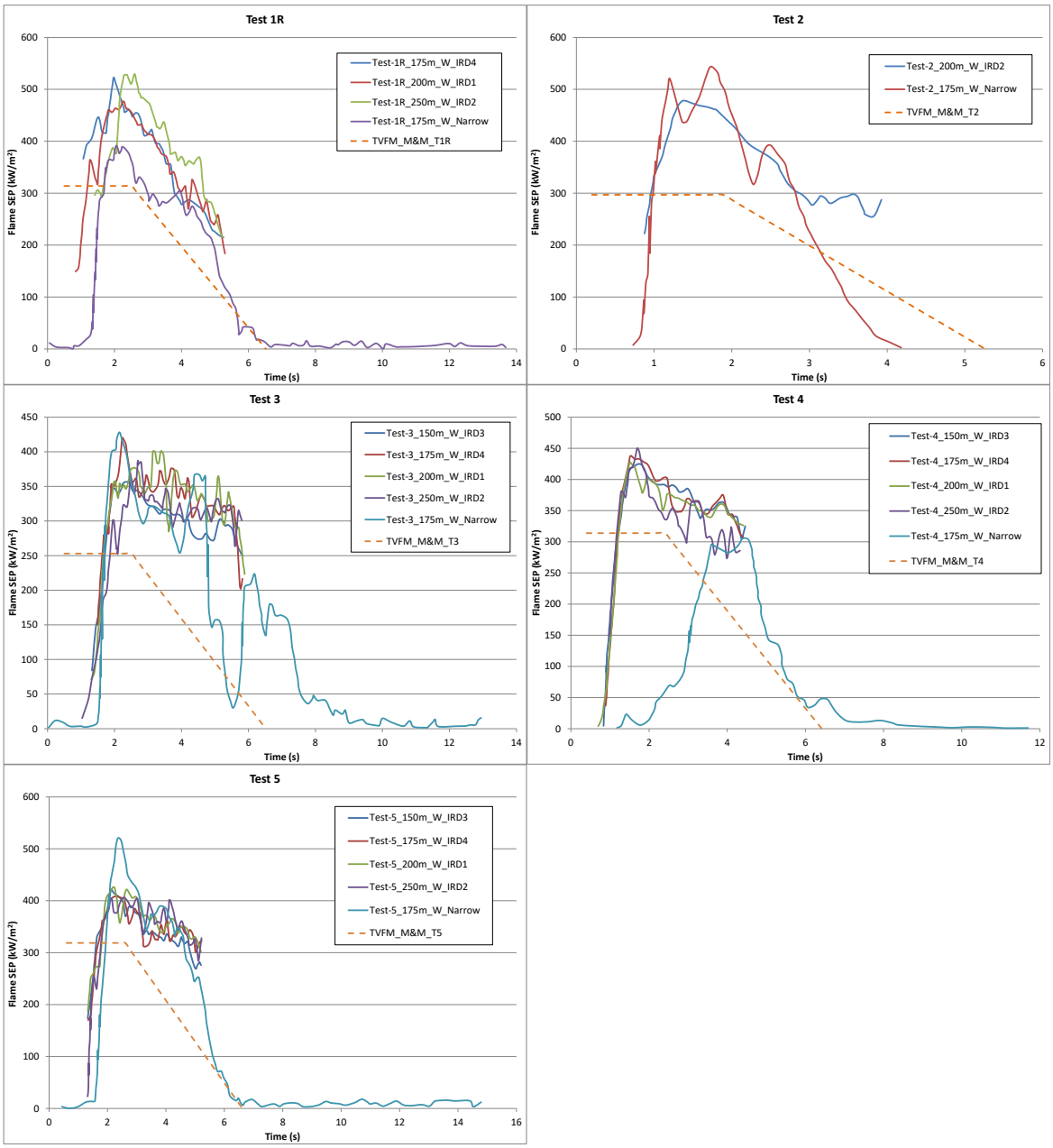

Figure 17. Validation of Martinsen and Marx model (Tests 1R – 5, Johnson et al., 1991) – flame SEP versus time

The plots depict the measured and predicted variation of flame SEP with time for butane (tests 1R–4) and propane (test 5) BLEVEs.

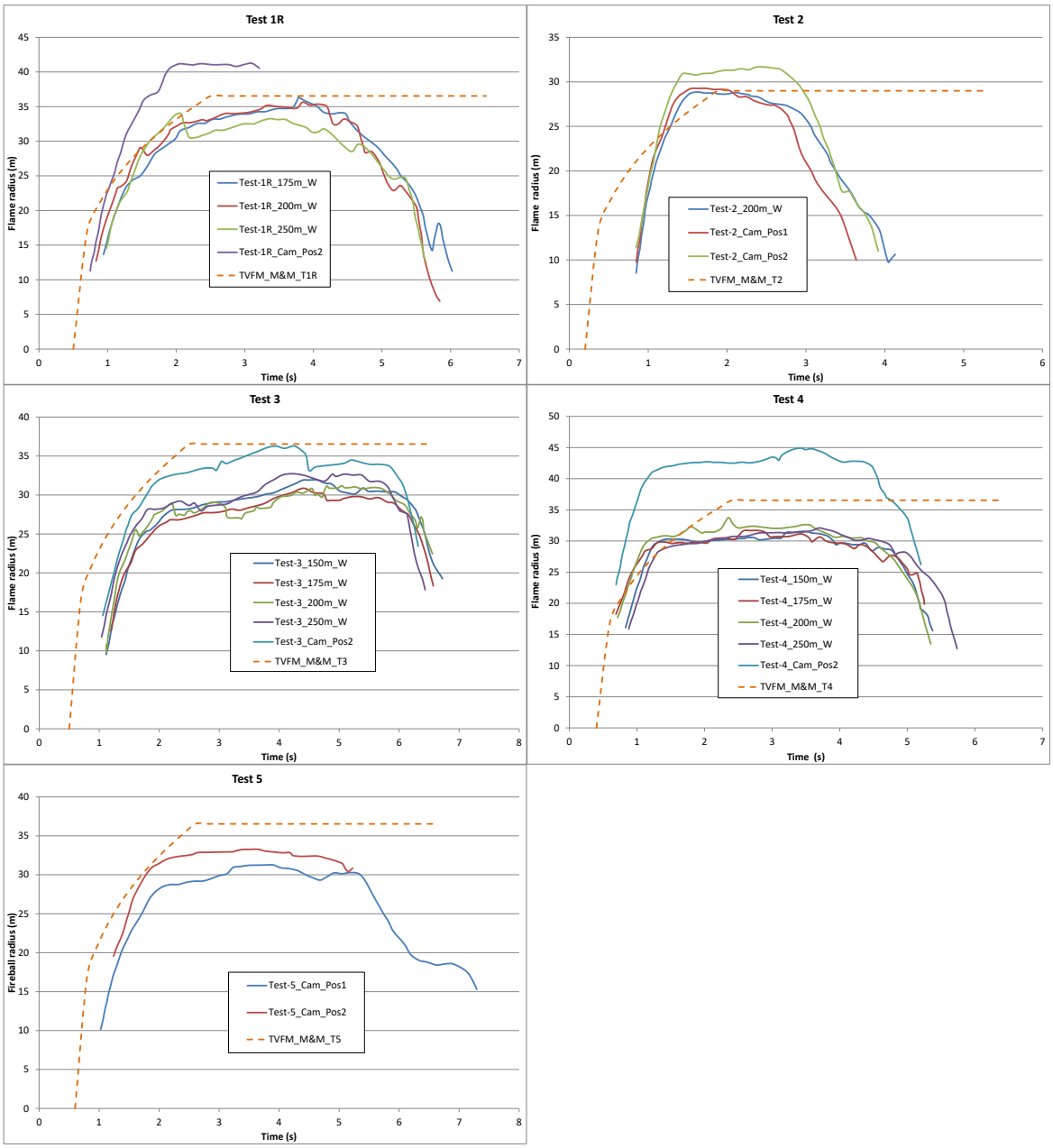

Figure 18. Validation of Martinsen and Marx model (Tests 1R – 5, Johnson et al., 1991) – flame radius versus time

The plots depict the measured and predicted variation of flame radius with time for butane (tests 1R–4) and propane (test 5) BLEVEs.

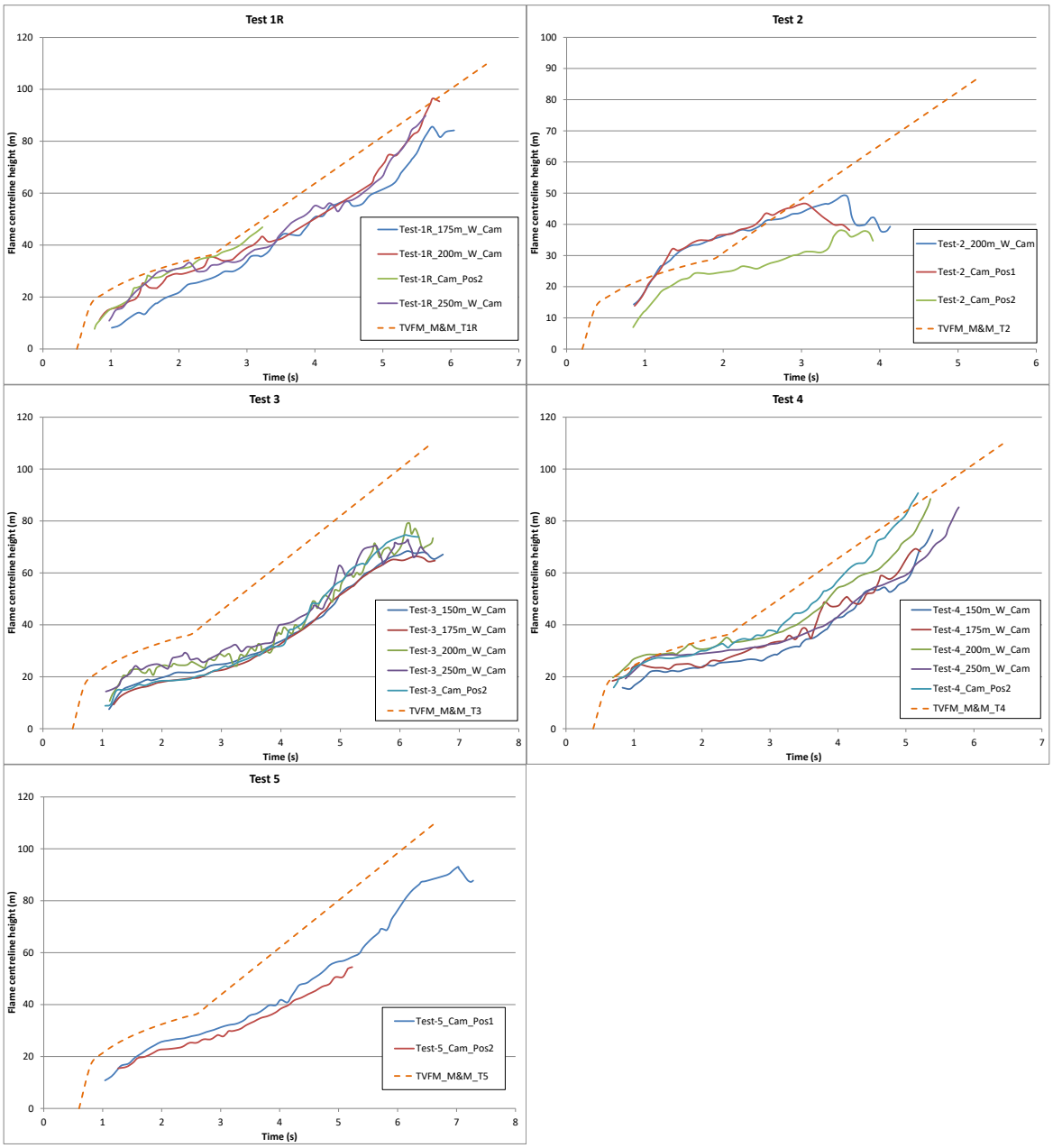

Figure 19. Validation of Martinsen and Marx model (Tests 1R – 5, Johnson et al., 1991) – flame centroid height versus time

The plots depict the variation of measured and predicted flame centroid height with time for butane (tests 1R–4) and propane (test 5) BLEVEs.

4.2 Roberts (2000) medium to large scale tests: Propane (LPG) BLEVEs

Table 8 presents a summary of the prevailing test and ambient conditions during the propane BLEVEs reported by Roberts et al. (2000)[8] (see section 3.1.5.2 for further details).

Description	Test number / identifier			
	1	2	3	4
Released Material	Propane	Propane	Propane	Propane
Released mass [kg]	279	710	1272	1708
Liquid fill ratio [%]	20	41	60	85
Burst pressure [Mpa]	1.65	2.13	1.86	2.44
Average wind speed [m/s]	4[28]	3[28]	5	2.5
Wind direction relative to direction of jet fire [°]	180	180	0	180
Wind direction relative to true North (see Figure 20)	Westerly	Westerly	South-easterly	Westerly
Ambient temperature [°C]	19	20	17	18
Relative humidity [%]	80	60	95	90
Ambient pressure [bara]	0.976	0.98	0.982	0.994

Table 8 Summary of test and ambient conditions: propane BLEVEs (Roberts et al., 2000)

Incident thermal radiation measurements were taken at between 50m and 250m along fixed lines, A, B, C, D and E relative to the propane vessel as illustrated in Figure 20. Lines A, B, C, D and E are inclined at 270°, 310°, 355°, 45° and 90°, respectively, relative to true North. The ruptured vessel's principal axis (horizontal cylinder with tori-spherical ends) is oriented 15° relative to true North. Both slow response (Land / Medtherm) and fast response (Medtherm / International Research and Development [WIRD]) wide-angle radiometers were employed.

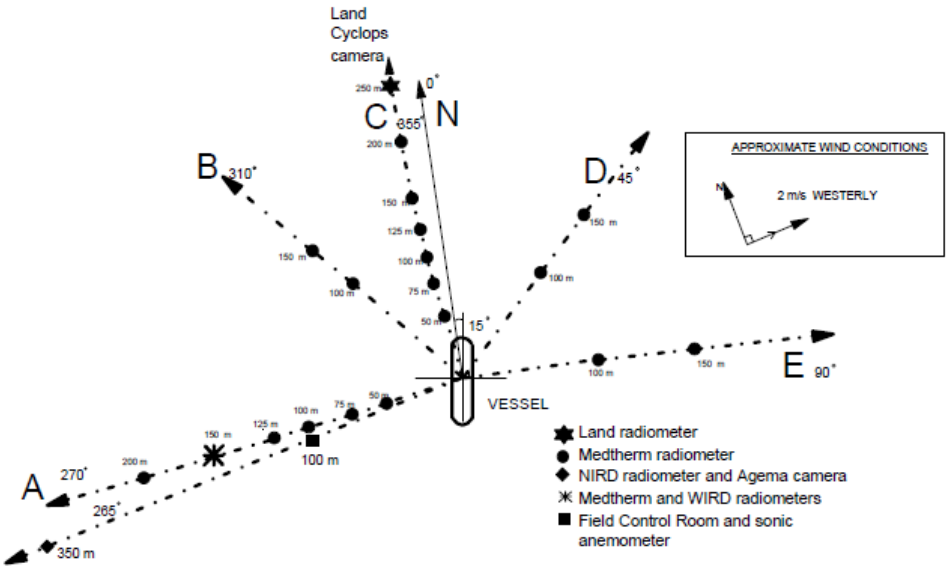

Figure 20. Instrument layout for (1708kg) propane BLEVEs (Roberts et al., 2000)

Flame surface emissive power (SEP) measurements were taken using an Agema 900 Infrared Thermal Imaging System and by a narrow angle, fast response radiometer (NIRD). The thermal images of the fireballs (used in determining fireball dimensions) were recorded using thermal imaging cameras oriented 90° apart for crosswind and upwind flame imaging measurements. The errors in the flame SEP and flame imaging measurements were reported as ±15% and ±5%, respectively.

4.2.1 Radiation intensity versus time

Figure 21 shows the measured and predicted ("TVFM_M&M") variation in radiation intensity at fixed observer locations 100m away from the 1708kg (85% fill) propane BLEVE along lines A, B, C, D and E. In each case, the observer is tilted so as to receive approximately the maximum radiation from the fireball.

[28] CLARIFY: Corresponds to wind speed data reported in Table 1, Roberts et al., 2000. Different wind speeds are quoted for the 279kg and 710kg propane BLEVEs in Table 3 of Roberts et al., 2000 (i.e. 3m/s and 4m/s, respectively)

From Figure 21, the following can be observed:

- The Martinsen and Marx model generally shows good agreement with measured peak incident radiation intensities. The peak radiation intensity (measured along line E) is marginally under-predicted. Roberts et al. (2000) state that the measured crosswind (line C) radiation intensities (and dosage) are higher than the upwind (line A) results due to cloud-drift as a result of the prevailing wind.
- The predicted radiation intensity versus time profiles are rather similar to measured data, each showing a relatively rapid increase to a peak value followed by a gradual decay in intensity as the flame goes to extinction. The Martinsen and Marx model appears to predict quicker radiation rise and shorter duration as compared to measured data.

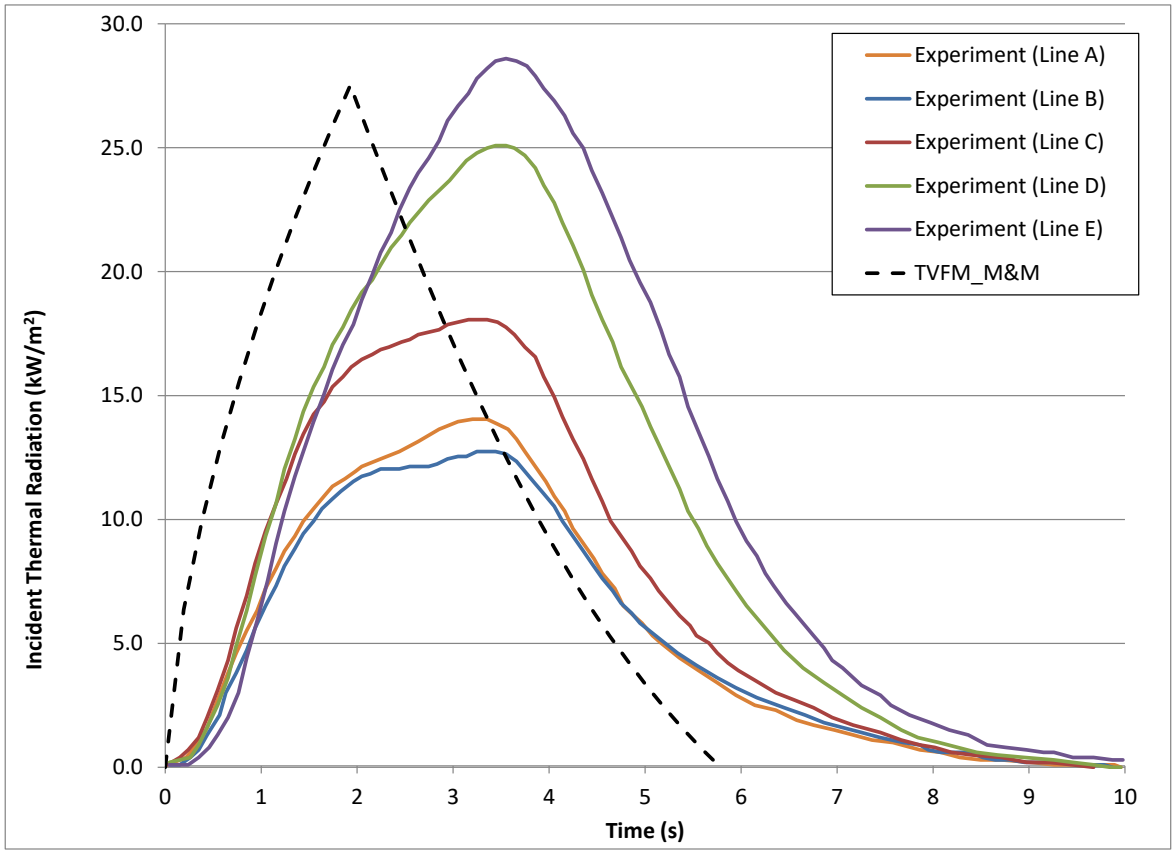

Figure 21. **Validation of Martinsen and Marx model (Roberts et al., 2000) – radiation intensity versus time**
The plot depicts the variation of measured and predicted radiation intensity with time at various observer locations: 1,708kg propane BLEVE from an initial pressure of 24.4barg. The observer locations are at a fixed distance of 100m relative to the propane vessel but inclined at 270° (Line A), 310° (Line B), 355° (Line C), 45° (Line D) and 90° (Line E) relative to the true North. The ruptured vessel's principal axis (horizontal cylinder with tori-spherical ends) is oriented 15° relative to the true North.

4.2.2 Radiation dose versus distance

Figure 22 shows the measured and predicted ("TVFM_M&M") variation in radiation dosage at various observer locations along lines A, B, C, D and E following the BLEVE of the 1708kg (85% fill) propane vessel. For comparison, Figure 22 also shows the predicted variation in radiation dosage at pertinent observer locations as derived from the PHAST/SAFETI 6.7 "Roberts/TNO hybrid" static fireball and radiation model ("TVFM_DNVR").

From Figure 22, the following can be observed:

- Both the "Roberts/TNO hybrid" and Martinsen and Marx models show good agreement with the range of measured radiation dosage data. On average, the Martinsen and Marx model shows better agreement with measured data as compared to the static "Roberts/TNO hybrid" fireball model, with the "Roberts/TNO hybrid" model tending to predict lower radiation doses in the near field and higher values in the far-field. Over or under-prediction in simulated data are likely to be influenced by cloud drift effects observed by Roberts et al. (2000) together with the reasons proffered in section 4.1.2 for the "Roberts/TNO hybrid" model.
- As with the Johnson et al. (1991) data, the predicted trend in the decay of radiation dosage with distance generally shows good agreement with measured data, with radiation dose showing a rapid decay in the near field and a less dramatic decrease in slope with increasing separation distance.

4.2.3 Flame SEP versus time

Figure 23 shows the measured and predicted ("TVFM_M&M") variation in flame SEP with time following the BLEVE of the 1708kg (85% fill) propane vessel.

From Figure 23, the following can be observed:

- The Martinsen and Marx model generally under-predicts the peak measured flame SEP, while showing good agreement with the crosswind averaged (Line C) data, noting that the predicted flame SEP should, by definition, be compared against the time-averaged flame SEP (i.e. prior to flame lift-off).
- The predicted trend in flame SEP with distance generally shows good agreement with measured data. The Martinsen and Marx model assumes instantaneous rise to peak flame SEP, i.e. upon ignition. This modelling assumption is to a large extent confirmed by measured data. Following the attainment of the peak flame SEP, measured data appears to suggest the flame SEP to remain relatively constant before decaying to a finite value upon flame extinction. The Martinsen and Marx model is observed to show relatively good agreement with the observed trend in the flame SEP as it assumes (i.e. post maximum flame SEP) flame SEP to remain constant prior to flame lift-off (for a third of the fireball duration) and to linearly decrease to zero upon flame extinction.

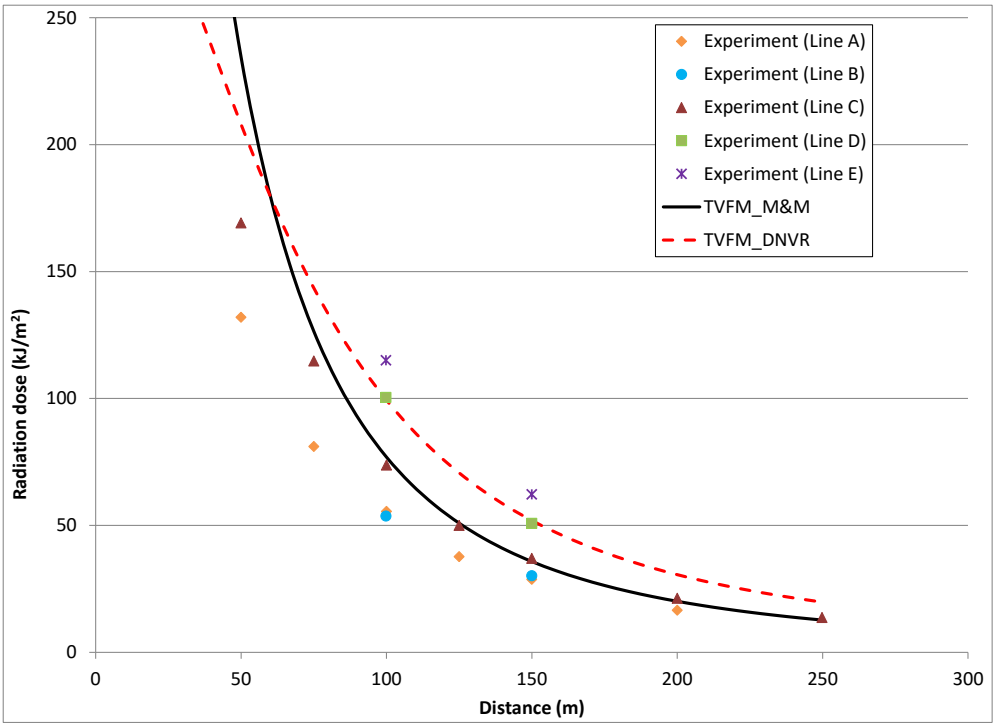

Figure 22. **Validation of Martinsen and Marx model (Roberts et al., 2000) – radiation dose versus distance** The plot depicts the variation of measured and predicted radiation dose with distance at various observer locations: 1,708kg propane BLEVE from an initial pressure of 24.4barg. Lines A, B, C, D and E are inclined at 270°, 310°, 355°, 45° and 90°, respectively, relative to the true North. The ruptured vessel's principal axis (horizontal cylinder with tori-spherical ends) is oriented 15° relative to the true North.

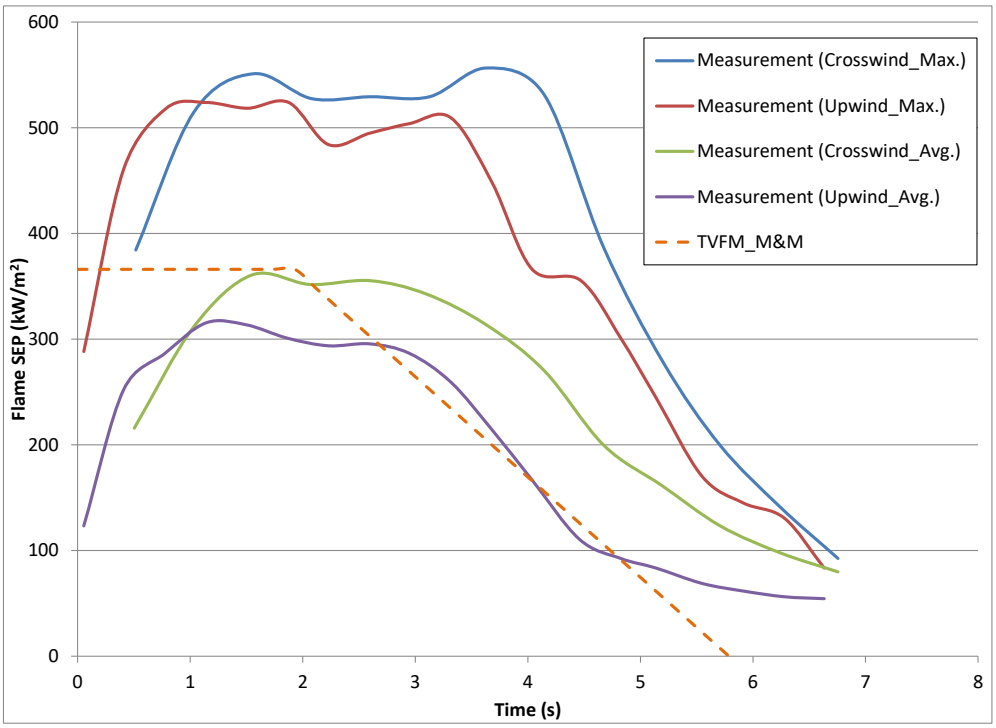

Figure 23. **Validation of Martinsen and Marx model (Roberts et al., 2000) – flame SEP versus time**
The plots depict the measured and predicted variation of flame SEP with time: 1,708kg propane BLEVE from an initial pressure of 24.4barg.

4.3 Overall results

Figure 24 and Figure 25 show the overall predicted radiation dose and peak intensities at various observer locations based on the "Roberts/TNO hybrid" ("TVFM_DNVR") and Martinsen and Marx ("TVFM_M&M") fireball models as compared to measured data for the Johnson et al. (1991) and Roberts et al. (2000) experiments.

From Figure 24 and Figure 25 it can be observed in general that:

- The Martinsen and Marx model shows very good agreement with measured data particularly in the far field, while tending to under-predict measured data in the near field (i.e. high radiation dose or peak intensity observer locations, or locations close to the ensuing fireball). On average, the Martinsen and Marx model shows better agreement with measured data as compared to the static "Roberts/TNO hybrid" fireball model.
- The "Roberts/TNO hybrid" fireball model tends to under-predict peak radiation intensity data for the various close-to-ground level observer locations studied, as the model assumes ensuing flames to be permanently elevated (i.e. increased flame-to-ground-level-observer distances). Furthermore, as with the Martinsen and Marx model, the "Roberts/TNO hybrid" fireball model tends to under-predict measured radiation dose data in the near field and over-predict in the far-field.
- It is judged that the poor agreement of predicted results against measured data in the near-field are driven by the reasons proffered in section 4.1.1 (i.e. flame directionality / non axi-symmetry and wind-drift effects) together with the reasons proffered in section 4.1.2 for the static "Roberts/TNO hybrid" model.

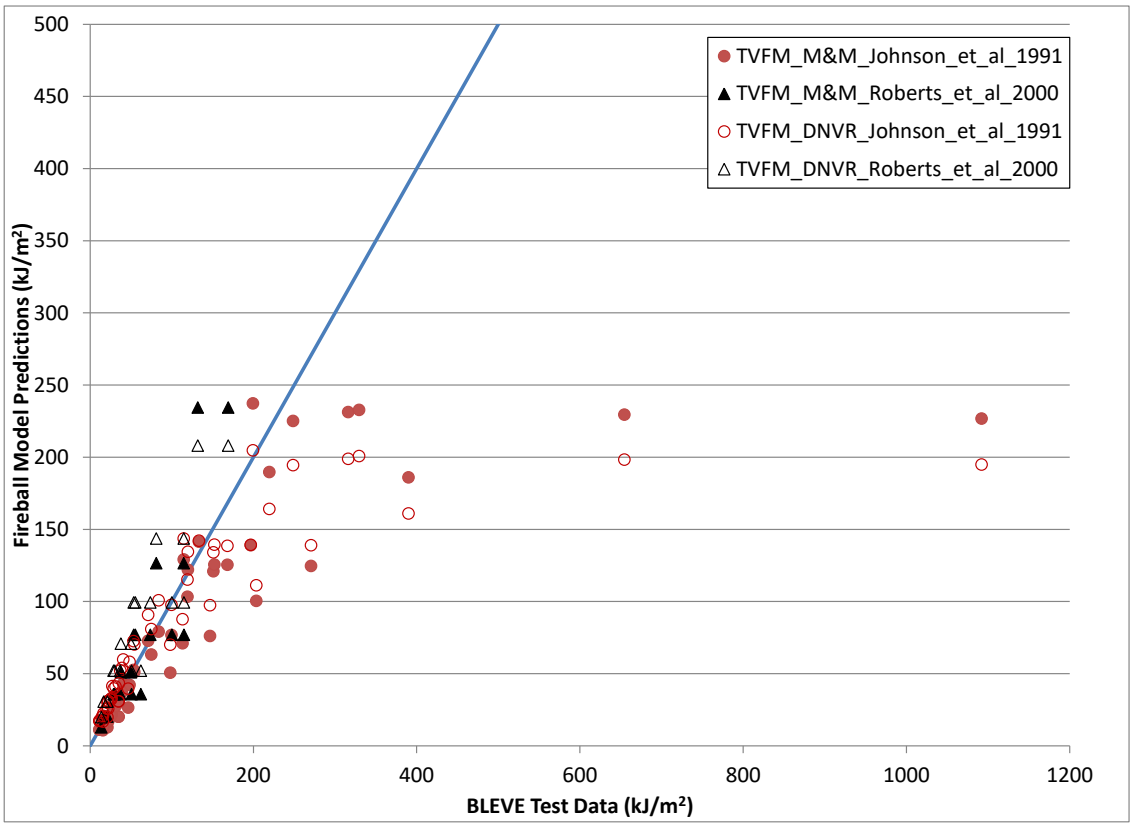

Figure 24. **Validation of Martinsen and Marx model (Johnson et al., 1991; Roberts et al., 2000) –radiation dose**

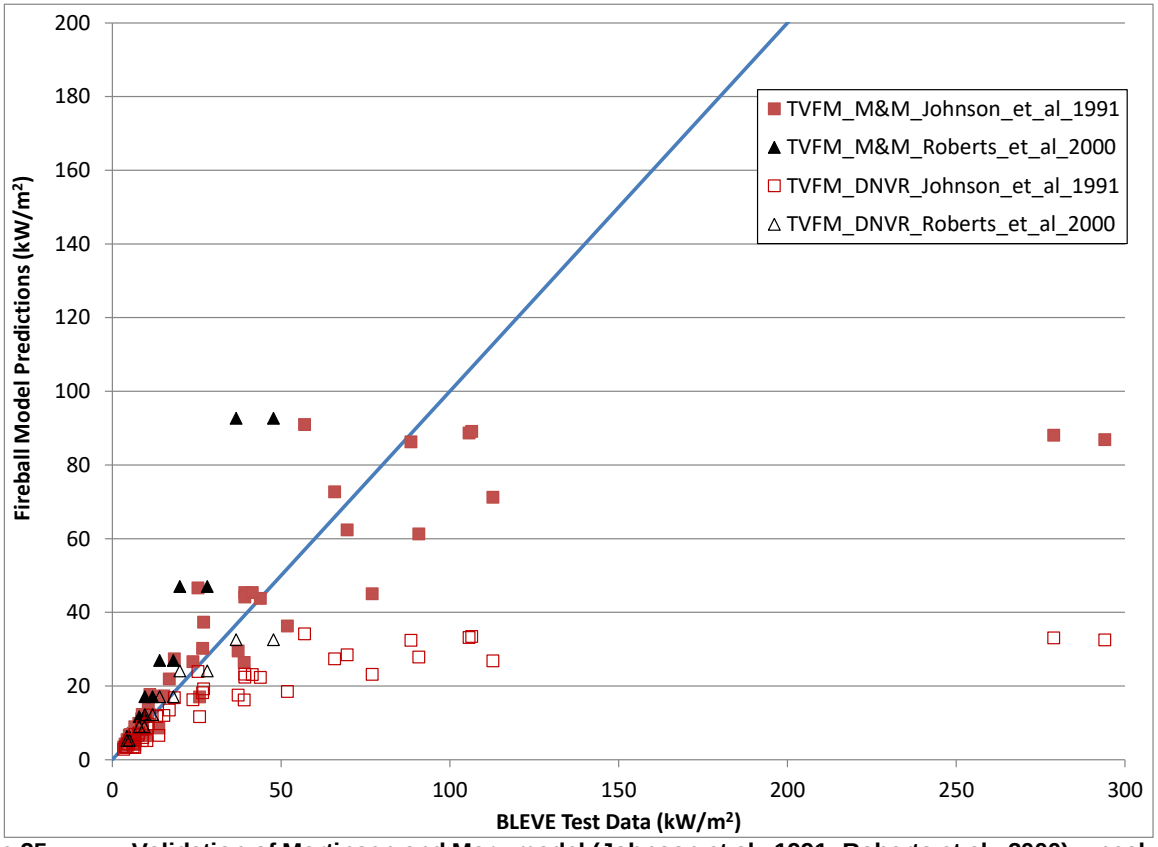

Figure 25. **Validation of Martinsen and Marx model (Johnson et al., 1991; Roberts et al., 2000) – peak radiation intensity**

5 CONCLUSIONS AND RECOMMENDATIONS

5.1 Conclusions

This document describes the theory of the time-varying (Martinsen & Marx) and static (HSE and TNO) fireball models (BLEV-HSE/BLEV-TNO) which are implemented in PHAST/SAFETI. The document also details a review of literature on static and dynamic fireball models together with an overview of previous literature studies undertaken including the review by DNV Benelux for the Flemish Government.

Attention has been paid to models describing the dynamic behaviour of fireballs. Literature on dynamic fireball models have been discussed under two categories:

- Catastrophic vessel failure fireball models: these cover fireballs stemming from BLEVEs or pressure vessel bursts. Three models have been identified and reviewed in this document, these include:
  - The BG/GL fireball model as reported by Pritchard (1985)
  - The Shell fireball model as detailed in Shield (1993 / 1995)
  - The Quest fireball model as described by Martinsen and Marx (1999) and implemented within PHAST/SAFETI.
- Pipeline release fireball models: these cover fireballs stemming from immediate/delayed ignited vertical (impulsive) jet releases from pipelines. Two models have been reviewed in this report, these include:
  - The GL impulsive fireball model as reported by Cleaver and Halford (2014)
  - The Shell vertical jet fireball model as reported by Cracknell and Carlsey (1997)

A comparative analysis of the key characteristics of each model and associated performance of model predictions against experimental / field data has also been undertaken. Also included are results of model validation of the Martinsen and Marx time-varying fireball model, as implemented in PHAST/SAFETI, against published experimental data for large scale (2tonne) propane and butane BLEVEs (Johnson et al., 1991) and medium to large scale propane BLEVEs reported by Roberts et al., 2000. For the model validation exercise, the predicted radiation dose and peak intensities at various observer locations based on the PHAST/SAFETI “Roberts/TNO hybrid” static fireball model (“TVFM_DNVR”) has been presented for comparison.

The key conclusions from the model review, validation and comparative analysis are summarized below, where:

In terms of catastrophic vessel failure fireball models:

- The Shell (Shield 1993, 1995) appears to be the most complex in terms of formulation, rigour and ease of implementation of the three studied models followed by the BG/GL model.
- The Shell (Shield 1993, 1995) model appears to be particularly suited for fireballs stemming from grounded (or close-to-ground) catastrophic vessel failures as it assumes the flame to start-off as a grounded hemisphere.
- The BG model conservatively assumes the entire contents of the ruptured containment to contribute to the developing fireball, while the Shell and Quest models allow for potential droplet rainout. The Shell model, however, appears to be only suitable for modelling fireballs stemming from BLEVEs and not the rupture of pure gas/vapour vessels.
- All three models account for three distinct regimes in the fireball development, i.e., flame ignition to lift-off, lift-off to break-up and break-up to extinction and primarily differ in assumptions as to flame behaviour during these regimes.
- In terms of performance against experimental / field data:
  - In general, the Quest model is observed to give the closest agreement with the range of data recorded during the propane and butane BLEVE tests. The above observation may not totally apply to the Shell model as only a limited amount of data (Test 4) was considered in the comparative analysis. It should be noted that both the Quest and Shell models were largely fitted against the Johnson et al. (1991) test data and as such, the latter may not constitute an independent basis for model performance assessment.
  - The Quest model shows overall very good agreement for radiation dose predictions except in the near-field for a limited number of cases. Thus, excellent results would be obtained for lethalities (presuming an accurate probit function).
  - As with the Martinsen and Marx model, the “Roberts/TNO hybrid” static fireball model tends to under-predict measured radiation dose data in the near field and over-predict in the far-field; while, on average, the Martinsen and Marx model is observed to show better agreement with measured data.
  - Only a limited amount of data (flame duration) was considered in the comparative analysis involving the Shell model, as such only limited conclusions may be drawn from the analysis undertaken. In general, for the cases considered, comparisons undertaken and dynamic fireball models studied, the Shell model is observed to give the closest agreement with measured data for flame durations. Furthermore, the BG model is observed to give generally closer agreement with the range of data recorded during the JIVE (Roberts et al., 2000) propane BLEVE tests when compared against simulated data using the Quest model.

In terms of the impulsive pipeline release fireball models:

- The Shell model is relatively simple and employs empirical correlations in describing flame characteristics. However, the BG/GL model is significantly more complicated and flame characterization requires the solution of mass, momentum and combustion differential equations.
- The BG/GL impulsive fireball model may only be applied to gas / vapour phase time-varying releases where the material is naturally buoyant. However, the Shell model may be applied to a wide variety of fluid states and materials but is only suited for steady state releases.

5.2 Recommendations

In general, it is not recommended to model the development of fireballs from impulsive pipeline releases using catastrophic vessel failure fireball models and vice-versa. For impulsive jet releases, the models described in this document may be used, albeit with care; readers are advised to take particularly note of the various model limitations documented in this report (see sections 3.1 and 3.2).

5.2.1 Catastrophic vessel failure fireball models

The key recommendations relating to catastrophic vessel failure fireball models within the PHAST/SAFETI product suite are as follows:

- Extend the Martinsen and Marx (1999) model to account for wind-drift effects and the modelling of non axi-symmetrical flames (e.g. using vessel-shape correction factors).
- Undertake additional validation of the Martinsen and Marx (1999) model against any additional independent field data on BLEVEs / fireballs as this information become available.
- Undertake a detailed comparison of the BG and Shell fireball models against available experimental data with the aim of confirming the overall performance of the studied models.
- Combination of the fireball and BLEVE-blast explosion models into a composite model
- Incorporation of a new model to the BLEVE-blast-Fireball models to predict the maximum range of different sized projectiles resulting from pressure-vessel bursts.

5.2.2 Impulsive pipeline release fireball models

The key recommendations from the literature review detailed in this document relating to impulsive pipeline release fireball models are as follows:

- Given its simplicity, wider range of applicability and subject to further feedback from Shell, implement the Shell (Cracknell and Carlsey, 1997) model
- Undertake detailed validation of the Shell (Cracknell and Carlsey, 1997) model against additional independent experimental/field data.
- Subject to the outcome of the above, incorporate model within future versions of Phast, Safeti and SAFETI-NL.
- Extend the Shell impulsive jet fireball model to account for wind-drift effects.

NOMENCLATURE

$C_{p,Liq}$	=	Specific heat capacity of the fluid at constant pressure [J/kg/K]
E_f	=	Surface emissive power of the flame [W/m^2]
$f_{correction}$	=	3 (mass correction factor based on CCPS recommendation) [-]
f_s	=	Fraction of total available heat energy radiated by the flame [-]
f_{Vapour}	=	Mass fraction of vapour released following vessel rupture [-]
H_{Flame}	=	Fireball lift-off height [m]
ΔH_C	=	Net available heat for radiation [J/kg]
ΔH_{Comb}	=	Heat of combustion of the fuel [J/kg]
ΔH_{Vap}	=	Latent heat of vaporisation of the fuel at its boiling point [J/kg]
i	=	Circles index (i varies from 1 to N)
$M_{Flammable}$	=	Mass of fuel involved in the fireball [kg]
M_{Input}	=	Total inventory released following vessel rupture [kg]
N	=	Total number of circles (N is currently equal to 10)
P_{Sat}	=	fuel's saturated-vapour/vessel-burst pressure at the point of vessel failure [N/m^2]
r_{Flame}	=	Maximum fireball radius [m]
t_{Flame}	=	Fireball duration [s]
T_{Amb}	=	Ambient temperature [K]
T_{Flame}	=	Flame temperature (≈2250K) [K]
x_i	=	Horizontal position of the centre of circle i [m]
z_i	=	Vertical height of the centre of circle i above ground level[m]

Greek letters

φ_i	=	Angle of inclination of circle i with respect to the horizontal [º]
ϑ_i	=	Angle between the vertical and the cord joining the fireball centre to the circumference of circle i [º]

APPENDICES

Appendix A. Verification of the static fireball (BLEV-HSE and BLEV-TNO) models

The following discusses the results of the verification of the BLEV-HSE and BLEV-TNO models. The first case relates to the simulation of the fireball characteristics following the rupture of an LPG (propane) tank using the BLEV-TNO model. This case attempts to reproduce the simulated results in the "TNO-Yellow Book" example 6.6.5[4]. Subsequent verification of the BLEV-TNO and BLEV-HSE models involve the comparison of simulated flame radius and duration for different values of $M_{Flammable}$ against similar data generated in Microsoft Excel.

A1. Yellow Book example 6.6.5[4]

Table 9 lists pertinent information supplied in the "TNO-Yellow Book" example 6.6.5[4] for the simulation of the BLEVE of a propane road tanker.

Table 9 Pertinent information relating to the simulation of fireball characteristics following the failure of a propane road tanker

	Description	Value
1	Failure pressure [N/m^2]	16. x 10^5
2	Amount of liquid LPG released [kg]	19775
3	Flame temperature [K]	2000
4	Ambient temperature [K]	283
5	Fraction of vaporised LPG from liquid inventory	1
6	Vapour inventory at the point of vessel failure [kg]	Ignored

To simulate the complete vaporisation of the liquid inventory using the BLEV-TNO model, values of 10^{-5} and 10^5 are assumed for f_{Vapour} and $f_{correction}$ respectively. A comparison of the fireball characteristics simulated using the BLEV-TNO model and published results in the "TNO-Yellow Book" example 6.6.5[4] are summarised in Table 10.

Table 10 Comparison of simulated fireball characteristics using the BLEV-TNO model against published results in the "TNO- Yellow Book" example 6.6.5[4]

Fireball Characteristic	Published Result ("TNO- Yellow Book" example 6.6.5[4]	BLEV-TNO (Simulated data)
Fireball Radius [m]	80.7	80.7
Fireball Duration [s]	11	11
Flame Lift-off Height [m]	161.4	161.4
Flame SEP [kW/m^2]	284.9	282.5

From Table 10, the published and simulated results are observed to be in very close agreement. The slight difference observed between the published and simulated flame SEP can be ascribed to differences in the adopted values of ΔH_{Comb}, ΔH_{Vap}, and $C_{p,Liq}$ used in their respective calculation steps.

A2. Fireball radius

Figure 26 shows the simulated variation of fireball radius with $M_{Flammable}$ based on plotting equations (2) and (3) in Microsoft Excel and the BLEV-HSE and BLEV-TNO models. From Figure 26, very close agreement between the results generated using Microsoft Excel for evaluating equations (2) and (3), and simulated results using the BLEV-HSE and BLEV-TNO models is observed.

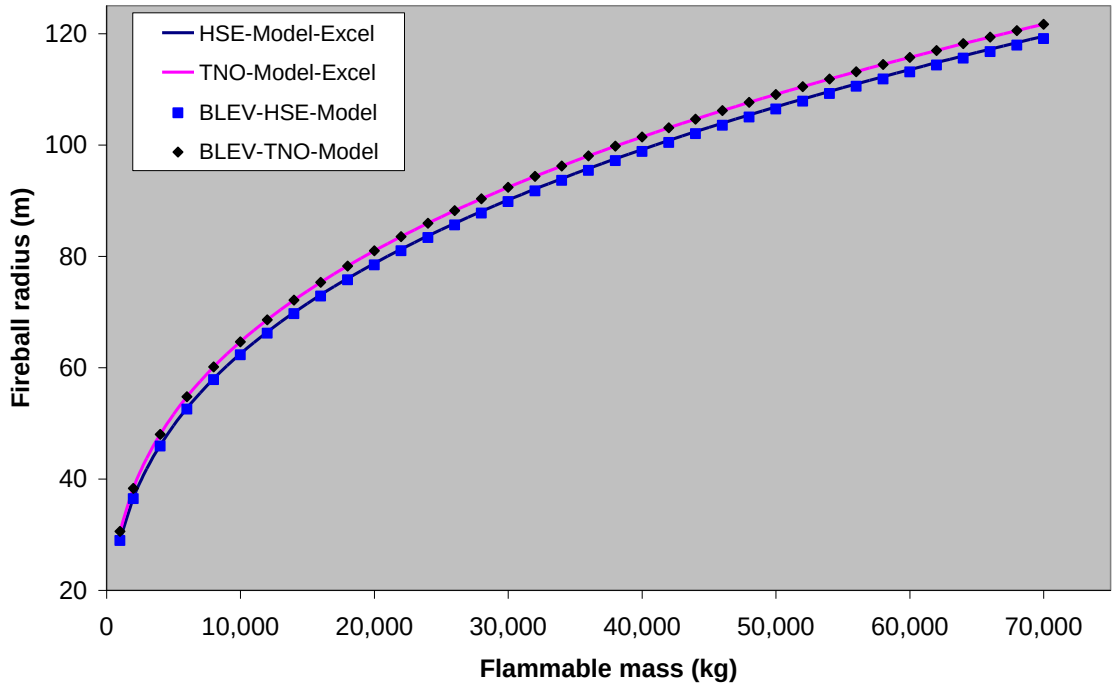

Figure 26 **Variation of predicted fireball radius with flammable mass using Microsoft Excel, the BLEV-HSE and BLEV-TNO models.**

A3. Fireball duration

Figure 27 shows the simulated variation of fireball duration with MFlammable based on plotting equations (4) and (5) in Microsoft Excel and the BLEV-HSE and BLEV-TNO models. From Figure 27, very close agreement between the results generated using Microsoft Excel for evaluating equations (4) and (5), and simulated results using the BLEV-HSE and BLEV-TNO models is observed. It can also be observed that simulated results using the BLEV-HSE model, in agreement with the inequality constraints in equation (4), switches from curve “HSE-Model (0.45*Mflame^1/3)-Excel” to curve “HSE-Model (2.59*Mflame^1/6)-Excel” when MFlammable ≥ 37,000kg.

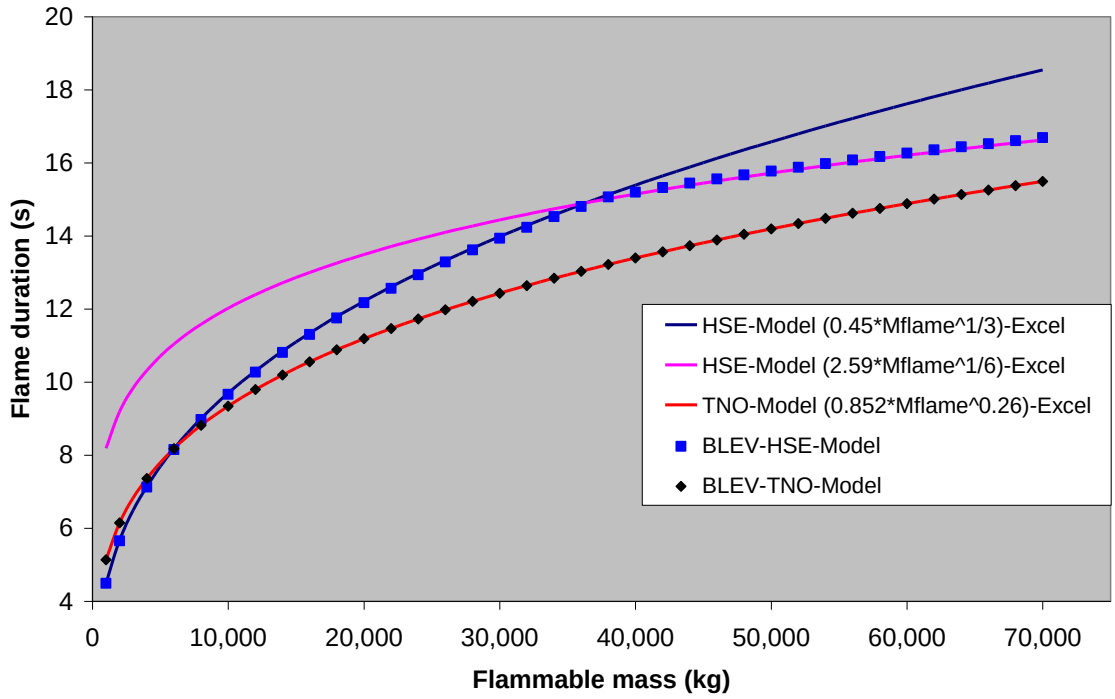

Figure 27 **Variation of predicted fireball duration with flammable mass using Microsoft Excel, the BLEV-HSE and BLEV-TNO models.**

Appendix B. Sensitivity analysis on the static fireball (BLEV-HSE and BLEV-TNO) models

The following summarises the observed trends following sensitivity analyses on the BLEV-HSE and BLEV-TNO models to model input parameters. Table 11 lists default parameter values and their corresponding variation during sensitivity tests on the BLEV-HSE and BLEV-TNO models. The method employed in these sensitivity tests involves the variation of an input parameter while all other default parameter values are kept constant.

Table 11 Parameter variations employed in the sensitivity analyses of the BLEV-HSE and BLEV-TNO models

No	Parameter/Input Variable	BLEV-HSE/ BLEV-TNO	
		Default	Parameter Variation
1	Flammable mass [kg]	1000	10, 10^2, 10^3, 10^4, $5x10^4$, 10^5, $5x10^5$, 10^6
2	Release temperature [K]	250	260, 270, 280, 290, 300, 310, 320
3	Atmospheric pressure [bara]	1.01325	0.5, 0.7, 0.9, 1.0, 1.1, 1.2
4	Vapour mass fraction [-]	0.5	0.0, 0.025, 0.05, 0.075, 0.1, 0.125, 0.15, 0.175, 0.2, 0.225, 0.25, 0.275, 0.3, 0.325, 0.35, 0.4, 0.5, 0.6, 0.7, 0.8, 0.9, 1

The effect of varying (i.e., increasing) the above input variables (within the ranges specified in Table 11) on r_{Flame}, t_{Flame}, H_{Flame} and E_f are summarised below:

B1. Effect of increasing flammable mass

Figure 28, Figure 29, Figure 30 and Figure 31, respectively, shows the effect of increasing the flammable mass on r_{Flame}, t_{Flame}, H_{Flame} and E_f based on the BLEV-HSE and BLEV-TNO models. From these figures, the following observations can be made:

- r_{Flame}, t_{Flame}, H_{Flame} and E_f increase with an increase in flammable mass.
- The BLEV-TNO model generally predicts wider fireball radius, initially shorter but later longer flame duration (i.e., longer flame duration when $M_{Flammable} \gtrsim$ 200, 000kg) and smaller flame surface emissive power when compared with simulated results based on the BLEV-HSE model.
- For the HSE model, below $M_{Flammable}$ = 37, 000kg, E_f is relatively constant and insensitive to increases in $M_{Flammable}$. Substituting equations (3) and (4) into equation (8) for the HSE model would yield an expression that is independent of $M_{Flammable}$ for $M_{Flammable}$ < 37, 000kg.

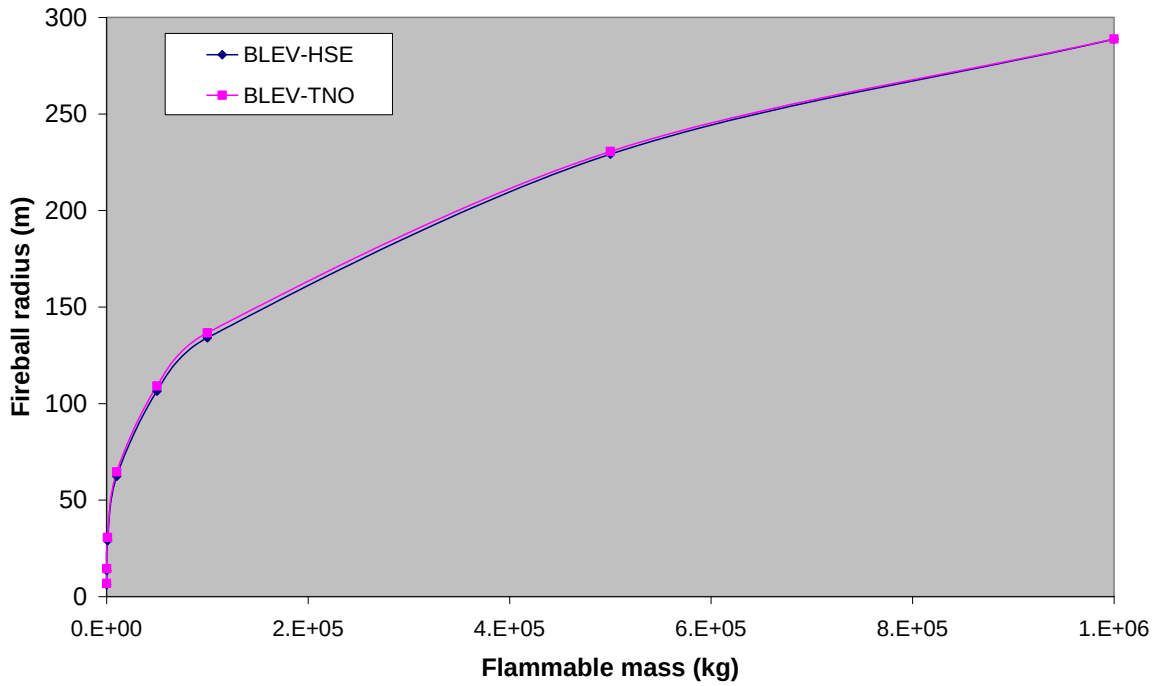

Figure 28 **Sensitivity analyses on the BLEV-HSE and BLEV-TNO models showing the variation of simulated fireball radius with flammable mass.**

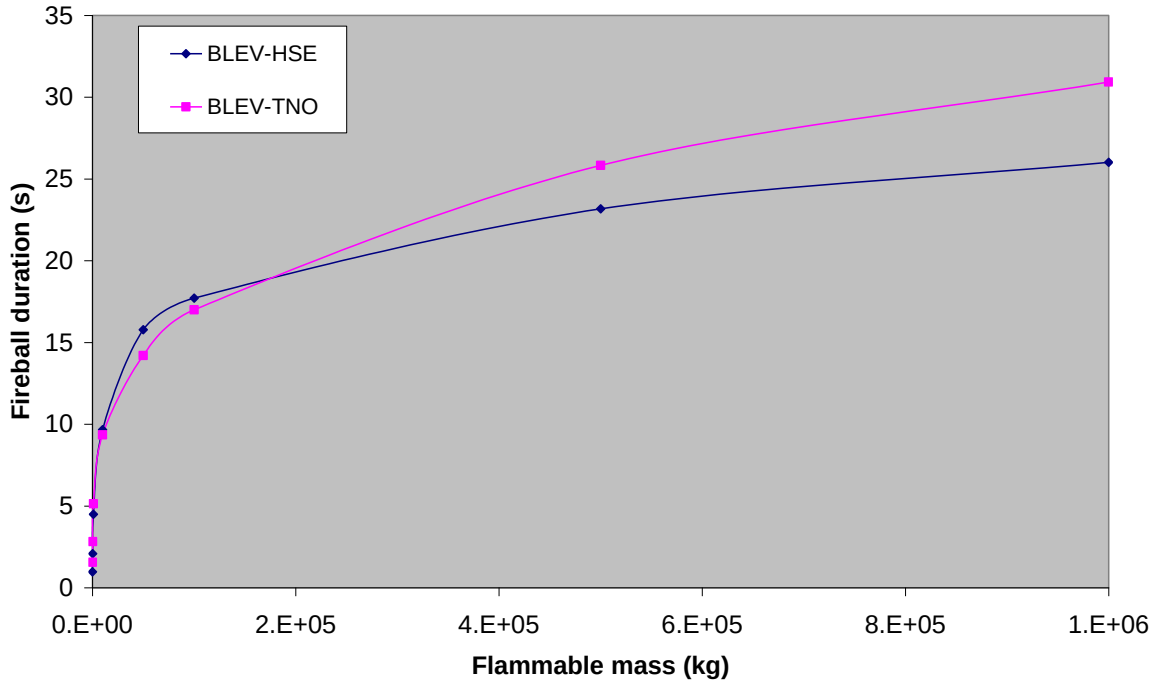

Figure 29 **Sensitivity analyses on the BLEV-HSE and BLEV-TNO models showing the variation of simulated fireball duration with flammable mass.**

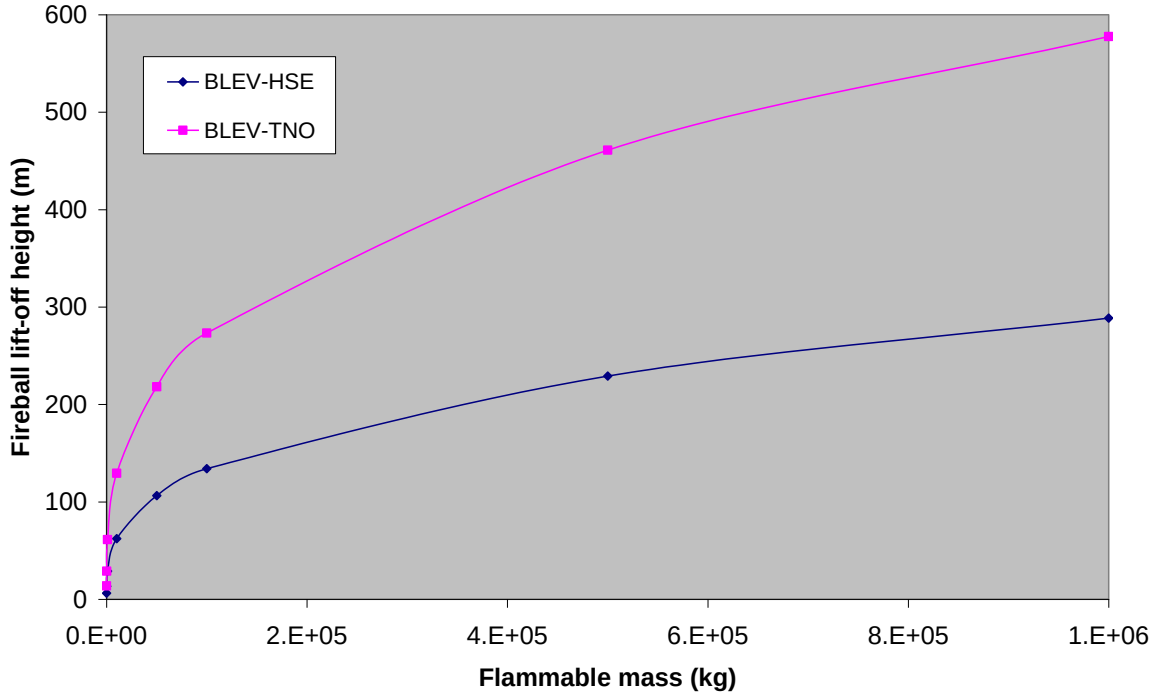

Figure 30 **Sensitivity analyses on the BLEV-HSE and BLEV-TNO models showing the variation of simulated fireball lift-off height with flammable mass.**

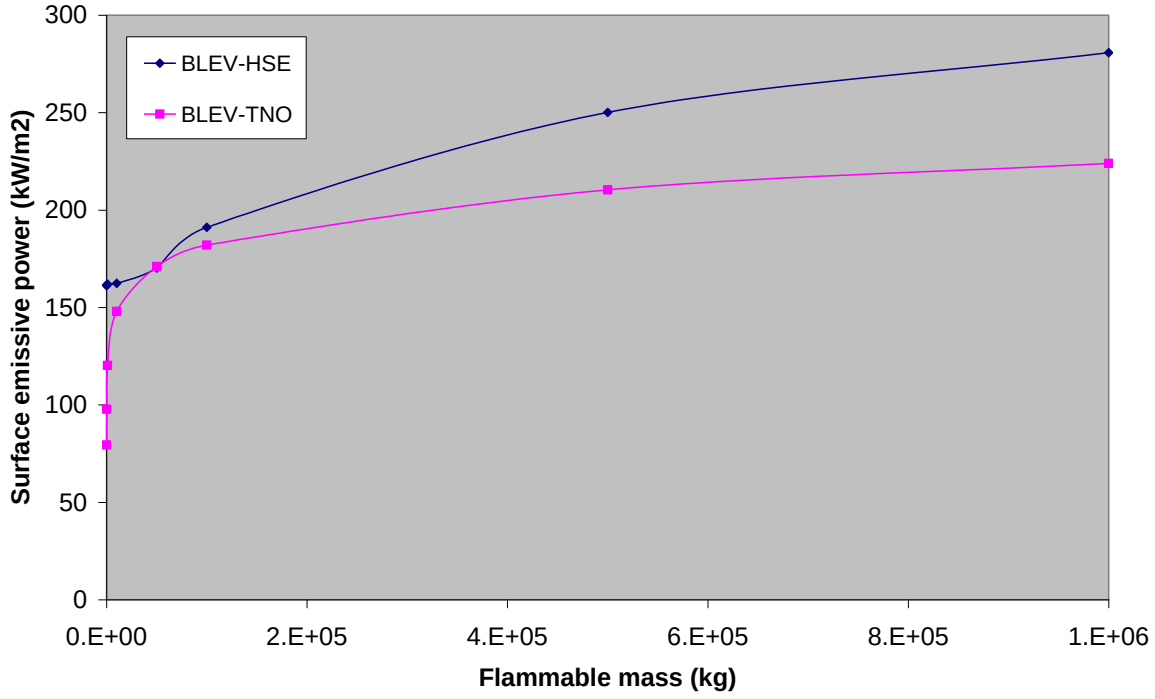

Figure 31 **Sensitivity analyses on the BLEV-HSE and BLEV-TNO models showing the variation of simulated fireball surface emissive power with flammable mass.**

B2. Effect of increasing burst temperature/pressure

For a fixed flammable mass, from equations (2) to (6), it can be easily deduced for the HSE and TNO fireball models that increase in the burst temperature/pressure will have no effect on r_{Flame}, t_{Flame}, and H_{Flame}. As such, only the behaviour of E_f with increase in the burst temperature/pressure is discussed below. Generally, for saturated fluids, increase in saturation

temperature corresponds to an increase in saturation pressure and vice-versa. Thus, results showing the behaviour of E_f following an increase in either the fluid's saturation temperature or pressure will suffice as an illustration for both cases.

Figure 32 shows the effect of increasing the burst temperature on the fireball's surface emissive power (E_f) as predicted by the BLEV-HSE and BLEV-TNO models. From Figure 32 the following can be observed:

- There is an approximate linear increase in E_f with a corresponding increase in saturation temperature.
- For a given saturation temperature, the BLEV-HSE model predicts a higher E_f when compared with simulated results using the BLEV-TNO model.

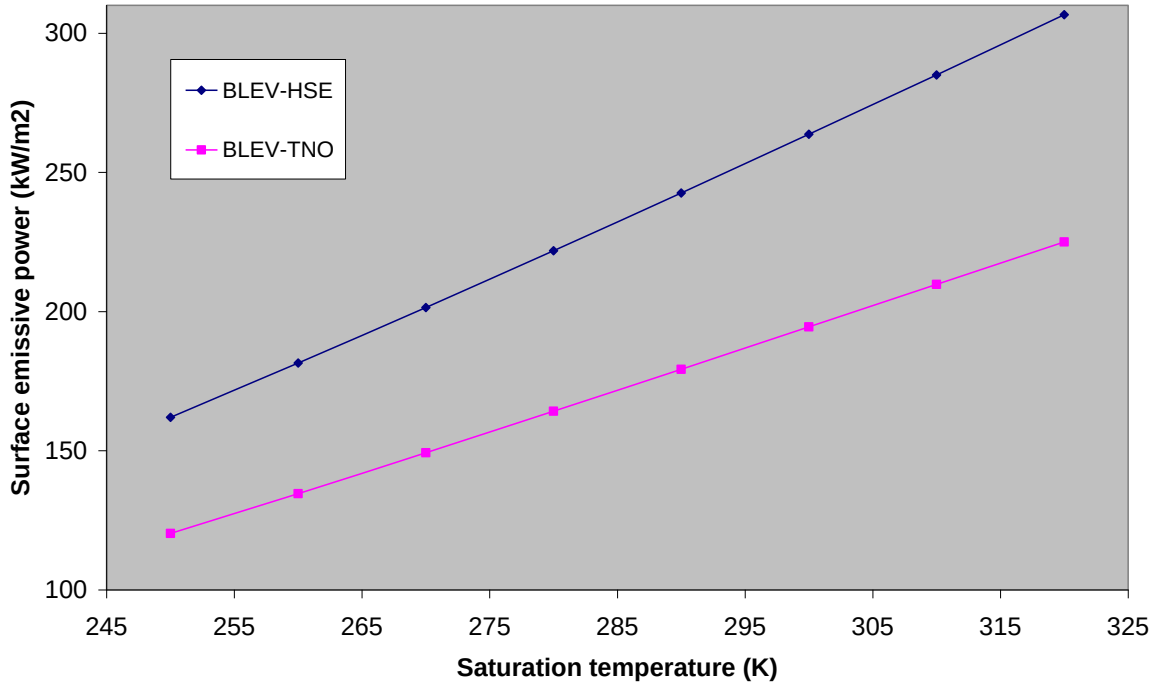

Figure 32 **Sensitivity analyses on the BLEV-HSE and BLEV-TNO models showing the variation of simulated fireball surface emissive power with fluid saturated vapour temperature at the moment of vessel rupture.**

B3. Effect of increasing atmospheric pressure

From equations (2) to (11), predicted r_{Flame}, t_{Flame}, H_{Flame}, and E_f, based on the HSE and TNO fireball models are expected to be insensitive to increase in the ambient pressure. However, the use of a modified form of equation (9) in the BLEV-HSE model (see footnote iii), makes the determination of E_f using the model sensitive to changes in ambient pressure.

Figure 33 shows the effect of increasing the ambient pressure on the fireball's surface emissive power (E_f) as predicted by the BLEV-HSE and BLEV-TNO models. From Figure 33 the following can be observed:

- Simulated results using the BLEV-HSE model show E_f as decreasing exponentially with increase in ambient pressure, while results obtained using the BLEV-TNO model show E_f as unaffected by changes in ambient pressure.

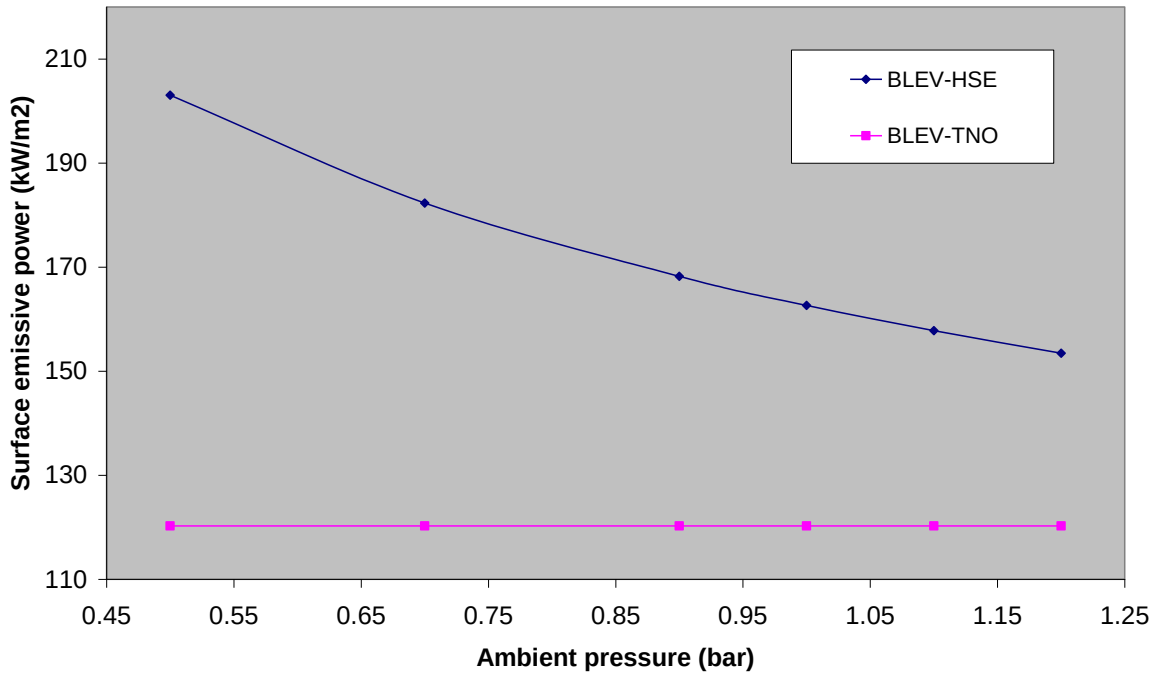

Figure 33 **Sensitivity analyses on the BLEV-HSE and BLEV-TNO models showing the variation of simulated fireball surface emissive power with the prevailing ambient pressure.**

B4. Effect of increasing burst vapour mass fraction

Figure 34, Figure 35, Figure 36 and Figure 37, respectively, show the effect of increasing the vapour mass fraction on r_{Flame}, t_{Flame}, H_{Flame} and E_f based on the BLEV-HSE and BLEV-TNO models. From these figures, the following observations can be made:

- Simulated results based on both models show r_{Flame}, t_{Flame} and H_{Flame} to increase exponentially from zero to a maximum value at vapour mass fraction ≈ 0.33 and thereafter remain constant at the maximum value.
- The BLEV-TNO model generally predicts wider fireball radius, higher flame lift-off heights, longer flame duration and smaller flame surface emissive power when compared with simulated results based on the BLEV-HSE model.
- Above zero vapour mass fraction, the predicted E_f based on the BLEV-HSE model is insensitive to increase in vapour mass fraction, while the simulated E_f, based on the BLEV-TNO model, increases with an increase in vapour mass fraction. The BLEV-TNO model, in its calculation of E_f, accounts for the effect of phase change and temperature rise in entrained liquid droplets that contribute to the flammable mass in a fireball. As such, the E_f calculated by the BLEV-TNO model is seen to be sensitive to the amount of liquid contributing to the fireball flammable mass. Based on the BLEV-TNO model, for a fixed fireball flammable mass, the higher the mass of entrained liquid, the lower the vapour mass fraction and estimated surface emissive power of the flame.

The results from the above sensitivity analyses also serve as added verification to the right implementation of the HSE and TNO fireball models in the BLEV models.

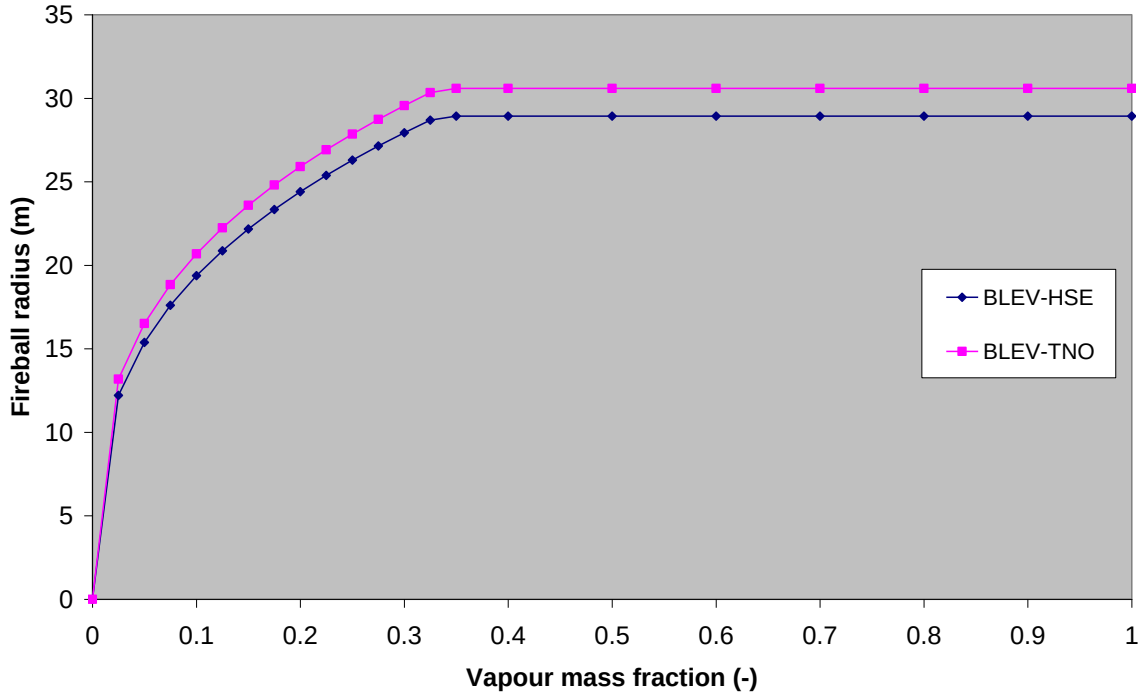

Figure 34 **Sensitivity analyses on the BLEV-HSE and BLEV-TNO models showing the variation of simulated fireball radius with vapour mass fraction from the released inventory.**

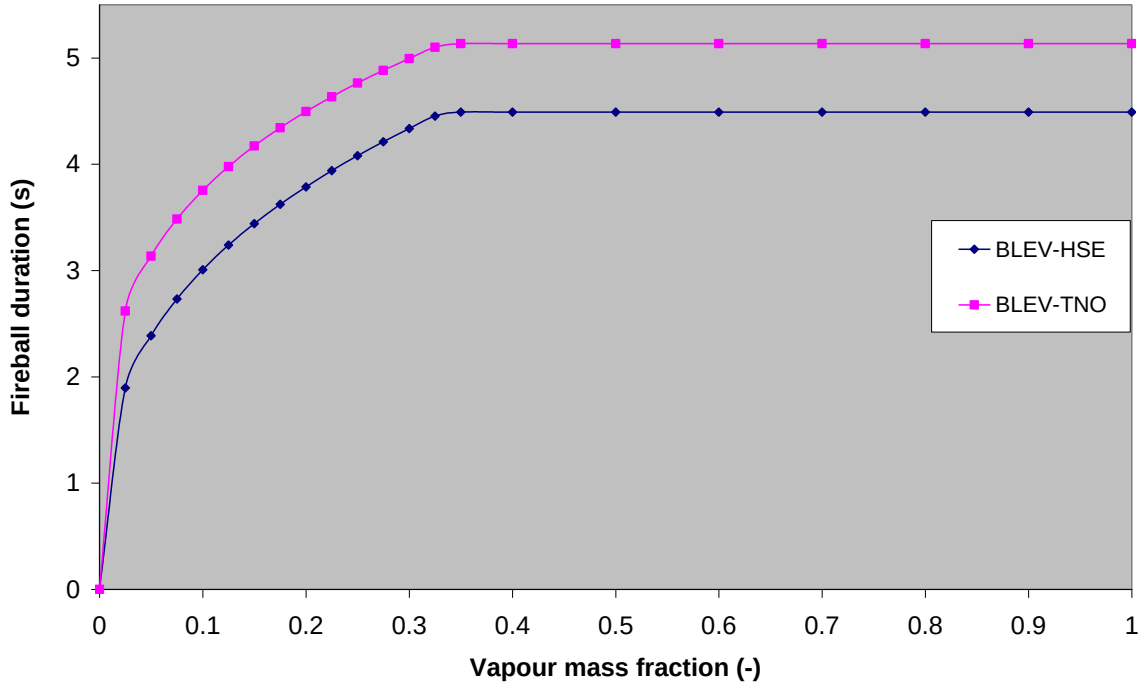

Figure 35 **Sensitivity analyses on the BLEV-HSE and BLEV-TNO models showing the variation of simulated fireball duration with vapour mass fraction from the released inventory.**

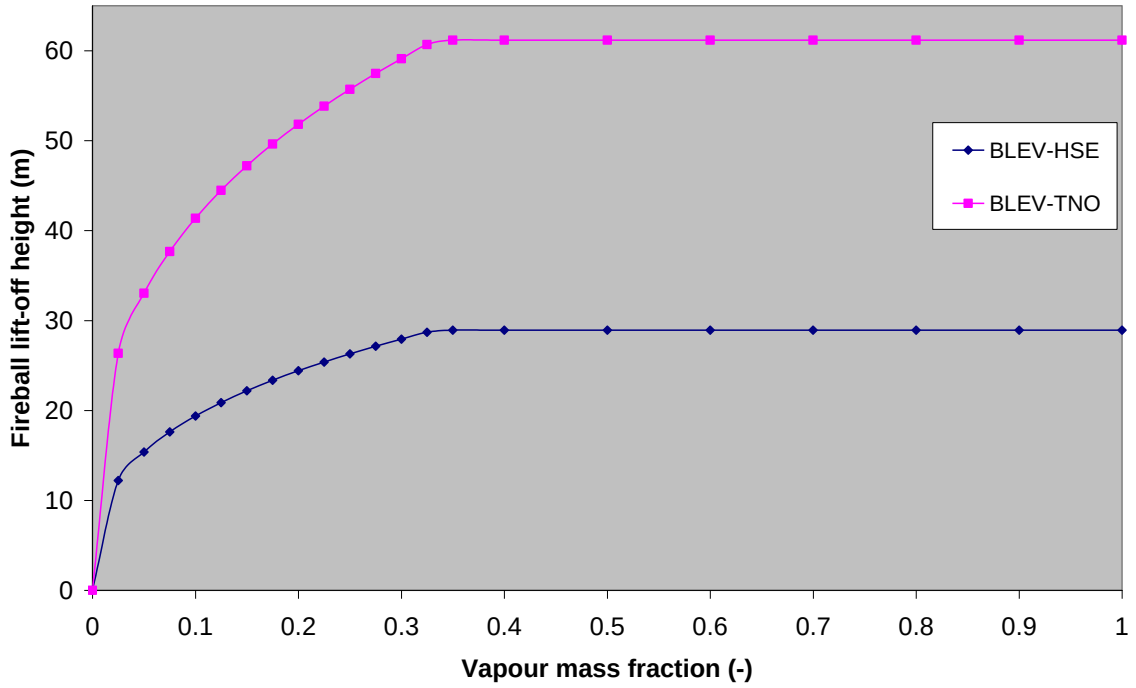

Figure 36 **Sensitivity analyses on the BLEV-HSE and BLEV-TNO models showing the variation of simulated fireball lift-off height with vapour mass fraction from the released inventory.**

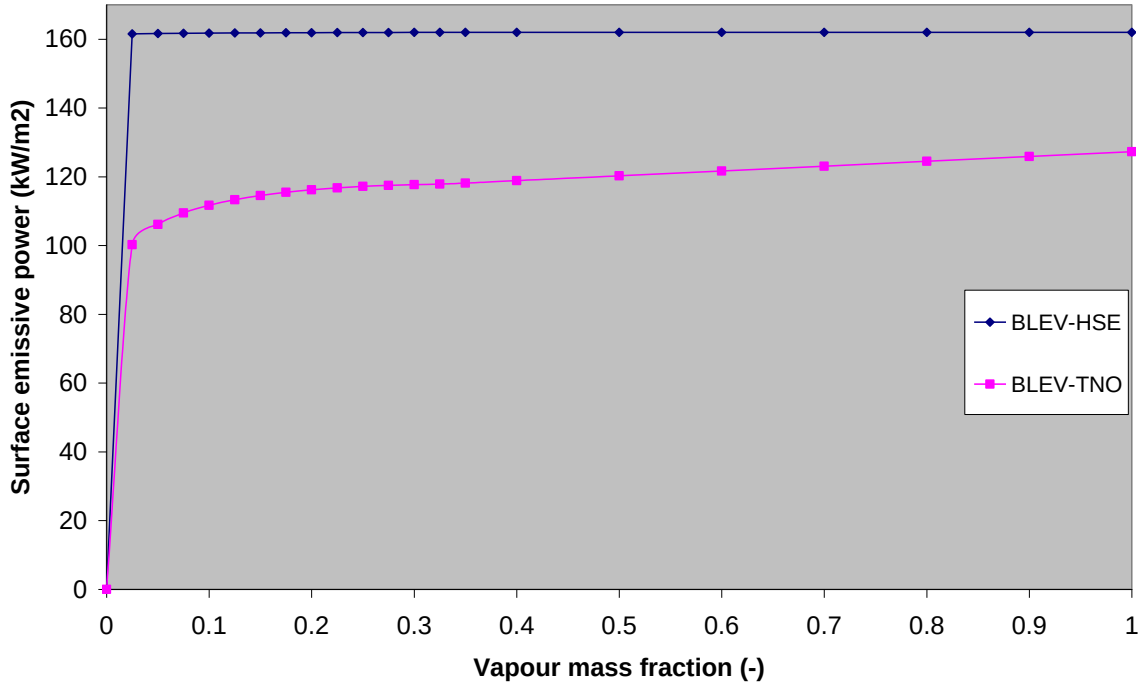

Figure 37 Sensitivity analyses on the BLEV-HSE and BLEV-TNO models showing the variation of simulated fireball surface emissive power with vapour mass fraction from the released inventory.

About DNV

We are the independent expert in risk management and quality assurance. Driven by our purpose, to safeguard life, property and the environment, we empower our customers and their stakeholders with facts and reliable insights so that critical decisions can be made with confidence. As a trusted voice for many of the world's most successful organizations, we use our knowledge to advance safety and performance, set industry benchmarks, and inspire and invent solutions to tackle global transformations.

Digital Solutions

DNV is a world-leading provider of digital solutions and software applications with focus on the energy, maritime and healthcare markets. Our solutions are used worldwide to manage risk and performance for wind turbines, electric grids, pipelines, processing plants, offshore structures, ships, and more. Supported by our domain knowledge and Veracity assurance platform, we enable companies to digitize and manage business critical activities in a sustainable, cost-efficient, safe and secure way.

DNV | digital@dnv.com | dnv.com/digital

REFERENCES

[1] Martinsen, W. E., and Marx, J. D., "An improved model for the prediction of radiant heat from fireballs", *International conference and workshop on modelling the consequences of accidental releases of hazardous materials*, San Francisco California, pp 605-621 (September, 1999)

[2] Bagster, D. G., and Pittblado, R. M., "Thermal hazards in the process industry", *Chemical Engineering Progress*, pp 69-75 (July, 1989)

[3] Cowley, L. T., and Johnson, A. D., "Blast and fire engineering project for topside structures", F11 Oil and gas fires: Characteristics and impact, (1991)

[4] Van den Bosch C. J. H., and Wetterings R. A. P. M. (Eds), "Methods for the calculation of physical effects 'Yellow Book' CPR 14E (Part 2)", 3rd ed., Sdu Uitgevers, The Hague, pp. 6.17-6.138 (1997)

[5] Crossthwaite, P. J., Fitzpatrick, R. D., and Hurst, N. W., "Risk assessment for the siting of developments near liquefied petroleum gas installations", IChemE Symposium 110, pp. 373-400 (1988)

[6] Mannan, S. (editor), Lees' "Loss Prevention in the Process Industries", Elsevier, Amsterdam (2005)

[7] CCPS Book, "Guidelines for Vapor Cloud Explosion, Pressure, Vessel Burst, BLEVE and Flash Fire Hazards", 2nd ed., John Wiley and Sons, Inc., Hoboken, New Jersey, VS (2010)

[8] Roberts T., Gosse A. & Hawksworth S., "Thermal radiation from fireballs on failure of liquefied petroleum gas storage vessels", Trans IChemE 78, pp. 184 – 192 (2000)

[9] DNV, "Onderzoek naar modellen voor gebruik in de kwantitatieve risicoanalyse", Report by DNV for Flemish authorities (Department Leefmilieu, Natuur en Energie), February 2012

[10] Acton, M.R., Baldwin, T.R., Jager, E.R., "Recent developments in the design and application of the Pipesafe Risk Assessment Package for Gas transmission pipelines", Paper IPC02-27196M Proceedings of IPC 2002 , Int. Pipeline Conf., Calgary, Canada (2002)

[11] Acton, M.R., Baldwin, P.J., Baldwin, T.R., Jager, E.R., "The Development of Pipesafe Risk Assessment Package for Gas transmission pipelines", Proceedings of the International Pipeline Conference, ASME International, Book No. G1075A-1998 (1998)

[12] "Shell Shepherd Desktop Technical Guide", Version 1.04.5 (2003)

[13] Shield, S.R., "A model to predict radiant heat and blast hazards from LPG BLEVES", AICHE 29th National Heat Transfer Conference, pp. 139-149 (1993)

[14] Shield, S.R., "Consequence modelling for LPG distribution in Hong Kong", Thornton Research Centre, United Kingdom, Research Note TNRN.95.7001, December 13 (1994)

[15] Shield, S. R., "Modelling of BLEVE fireball transients", IChemE symposium series, 139, pp. 227 – 236 (1995)

[16] Hasegawa, K., and Sato, K., "Study on the fireball following steam explosion of n-Pentane", *Proceedings of the Second International Symposium on Loss Prevention and Safety Promotion in the Process Industries*, Heidelberg, Germany, pp 297-304, (September, 1977)

[17] Roberts, A. F., "Thermal radiation hazards from releases of LPG from pressurised storage", *J. Fire Safety Studies*, **4**, pp 197-212 (1982)

[18] CCPS Book, "Guidelines for Vapor Cloud Explosion, Pressure, Vessel Burst, BLEVE and Flash Fire Hazards", 2nd ed., John Wiley and Sons, Inc., Hoboken, New Jersey, VS (2010)

[19] Pritchard, M.J., "A review of experimental data on the time-dependent behaviour of fireballs, Report MRS I 3701, Midland Research Station, British Gas R&D, April 1985 (1985)

[20] Pritchard, M.J., "An improved technique for predicting the thermal radiation hazards from fireballs, Report MRS I 3700, Midland Research Station, British Gas R&D, April 1985 (1985)

[21] Halford, A. R., Private communication, DNV, Loughborough, 18th February (2014)

[22] Maurer, B., Hess, K., Giesbrecht, H., and Leuckel, W., "Modelling of vapour cloud dispersion and deflagration after bursting of tanks filled with liquefied gas", 2nd Lit. Symposium on Loss Prevention, European Federation of Chemical Engineers, pp. 305-321 (1977)

[23] Schulz-Forberg, B., Droste, B., and Charlett, H., "Failure mechanisms of propane-tanks under thermal stresses including fire engulfment", Transport and Storage of LPG and LNG, Proceedings, 1, Brugge, Belgium, pp. 295-305 (1984)

[24] Johnson, D.M., Pritchard, M.J., and Wickens, M.J., "A large scale experimental study of BLEVEs", Contract report on Commission of the European Communities (CEC) co-funded research project, Report number I5367 (1991)

[xxv] Beyler, 'Fire hazard calculations for large, open hydrocarbon fires, Chapter 11, Section 3, the SFPE Handbook of fire protection engineering, SFPE, Quincy, USA (2002)

[xxvi] Cleaver, R. P., and Halford, A. R., “A model for the initial stages following the rupture of a natural gas transmission pipeline”, DNV (2014)
[xxvii] Turner, J. S., “The Starting Plume in Neutral Surroundings”, J.Fluid Mech., Vol 13, Part 3, pp 356-368, (1962)
[xxviii] Acton, M.R., Hankinson, G., Ashworth, B.P., Sanai, M. and Colton, J.D., “A full scale experimental study of fires following the rupture of natural gas transmission pipelines”, IPC2000, Calgary, October 2000
[xxix] Norris H.L., “Hydrocarbon blowdown from vessels and pipelines”, Presented at the SPE 69th Annual Technical Conference, New Orleans (1994).
[xxx] Hirst, W.J.S., “Combustion of large scale releases of pressurized liquid propane”, Proceedings 3rd Symposium on heavy gas risk assessment, S Hartwig (ed.), Reidel, Dordrecht, Netherlands (1986)
[xxxi] Cracknell, R.F., and Carlsey, A.J., “Cloud fires – A methodology for hazard consequence modelling”, IChemE symposium series, 141, pp. 139 – 150 (1997)